GeoProc 2025

20-23 October, 2025
University of Cyprus, Nicosia, Cyprus

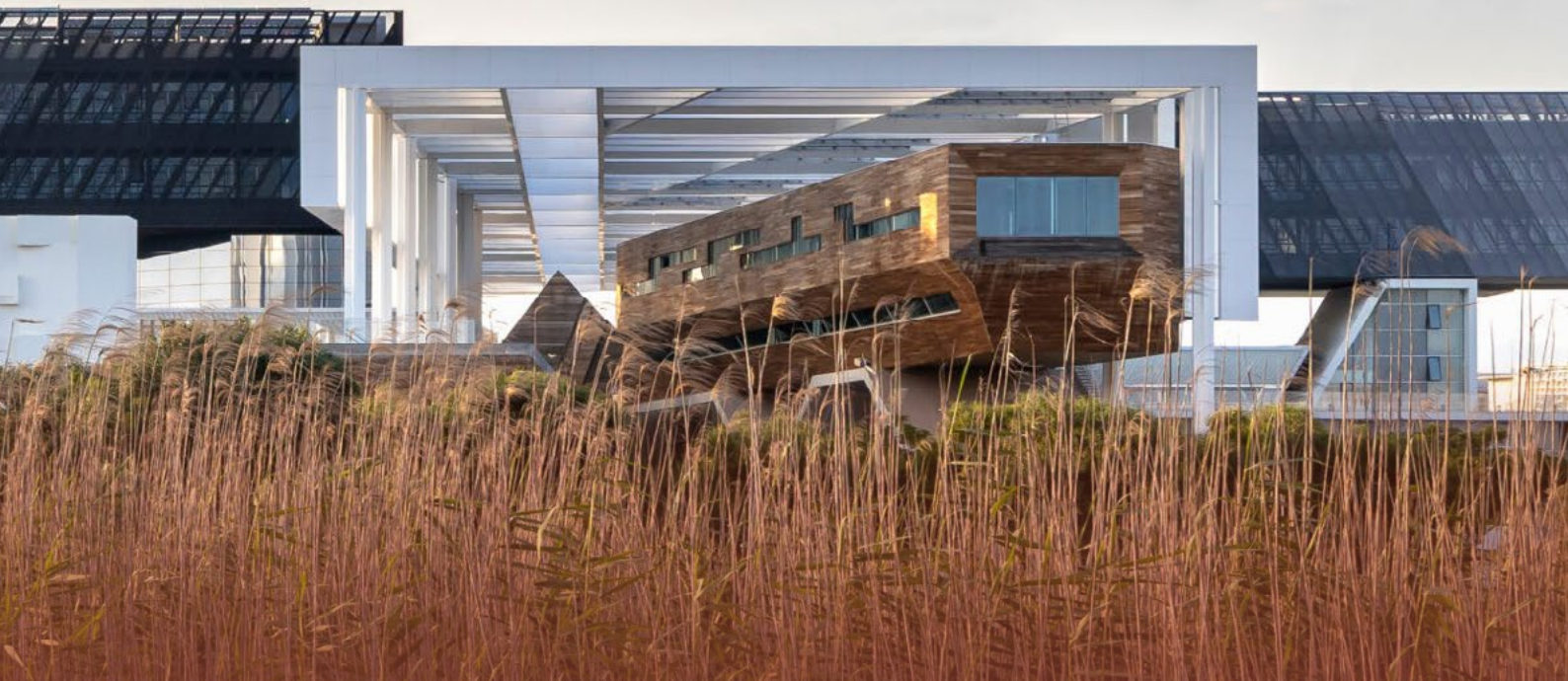

8th International Conference on Coupled THMC Processes: Geomechanics for Energy and Environmental Applications

https://cyprusconferences.org/geoproc2025/

Committees

Organizing Committee GeoProc2025

Prof. Panos Papanastasiou (UCY, Chairman)
Prof. Euripides Papamichos (AUTh, Co-Chairman)
Dr. Charalampos Konstantinou (UCY, Co-Chairman)
Prof. Ioannis Ioannou (UCY)
Prof. Theodora Kyratsi (UCY)
Prof. Dimitrios Loukidis (UCY)
Dr. Nikolaos Papadimitriou (GSD-CY)
Prof. Salah Sadek (American University of Beirut Mediterraneo, Cyprus)
Prof. Ernestos Sarris (AUTh, Greece)

Scientific Committee GeoProc2025

Prof. Khalid Alshibli (The University of Tennessee, Knoxville, USA)
Dr. Jianye Chen (Institute of Geology, China Earthquake Administration, China)
Dr. David Dempsey (University of Auckland, New Zealand)
Dr Christine Detournay (ITASCA, Minnesota, USA)
Prof. Emmanuel Detournay (University of Minnesota, USA)
Prof. Yaniv Edery (Technion, Israel)
Dr. Jan van Elk (Nederlandse Aardolie Maatschappij, The Netherlands)
Prof. Nicolas Espinoza (University of Texas at Austin, USA)
Prof. Alessio Ferrari (EPFL, Switzerland)
Dr Roar Egil Flatebø (AkerBP, Norway)
Dr. Eiichi Fukuyama (National Research Institute for Earth Science and Disaster Resilience, Japan)
Prof. Kenji Furui (Waseda University, Japan)
Dr. Vincenzo De Gennaro (SLB, France)
Prof. Eleni Gerolymatou (Technical University of Clausthal, Germany)
Prof. Yves Guglielmi (Lawrence Berkeley National Laboratory, USA)
Dr. Suzanne Hangx (Utrecht University, The Netherlands)
Prof. Rune Holt (NTU, Norway)
Dr. Manman Hu (The University of Hong Kong, Hong Kong)
Prof. Gangqiang Kong (Hohai University, China)
Dr. Charalampos Konstantinou (University of Cyprus, Cyprus)
Prof. Joe Labuz (University of Minnesota, USA)
Prof. Lyesse Laloui (EPFL, Switzerland)
Prof. Nadia Lapusta (California Institute of Technology, USA)

Prof. Alexandre Lavrov (NTNU, Norway)
Prof. Brice Lecampion (EPFL, Switzerland)
Assoc. Prof Hossein Masoumi (Monash University, Australia)
Assist. Prof Johannes Miocic (University of Groningen, The Netherlands)
Prof. Charles Wang Wai Ng (HKUST, Hong Kong)
Dr. Hamid Nick (DTU, Denmark)
Dr. André Niemeijer (Utrecht University, The Netherlands)
Dr. Edvard Omdal (ConocoPhillips Norway, Norway)
Prof. Jean-Michel Pereira (École des Ponts ParisTech, France)
Prof. Euripides Papamichos (Aristotle University Thessaloniki, Greece)
Prof. Panos Papanastasiou (University of Cyprus, Cyprus)
Dr. Thomas Poulet (CSIRO, Australia)
Prof. Klaus Regenauer-Lieb (University of New South Wales, Australia)
Prof. François Renard (University of Oslo, Norway)
Prof. Roman Makhnenko (University of Illinois at Urbana, USA)
Dr. Jonny Rutqvist (Lawrence Berkeley National Laboratory, USA)
Prof. Jianfu Shao (University of Lille, France)
Dr. Elena Spagnuolo (National Institute of Geophysics and Volcanology, Italy)
Prof. Chris Spiers (Utrecht University, The Netherlands)
Prof. Ioannis Stefanou (Ecole Centrale de Nantes, France)
Prof. Jean Sulem (École des Ponts ParisTech, France)
Prof. Manolis Veveakis (Duke University, USA)
Dr. Futoshi Yamashito (National Research Institute for Earth Science and Disaster Resilience, Japan)
Prof. Chunhe Yang (Chinese Academy of Sciences, Wuhan, China)
Dr Roar Egil Flatebø (AkerBP, Norway)

Mechanics of Fluid-Driven Fracture: Recent Results

Emmanuel Detournay[1]

[1] *Department of Civil, Environmental & Geo- Engineering, University of Minnesota*
Minneapolis, Minnesota, USA
E-mail: detou001@umn.edu

Keywords: Hydraulic fracture, receding fracture, poroelastic medium, shallow fracture

1. Introduction

Modeling of hydraulic fractures has been the subject of intense research in the last 30 years. These efforts, triggered by the seminal paper of Spence and Sharp [1], have led to new classes of solutions and algorithms, see [2-4] for recent reviews. It has been shown that the combination of elasticity, lubrication, and leak-off leads to the existence of a multiscale tip asymptote that account for the shifting nature of the dissipation in the tip region and to the existence of multiple time scales that are associated with the transition between different regimes of solution. Here we review recent results obtained by the author and his collaborators on topics that have so far received limited attention.

2. Receding Hydraulic Fracture: The Sunset Solution

A receding hydraulic fracture, which is closing due to fluid loss to the surrounding permeable medium, has a linear aperture asymptote $\widehat{w} \sim \hat{x}$ in the tip region, where $\hat{x}$ is the distance from the fracture front [5]. This asymptotic result enables the identification of a similarity solution for a radial fracture [6], the so-called Sunset Solution, which emerges close to the ultimate collapse of the fracture. As the fracture approaches closure, its aperture profile is described by a second-degree polynomial, with the aperture being proportional to the reverse time t' measured from closure. Furthermore, the fracture radius recedes in its final gasp as $R \sim \sqrt{t'}$. The existence of the Sunset Solution is due to a fundamental decoupling of the kinematics from the dynamics in the governing equations, which leads to a robust way to measure the Carter leak-off coefficient from the rate of change in the fracture aperture at the wellbore.

3. Hydraulic Fracture Induced by Water Injection in Weak Rock

A two-dimensional model of a hydraulic fracture propagating in a weakly consolidated, highly permeable reservoir rock during a waterflooding operation has been constructed, by combining equations from linear elastic fracture mechanics, porous media flow, and lubrication theory [6]. The model recognizes the essential differences that exist between this class of fractures and conventional hydraulic fracturing treatments of oil and gas wells, namely: (i) the large scale perturbations of pore pressure and the associated poroelastic effects caused by extended injection time; (ii) the extremely small volume of fluid stored in the fracture compared to the injected volume; and (iii) the leakage of water from both the borehole and the propagating fracture. The solution reveals that the

injection pressure does not evolve monotonically, as it increases with time in the early-time radial-flow regime but decreases in the late-time fracture-flow regime. Thus, the peak injection pressure does not correspond to a breakdown of the formation, as usually assumed, but rather to a transition between two regimes of porous media flow.

4. Growth Rate of Natural Hydraulic Fracture

Natural hydraulic fractures (NHFs) are tensile fractures that form in fluid-saturated rocks when in-situ pore pressure exceeds the minimum compressive stress. Their propagation is controlled by the inflow of pore fluid, which depends on both pore pressure diffusion in the surrounding rock and the evolving fracture size. However, the long-term growth behavior of NHFs remains an open question. A recent study [7] demonstrates that, after an initial transient phase triggered by a perturbation that caused the fracture to grow, an NHF attains a steady-state propagation rate. An explicit expression for this rate is derived, linking it to the rock poromechanical properties and to the difference between in-situ pore pressure and minimum compressive stress. This result is achieved by recognizing that, over time, fracture growth outpaces diffusion, effectively confining pore pressure evolution to a one-dimensional diffusion process within thin layers adjacent to the fracture plane.

5. Near-tip Behavior of a Shallow Hydraulic Fracture with Small Toughness

The coupled problem of steadily moving semi-infinite fractures driven by a viscous fluid in the proximity of a free surface has been studied recently [9]. A scaling analysis indicates that the solution depends on a single parameter, which can be interpreted as a dimensionless toughness κ. Because of the existence of a free surface, a sliding zone emerges at the fracture tip when κ is less than a critical value κ_*. The length of the sliding zone increases with smaller values of κ below κ_*.

6. References

[1] Spence, D.A., Sharp, P.W., "Self-similar solution for elastohydrodynamic cavity flow", Proc. Roy. Soc. London, Ser. A, 400:289–313 (1985).
[2] Detournay, E., "Mechanics of hydraulic fractures", Annual Review of Fluid Mechanics, 48:311–339 (2016).
[3] Peirce, A.P., "Implicit level set algorithms for modelling hydraulic fracture propagation", Philosophical Transactions of the Royal Society A: 374(2078):20150423 (2016).
[4] Lecampion, B., Bunger, A.P., Zhang X., "Numerical methods for hydraulic fracture propagation: A review of recent trends", Journal of Natural Gas Science and Engineering, 49:66–83 (2018).
[5] Peirce, A.P., Detournay, E., "Multiscale Tip Asymptotics for a Deflating Hydraulic Fracture with Leak-off", Journal of Fluid Mechanics, 947: A17 (2022).
[6] Peirce, A.P., Detournay, E., "Sunset similarity solution for a receding hydraulic fracture", Journal of Fluid Mechanics, 944:A7 (2022).
[7] Gao, Y., Detournay E., "Hydraulic Fracture Induced by Water Injection in Weak Rock", Journal of Fluid Mechanics, 927, A19 (2021)
[8] Liu, C., Zhang, F., Detournay, E., "Growth Rate of Natural Hydraulic Fracture", Journal of Engineering Mechanics, 151:8 (2025).
[9] Zhang, Y.H., Wang, Z.Q., Detournay, E., Zheng, L.T., "Near-tip Behavior of a Shallow Hydraulic Fracture with Small Toughness", ARMA 25-743, 59th US Rock Mechanics/Geomechanics Symposium, Santa Fe, New Mexico, 8-11 June 2025, (2025).

High-Temperature K-Feldspar Dissolution and Lithium Enrichment in the Cooper Basin: A THMC(E) Perspective

Klaus Regenauer-Lieb[1*], Yongqiang Chen[1], Manman Hu[2]

[1] *WA School of Mines: Minerals, Energy and Chemical Engineering, Curtin University., Perth 6102, Australia.*
E-mail: klaus@curtin.edu.au, yqzchen@gmail.com,
[2] *Department of Civil Engineering, The University of Hong Kong, Hong Kong, China*
E-mail: mmhu@hku.hk

Keywords Lithium-rich fluid generation, granite reservoirs, creep fractures, reaction-cross-diffusion modelling

Abstract:

Building upon a proposed THMC pathway for lithium genesis in the Cooper Basin, this study explores the significant role of high-temperature (above 250°C) K-feldspar dissolution, driven by H+ and tectonic stress, in contributing to Li-enrichment. We emphasise the additional role of electrical processes THMC(E) that can support processes of micro fracturing [1], feldspar dissolution [2], and lithium enrichment observed in the recent (<10 Myrs) high-temperature reactivation of the Cooper basin granite due to tectonic plate collision. The hydrolysis reaction, triggered by the presence of H+ ions is the main driver of the release of cations such as (potassium and lithium) causing the breakdown of the feldspar structure. A prominent dissolution reaction is K-Feldspar ($K\,Al\,Si_3\,O_8$) dissolution into Muscovite and aqueous silica:

$$3K\,Al\,Si_3\,O_8 + 2H^+ \rightleftarrows K\,Al_3\,Si_3\,O_{10}(OH)_2 + 2K^+ + 6Si\,O_2(aq.)$$

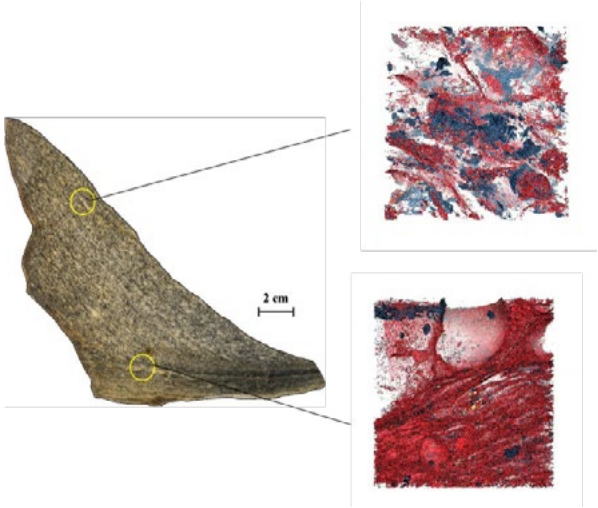

Figure 1Micro-tomography results showing microporosity (red) increasing towards a deformation band transporting fluids through a creep fracturing mechanism [1]. Quartz and Feldspar are transparent, Mica is blue.

Micro-CT analysis of a high-temperature deformation band within granite, now exposed by the Redbank shear zone (Australia), reveals creep fractures formed through coupled dissolution and tectonic stress at elevated temperatures (Fig. 1). These creep fractures generate fresh, chemically reactive surfaces, significantly enhancing hydrolysis. The increased surface area promotes accelerated feldspar breakdown and alkali ion release, potentially influenced by deformation-induced electrical fields. A simplified damage model has been used to simulate these processes [3].

In the present work, we have formulated a Multiphysics THMC(E) model intending to explicitly consider the following feedbacks: **Thermal (T)** where high temperatures drive the dissolution reactions; **Hydrological (H)** in which released fluids alter pore pressure and flow, influencing further reactions; **Mechanical (M)** through the application of tectonic stress enhancing fracturing and fluid flow; **Chemical (C)** reactions such as K-feldspar dissolution that release lithium and other ions; and finally **Electrical (E)** charge exchange plays a significant role in high-temperature hydrolysis by influencing ion mobility, mineral stability, and fluid-rock interactions. To simplify the numerical analysis a semi-analytical approach based on identifying dynamically stable modes of cross-coupled Onsager matrix of multiphysics transport coefficients has been developed to evaluate the dominant feedback mechanism:

$$J_i = -\begin{bmatrix} L_{TT} & L_{TH} & L_{TM} & L_{TC} & L_{TE} \\ L_{HT} & L_{HH} & L_{HM} & L_{HC} & L_{HE} \\ L_{MT} & L_{MH} & L_{MM} & L_{MC} & L_{ME} \\ L_{CT} & L_{CH} & L_{CM} & L_{CC} & L_{CE} \\ L_{ET} & L_{EH} & L_{EM} & L_{EC} & L_{EE} \end{bmatrix} X_j.$$

Here, J_i refers to the generalised thermodynamic flux and X_j to the generalised thermodynamic force. This model reinstates a linear combination of known laws, including Fourier's law (thermal L_{TT}), Darcy's law (hydraulic L_{HH}), Stokes' law (hydromechanical L_{MM}), Fick's law (chemical L_{CC}), and Ohm's law (electrical L_{EE}), each described by a particular coefficient. Additionally, it sheds light on the interesting cross-effects among various Thermal-Hydraulic-Mechanical-Electrical THMC(E) processes through the introduction of crossed coefficients.

Using a simplified version, a steady-state analytical solution has been used to model fluid release of the sheet silica reactions in the equivalent low-temperature from spacing and width of deformation bands in overpressured shales [4]. We have also explored the approach for dynamic GPS observations of episodic-tremor and slip cycles in subduction zones [5]. A linear stability analysis of the system of equations followed by a subsequent numerical solution has been successful in deriving the dehydration reaction of serpentinite minerals in subduction zones. In future work we aim to quantify the unknown rate of Feldspar dissolution and Li-release reactions using all available geophysical, geological, and >5km deep drilling data from the Cooper Basin geothermal project.

References

1 *Fusseis, F., Regenauer-Lieb, K., Liu, J., Hough, R. M. & De Carlo, F. (2009), Nature, 10.1038/nature08051*

2 *Wintsch, R. P. (1975), Geological Society of America bulletin, 10.1130/0016-7606(1975)86<35:FAAROD>2.0.CO;2*

3 *Regenauer-Lieb, K. et al. (2015), Philosophical Magazine,*

4 *Alevizos, S. et al. (2017), Rock Mechanics and Rock Engineering, https://doi.org/10.1007/s00603-016-0996-y*

5 *Sun, Q., Regenauer-Lieb, K. & Hu, M. (2024), Physics of the Earth and Planetary Interiors, 10.1016/j.pepi.2024.107223*

Deformation Modes of a Porous Limestone: Quantifying the Influence of Initial Porosity Distribution

Catherine Doré-Ossipyan[1,2], Adriana Quacquarelli[1], Jean Sulem[1], Michel Bornert[1], Alexandre Dimanov[2]

[1] *Laboratoire Navier, École Nationale des Ponts et Chaussées, Institut Polytechnique de Paris, Univ. Gustave Eiffel, CNRS UMR 8205, Marne-la-Vallée, France*
[2] *Laboratoire de Mécanique des Solides, École Polytechnique, Institut Polytechnique de Paris, CNRS UMR 7649, Palaiseau, France*

Keywords: Strain localization, triaxial testing, porous limestone

1. Introduction

Failure in porous geomaterials has been demonstrated to be characterized by heterogeneous strain through field and laboratory studies. Identification of the mechanical processes involved in the formation of strain localization patterns in porous carbonate rocks is challenging due to the complexity of their microstructure. This is due to the intricate geologic processes involved in limestone formation, resulting in a wide variety of carbonate rock facies [1] and observed behaviors.

2. Methodology

We experimentally explore the relationship between initial porosity distribution of the heterogeneous Saint-Maximin limestone (SML) and its deformation modes at micrometre scale. From previous work on SML [2], it was established that the alternation of more porous and denser centimetre-wide zones controls strain localization at all confining pressures. In the present study, we analyse how these zones individually accommodate strain.

A series of *in situ* tests on small, 8 mm in diameter samples – cored either in the porous or dense zones of SML – have been conducted, together with high resolution synchrotron imaging and Digital Volume Correlation (DVC) [3]. The deformation modes of porous and dense 8 mm samples are then compared with the standard 40 mm heterogenous samples [2].

3. Main Results

The *in situ* mechanical data for all tests are summarized in Fig. 1a. Dense 8mm samples (blue squares) exhibit a significantly larger elastic domain than porous ones (red circles), despite the relatively small difference in their initial porosity (35-37% vs 42% respectively). The yield surface obtained on samples of 40 mm in diameter is also reported and lies between that of the dense and porous samples.
DVC showed that strain is accommodated heterogeneously at all confining pressures, even under hydrostatic loading (Fig 1b): localized failure at low pressure (LC), diffuse deformation at high confining pressure (HC). A transition from brittleness to ductility was observed in dense samples only at intermediate confining pressures (IC). Localized

bands form in the most porous zone of the sample at LC. At IC, both contractant and dilatant shear bands develop in porous and dense zones respectively. At HC and in hydrostatic loading conditions, a multiplicity of small contractant bands close to each other appear in the most porous zones and propagate progressively in the whole sample leading to a densification of the sample and a homogenization of the porosity (Fig 1b).

Comparison of global responses under hydrostatic loading of 40mm and 8 mm samples showed that the larger sample's response is governed by that of its porous zones at a scale of one centimetre.

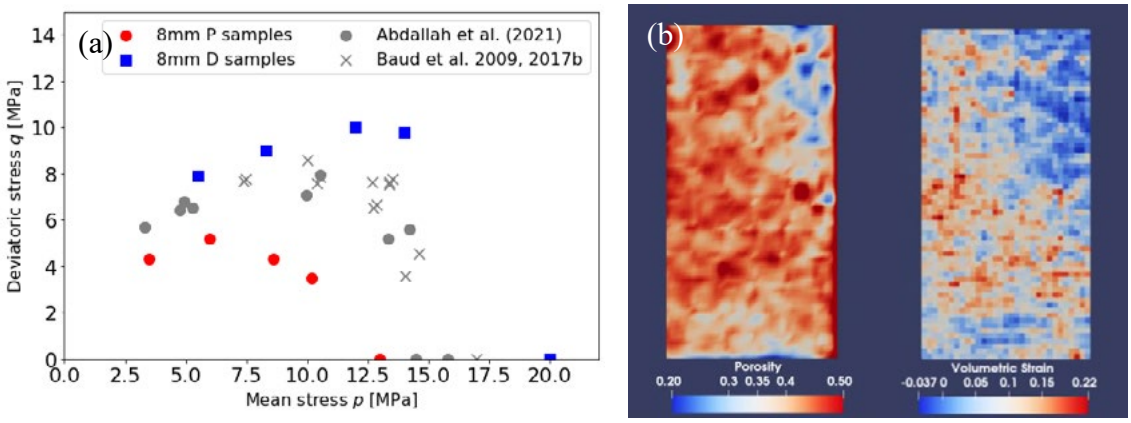

Fig. 1: (a) Yield stresses for porous (red circles) and dense (blue squares) samples in a mean stress versus deviatoric stress plane, and comparison with existing data (grey circles and x-es). (b) Vertical cross sections of an initial porosity map (left) and volumetric strain map (right) of a porous sample ($\varphi_{initial} = 42\%$) brought to $\sigma_c = 20$ MPa. Compaction is positive.

4. Conclusions

Initial porosity exerts a first order control on strain pattern, from the micro to the centimetre scale. In brittle conditions, strain localises in bands and is accommodated in the more porous areas, while the denser ones remain almost intact. Heterogeneity promotes transitional behaviour at intermediate confining pressure with coexistence of both diffuse and localized deformation. In ductile conditions multiple small contractant bands progressively saturate the sample and lead to a homogenization of its porosity.

5. References

[1] Flügel, E. 2004. Microfacies of Carbonate Rocks. In Microfacies of Carbonate Rocks.

[2] Abdallah, Y., Sulem, J., Bornert, M., Ghabezloo, S., Stefanou, I. 2021. Compaction Banding in High-Porosity Carbonate Rocks: 1. Experimental Observations. Journal of Geophysical Research: Solid Earth 126 (1): 1–24.

[3] Lenoir, N., Bornert, M., Desrues, J., Bésuelle, P., & Viggiani, G. 2007. Volumetric digital image correlation applied to x-ray microtomography images from triaxial compression tests on argillaceous rock. Strain, 43(3), 193–205.

FFT-based solver for computing the thermoporoelastic response of porous composites

Maria Camila Olarte[1], Jean-Michel Pereira[1], Patrick Dangla[1]

[1] *Navier, ENPC, Institut Polytechnique de Paris, Univ Gustave Eiffel, CNRS, Marne-la-Vallée, France*

E-mail : maria-camila.olarte-garzon@enpc.fr, jean-michel.pereira@enpc.fr, patrick.dangla@univ-eiffel.fr

Keywords: thermoporoelasticity, FFT-based method, homogenization, porous materials

1. Introduction

Since the pioneering work of Moulinec and Suquet [1], considerable attention has been paid to the application of the Fast Fourier Transform (FFT) based homogenization method to address problems in geomechanics. In this paper we present an FFT-based solver that includes the framework of thermoporomechanics in porous materials with direct applications to image-based fast homogenization. We optimize the original algorithm for the determination of the strain $\underline{\varepsilon}^{n+1}$ as:

$$\begin{cases} \text{Setup} \\ p^0 \wedge T^0 \end{cases} \begin{cases} \text{Iterations (n}\geq 0) \\ \underline{\varepsilon}^{n+1}(\underline{x}) = -\mathbb{\Gamma}^0 * \left[\left(C(\underline{x}) - C^0 \right) : \underline{\varepsilon}^n(\underline{x}) - p\underline{b}(\underline{x}) - C(\underline{x}) : \underline{\alpha}(\underline{x}) T \right] \end{cases} \tag{1}$$

From the local value of $\underline{\varepsilon}$ it is possible to determine the local values of the Biot's tensor $\underline{b}(\underline{x})$, the Biot's tangent modulus $1/N\,(\underline{x})$, the dilatancy tensor $\underline{\alpha}(\underline{x})$, the dilatancy coefficient α_ϕ and the heat capacity h according to the equations proposed by Coussy [2].

2. Methodology

In order to validate our developments, we consider a 2D microstructure consisting of a circular inclusion embedded into a continuous matrix defined as Ω = [0,1]x[1,0]. The RVE is discretized with a *N*x*N* grid with N = 256, and the loading consists of a scalar pressure and temperature field of 1 MPa and 274.15 K, respectively. The inclusion radius was fitted within an interval spanning from 0.05 to 0.5. From equation (1) we can calculate the isotropic operators b^{hom}, $1/N^{hom}$, κ^{hom}, $\alpha_\phi{}^{hom}$, and H^{hom} by simply summing all the values of each local magnitude over the entire volume Ω and normalizing the sum by the total number of pixels. The analytical solutions of micro-poroelasticity and the homogenization of the poroelastic properties follow the formulation proposed by Ghabezloo [3].

3. Main results

The input parameters used in the analysis are presented in Table 1. The comparative results are presented in Fig. 1, where we obtained an accurate agreement between the

results of our FFT-based homogenization solver and the analytical solutions. Note that both solutions move in a closed range from the value of the matrix to near the value of the inclusion when the radius is increased. In terms of time of computation, the solver requires less than 10 seconds, which is approximatively 0.8 seconds per iteration. In higher resolutions, with a discretization 1024x1024, *i.e.*, 1 million Fourier points, only 50 second are required.

Table 1. Input parameters for the calculation of homogeneous thermoporoelastic operators.

	E [GPa]	υ [.]	b [.]	k_s [GPa]	ϕ_0 [.]	N [GPa^{-1}]	α [K^{-1}]	α_ϕ [K^{-1}]	h [MJ/K]
Matrix	2.67	0.33	0.58	31.8	0.25	$\frac{k_s}{b-\phi_0}$	30e^{-6}	$\alpha(b-b_0)$	1.47
Inclusion	5.34	0.35	0.68	30.8	0.25		32e^{-6}		1.40

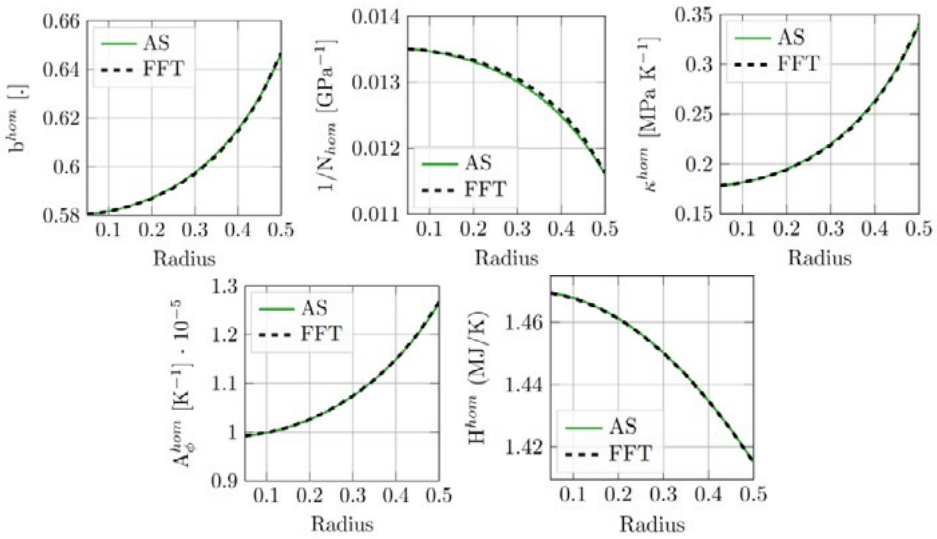

Fig. 1: Evolution of homogeneous operators as a function of radius for isotropic case.

4. Conclusions

In this paper, we introduce a numerical tool based on FFT homogenization that can determine the full thermo-hydro-mechanical coupled matrix for homogeneous porous materials. Through comparison with analytical solutions derived within the framework of micromechanics, we successfully validate the numerical results.

5. References

[1] Moulinec, H., Suquet, P., 'A fast numerical method for computing the linear and nonlinear mechanical properties of composites', Comptes rendus de l'Académie des sciences. Série II, Mécanique, physique, chimie, astronomie, 318, 1417-1423 (1994).
[2] Coussy, O., 'Poromechanics', John Wiley & Sons (2004).
[3] Ghabezloo, S., 'Micromechanics analysis of thermal expansion and thermal pressurization of a hardened cement paste', Cement and Concrete Research, 41, 520-532 (2011).

Shear strength recovery of rock salt fractures following healing process

Shihao Fu, Anne-Catherine Dieudonné, David Bruhn, Anne Pluymakers

Department of Geoscience and Engineering, TU Delft, The Netherlands
E-mail: s.fu-2@tudelft.nl, A.A.M.Dieudonne@tudelft.nl, D.F.Bruhn@tudelft.nl, Anne.Pluymakers@tudelft.nl

Keywords: Rock salt; Fluid-rock interaction; Healing process; Direct shear testing

1. Introduction

Rock salt is widely regarded as a potential host formation for underground storage applications, including CO_2 sequestration, radioactive waste disposal, and energy storage. However, fractures, whether preexisting or induced, can undermine the mechanical strength of the rock, posing risks to the safety, sustainability, and cost effectiveness of such operations. While solution-assisted fracture healing in rock salt has shown promise in restoring strength, most studies to date have focused on short-term healing over just hours to days [1, 2]. To ensure the reliable design and long-term performance of subsurface projects, a deeper understanding of prolonged healing processes and the differences in mechanical property evolution between dry and solution conditions is needed.

2. Methodology

Shear strength recovery in rock salt fractures is investigated through a two-step process. Samples consist of two separate plates, with the gap in-between representing an artificial fracture (Fig. 1). The samples are first subjected to static healing under a constant normal stress of 55 kPa. Healing is carried out either in dry conditions or in the presence of saturated brine. Healing duration is 192 days in the first case (dry) and 115 days in the later (saturated). Afterwards, the samples are tested in a direct shear box under an initial normal stress of 55 kPa and a shear rate of 0.5 mm/min. Healing strength (τ_H) is defined as the peak shear stress. Before and after testing, the topography of the sample surface is investigated using digital microscopy.

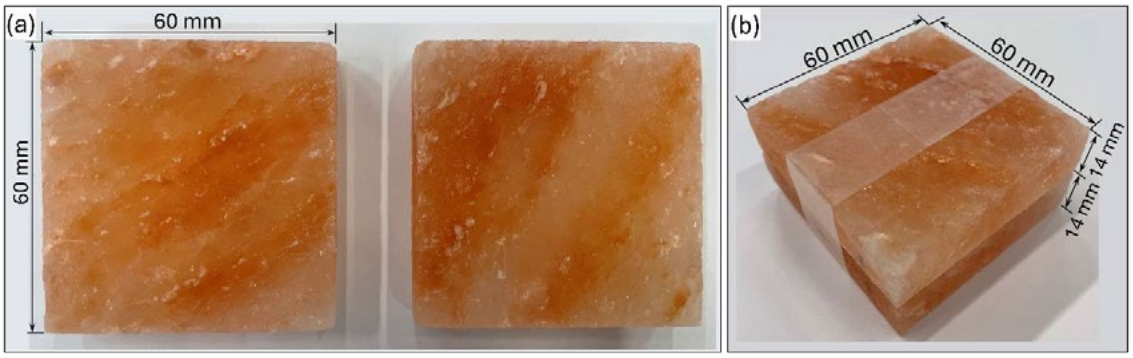

Fig 1: (a) and (b) show the dimensions of the rock salt plates used in the direct shear box test

3. Results

Healing strength increases under both dry and wet conditions (Fig. 2). Dry and unhealed sample (D-T000) shows a healing strength of 15 kPa. After 192 days of healing, the healing strength of the D-T192 sample reaches 31 kPa. However, when exposed to saturated solution, the unhealed sample (W-T000) shows a healing strength of 51 kPa, while the sample healed for 115 days (W-T115) reaches 251 kPa. The healing rate in the wet condition is about 1.7 kPa/day, which is 17 times higher than the 0.1 kPa/day observed in the dry condition. Digital microscopy shows the presence of post-shear striations only in dry healed sample, whereas the wet healed sample exhibits signs of dissolution, precipitation and recrystallization.

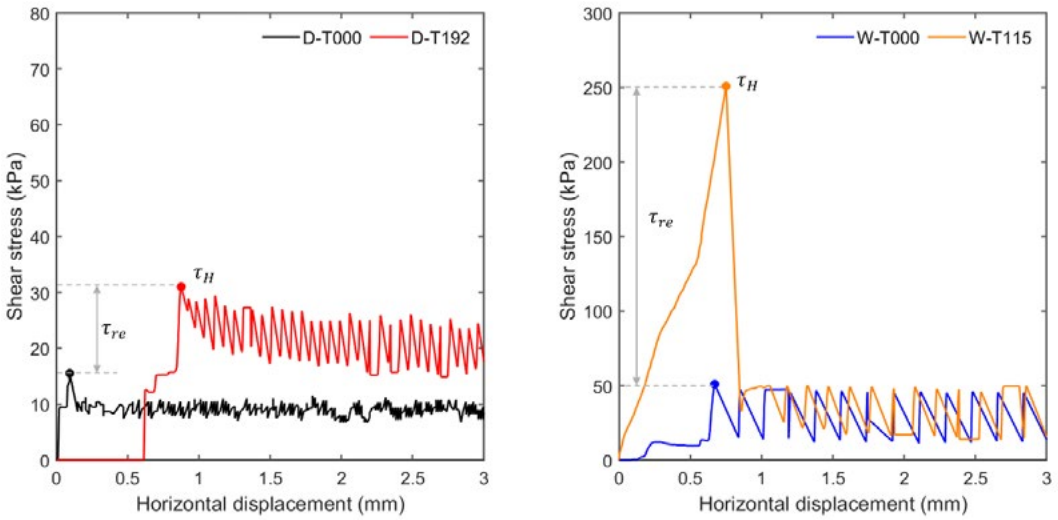

Fig. 2: (a) shows the shear stress versus horizontal displacement for the dry samples D-T000 and D-T192, while (b) presents the results for the wet samples W-T000 and W-T115.

4. Conclusions

Shear strength recovery depends on both healing duration and environmental conditions (dry/wet), with saturated solutions promoting greater strength restoration and nearly 20 times faster healing. These results have important implications for subsurface storage, suggesting that a saturated brine environment can enhance fracture healing. To better understand the mechanical evolution, additional samples with varying healing durations will be tested in the future. Furthermore, factors such as normal stress and temperature during static compaction also influence the healing process and should be considered in future studies.

5. References

[1] Fuenkajorn, K., & Phueakphum, D. Laboratory assessment of healing of fractures in rock salt. Bulletin of Engineering Geology and the Environment, 70(4), 665–672, 2011.
[2] Salzer K, Popp T, Böhnel H. Mechanical and permeability properties of highly pre-compacted granular salt bricks. In The Mechanical Behavior of Salt–Understanding of THMC Processes in Salt, 14, 239-248, 2007 Dec.

Chemo-Mechanical Couplings in a Numerical Twin

Alexandre Sac-Morane[1,2], Hadrien Rattez[1], Manolis Veveakis[2]

[1] IMMC, UCLouvain, Louvain-la-Neuve, Belgium
E-mail: alexandre.sac-morane@uclouvain.be, hadrien.rattez@uclouvain.be
[2] CEE, Duke University, Durham, NC, USA
E-mail: manolis.veveakis@duke.edu

Keywords: chemo-mechanical couplings, discrete element model, phase-field, pressure-solution, numerical twin

1. Introduction

The intricate interplay between chemical and mechanical processes in soil and rocks has emerged as a key factor to consider for many engineering applications like underground storage or geothermal energy or to understand geological processes like diagenesis or earthquake nucleation. Those reactions lead to mineral dissolution/precipitation that can modify the different properties of the sample.

2. Methodology

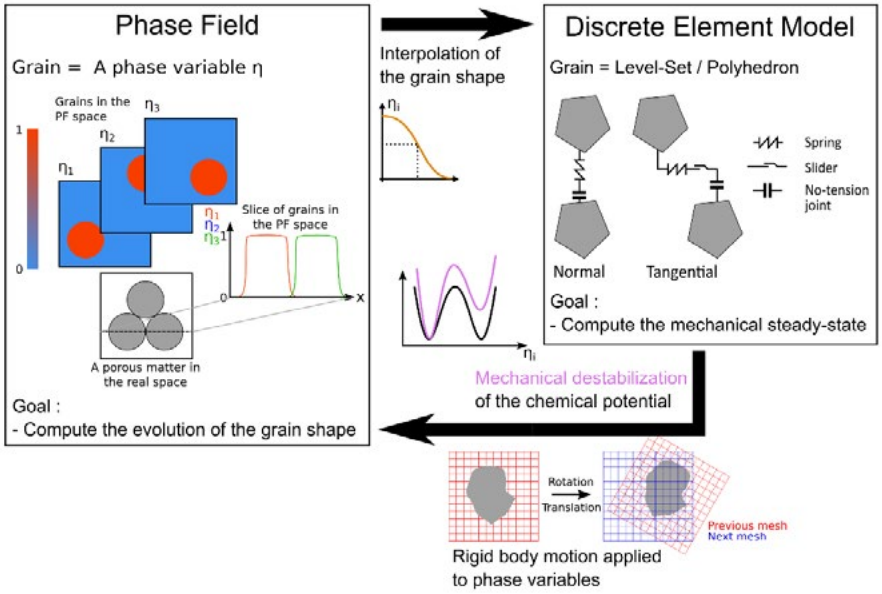

Fig. 1: framework of the PFDEM

A new coupling (PFDEM) between a Phase-Field (PF) method and a Discrete Element Model (DEM) has been recently developed to investigate deeper on chemo-mechanical couplings [1,2]. As depicted in Fig.1, the grains are modeled in the DEM part as polygonal (2D)/polyhedral (3D) particles to capture their complex shapes as they influence the macroscopic mechanical behavior of the material. Once a mechanical steady-state is reached in the DEM part, the transmission of stress can be extracted and employed to activate chemical reactions. Considering the granular material as a phase, the PF

description is a good candidate to model with physics-based laws a reduction/addition of the quantity of material locally. The dissolution/precipitation is controlled by the introduction of a destabilized chemical potential into the Allen-Cahn formulation on the phase variables, whereas the diffusion of the solute dissolved and the mass conservation are verified by a coupled diffusion formulation on the solute concentration.

3. Main Results

This method has been applied to reproduce results from previous works on the pressure-solution phenomenon. Pressure-solution has a pivotal role in earthquake nucleation and recurrence or in diagenetic processes, among others. As illustrated in Fig.2, it involves three chemo-mechanical processes at the micro-scale: dissolution due to stress concentration at grain contacts, diffusive transport of dissolved mass from the contact to the pore space, and precipitation of the solute on the less stressed surface of the grains. Once the formulation has been validated, it is applied to a numerical twin obtained by computed tomography scans of a granular sample [3].

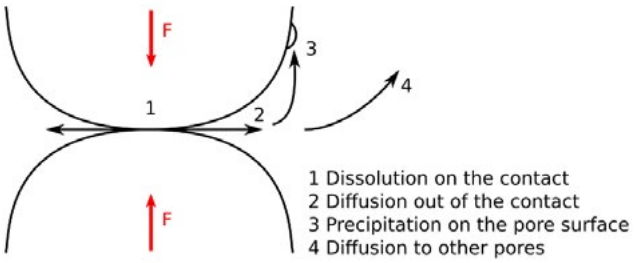

Fig. 2: scheme of the pressure-solution phenomenon

4. Conclusion

The proposed formulation opens up avenues for further exploration into the influence of various parameters on the creep behavior and the effect of grains characteristics. Parameters such as solute diffusivity, grains' morphology, and chemical/mechanical energy destabilization factors can now be systematically studied to gain insights into their impact on the overall behavior. This coupling of Discrete Element Model with Phase-Field theory provides a useful framework for investigating the mechanical response of geomaterials undergoing chemical solicitations.

5. References

[1] Sac-Morane, A., Veveakis, M., Rattez, H., 'A Phase-Field Discrete Element Method to study chemo-mechanical coupling in granular materials', Computer Methods in Applied Mechanics and Engineering, 424, 116900 (2024).

[2] Sac-Morane, A., Rattez, H., Veveakis, M., 'Importance of the precipitation on the slowdown of the creep behavior due to pressure-solution', under review in Journal of Engineering Mechanics.

[3] https://sand-atlas.scigem.com, accessed: Jan 30th 2025.

Stress versus damage-induced permeability anisotropy under true triaxial stress states in Etna Basalt

Ashley Stanton-Yonge, Thomas Mitchell, Philip Meredith, John Browning, David Healy

Fluids within low-porosity rocks are transported through networks of interconnected microcracks and fractures. Under crustal conditions, rocks are subjected to true triaxial stress states characterized by three unequal principal stresses, where $\sigma1>\sigma2>\sigma3$. These triaxial stress states can influence the magnitude and direction of fluid flow in two ways. First, cracks may open, close, and/or slip depending on their orientation with respect to the anisotropic stress field, and thereby potentially reducing fluid flow in certain directions while enhancing flow in others. Second, once the magnitude of differential stresses surpasses the onset of dilatancy in the rock, new cracks form, providing additional pathways for fluid transport. The geometry of these new fractures, and therefore the direction of fluid flow enhancement, is also controlled by the anisotropic stress field.

Despite the fundamental role of triaxial stresses in controlling the magnitude and direction of fluid flow through the crust, very little is known regarding the anisotropy of permeability under true triaxial stress states. This knowledge gap exists primarily because experimental permeability measurements are typically conducted under axisymmetric stress states ($\sigma1>\sigma2=\sigma3$) with fluid flow and permeability usually measured only parallel to the $\sigma1$-direction. To address this, we have developed a new True Triaxial Apparatus (TTA) at UCL equipped with a pore fluid system to deform cubic, saturated rock samples under true triaxial loading while contemporaneously measuring permeability along all three loading axes and recording the output of acoustic emissions (AEs) hits.

Results from tests conducted on 50 mm isotropic cubes of initially isotropic Etna basalt under true triaxial loading indicate that, under relatively low differential stresses (<180 MPa), fluid flow is reduced by over one order of magnitude in the direction parallel to $\sigma1$. Increasing the magnitude of stresses along the $\sigma2$ axis also results in a decrease in permeability along the same axis, although less pronounced. The increase of differential stresses eventually leads to an increase in AE hits, which further coincides with a sharp increase in permeability along the $\sigma2$-axis of one order of magnitude and, to a lesser extent, along the $\sigma3$-axis.

We have recognised a key differentiation in the magnitudes and orientations of permeability anisotropy before and after the onset of dilatancy. One stage is stress-controlled (involving the closing and slipping of pre-existing cracks), while the other is damage-induced (with the formation of new cracks or damage), resulting in entirely different permeability behaviours in these two stages.

Predicting the microstructural evolution of shear bands in crushable granular media

Nicholas Anton Collins-Craft[1], Ioannis Stefanou[2], Jean Sulem[1], Itai Einav[3]

[1] *Laboratoire Navier, École nationale des ponts et chaussées, Champs-sur-Marne, France*
E-mail: nicholas-anton.collins-craft@enpc.fr, jean.sulem@enpc.fr
[2] *IMSIA, École nationale supérieure de techniques avancées, Palaiseau, France*
E-mail: ioannis.stefanou@ensta-paris.fr
[3] *Particles and Grains Laboratory, University of Sydney, Sydney, Australia*
E-mail: itai.einav@sydney.edu.au

Keywords: shear bands, grain crushing, pore collapse, permeability, Cosserat

1. Introduction

The appearance of shear bands is a pervasive failure mode in geomaterials, whether at the laboratory scale of triaxial tests, or at field scales as large as the faults responsible for catastrophic earthquakes. Modelling shear band formation is thus a pressing challenge in both interpreting the results of calibration tests and making useful predictions, and to do so requires an accurate account of the width of the shear band. However, classical rate-independent models predict infinitely thin bands, and numerical simulations with tools such as the finite element method are unable to produce mesh-independent results. The origin of this pathology is the absence of an internal length scale [1], which can be rectified by recourse to a higher-order continuum such as a nonlocal, second-gradient or Cosserat continuum.

While previous works in the geomechanics community have successfully used the Cosserat continuum to predict shear band widths, they have systematically taken the internal length scale to be a fixed internal parameter related to the mean grain size. However, shear bands in the field reveal that the grain size distribution is radically different from that of the host rock, having undergone a process of grain crushing that produces a very wide spectrum of grain sizes, making the assumption of a fixed internal length unsustainable. To rectify this problem, in a previous work [2] we coupled the Cosserat continuum with the Breakage Mechanics theory [3] to derive a theory that was capable of predicting shear bands in crushable granular media. However, this model was not able to adequately account for pore-related phenomena, such as dilation orpore-collapse necessitating further refinement to address challenges such as fault modelling.

2. Methodology

We suppose that the internal energy of the system depends on a set of five state variables:

$$U = U\left(\gamma^e, \kappa^e, \rho, \phi, B\right), \tag{1}$$

where γ^{e} is the elastic (Cosserat) strain tensor, $\varkappa^{e}$ is the elastic curvature tensor, ρ the density, ϕ the solid fraction and B the breakage index. The (Cosserat) stresses, couple stresses, chemical potential and breakage energy are derived from this potential. We also specify a pseudo-potential of dissipation that depends on the plastic rates:

$$\Phi = \Phi\left(\dot{\kappa}^{p}, \dot{\phi}^{p}, \dot{B}\right) \tag{2}$$

The evolution laws of the system are obtained from this dissipation pseudo-potential.

Having derived a model, we carry out a linear stability analysis by first integrating a single element, and then perturbing the system with a variety of different wavelengths. We interpret the half-wavelength of the perturbation with the largest positive real Lyapunov exponent (if any) as the width of the shear band predicted by the material model. As the linear stability analysis is only strictly valid up until the moment that the shear band appears, we also conduct a finite element analysis to confirm our post-localisation predictions.

3. Main results

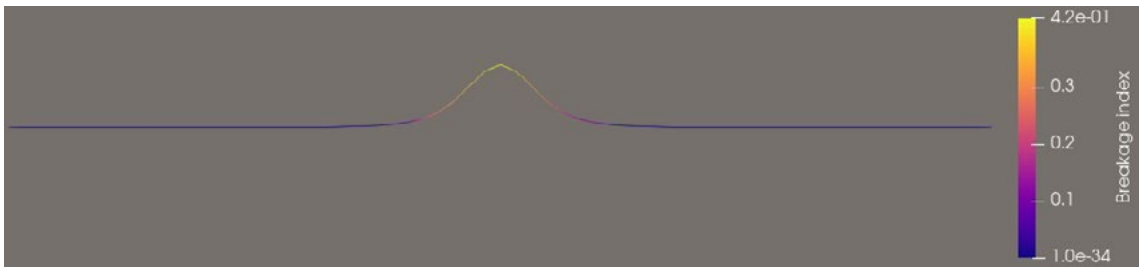

Fig 1: Plot of the breakage index over space in a one-dimensional finite element simulation.

As seen in Figure 1, our model is able to predict finite thickness shear bands, in this case in a system calibrated against Bentheim sandstone, and submitted to constant volume shear at an initial confining stress of 200 MPa.

4. Conclusions

By combining the Cosserat continuum with Breakage Mechanics, we are able to model the processes of grain crushing and pore collapse within a shear band of finite thickness. Access to these microstructural properties also allows us to make predictions of permeability reduction on the order of 10^{-3} to 10^{-4}, which has important implications for hydro-thermally coupled models that can more accurately model all of the processes involved in faulting.

5. References

[1] Mühlhaus, H.-B., Vardoulakis, I, 'The thickness of shear bands in granular media', Géotechnique, 37, 271–283 (1987)

[2] Collins-Craft, N.A., Stefanou, I., Sulem, J., Einav, I., 'A Cosserat Breakage Mechanics model for brittle granular media', Journal of the Mechanics and Physics of Solids, 141, 103975 (2020)

[3] Einav, I., 'Breakage mechanics — Part I: Theory', Journal of the Mechanics and Physics of Solids, 55, 1274–1297 (2007)

Spatiotemporal Evolution of Injection-Induced Seismicity in Fractured Rocks

Iman Vaezi and Qinghua Lei

Department of Earth Sciences, Uppsala University, Uppsala, Sweden
E-mail: iman.vaezi@geo.uu.se, qinghua.lei@geo.uu.se

Keywords: Induced seismicity, Discrete fracture network, Subsurface fluid injection

1. Introduction

Fluid injections related to industrial activities and subsurface energy production can modify the regional stress field within the Earth's crust, often leading to induced microseismicity, which, in certain cases, may exceed safety thresholds triggering large earthquakes (Mignan et al., 2017). Furthermore, such induced seismic events can occur at greater distances from the injection site than initially anticipated and may manifest over a wide range of timescales, spanning from days to months or even years (Keranen & Weingarten, 2018). These characteristics underscore the inherent variability and complexity of injection-induced seismicity evolution across spatiotemporal scales. To effectively mitigate the associated seismic hazard, a comprehensive understanding of the spatiotemporal evolution of induced seismicity, alongside the development of robust modeling approaches, is essential.

2. Methodology

We consider a 2D fractured reservoir with a domain size of L = 100 m situated at a depth of 3600 m below the ground surface. The material properties of rock matrix and pre-existing fractures, and in-situ stresses resemble those of the Fenton Hill geothermal test site (Norbeck et al., 2018). In the 2D square domain, we generate a series of fracture networks with the location of fractures assumed purely random and fracture lengths obey the power law scaling with different length exponents a and density values d. We study the injection-induced microseismic responses of each fracture network due to 1-hour fluid injection at the center of the domain. The fully coupled hydromechanical model considers fracture activation and damage growth, and calculates seismicity based on energy released from brittle failure of intact rock and activation of pre-existing fractures.

3. Main Results

We study the influence of the fracture network structure (such as density, length exponent, and percolation parameters) on the emergence and development of injection-induced seismicity (Fig. 1). The results show that the networks with less connected fractures (higher power law length exponent a) are prone to an enhanced hydraulic stimulation leading to better connectivity improvement and potentially more effective resource extraction. In contrast, well connected networks show less improvement in the

fracture system connectivity and exhibit a propensity for increased seismic activity due to the efficient transmission of pore pressure and elastic stresses across interconnected fractures. Furthermore, we observe hat poroelastic effects drive heterogeneous connectivity evolution during fluid injection, consistent with previous studies on fluid injection-induced fracture activation and seismicity occurrence in naturally fractured rocks (Lei et al., 2021).

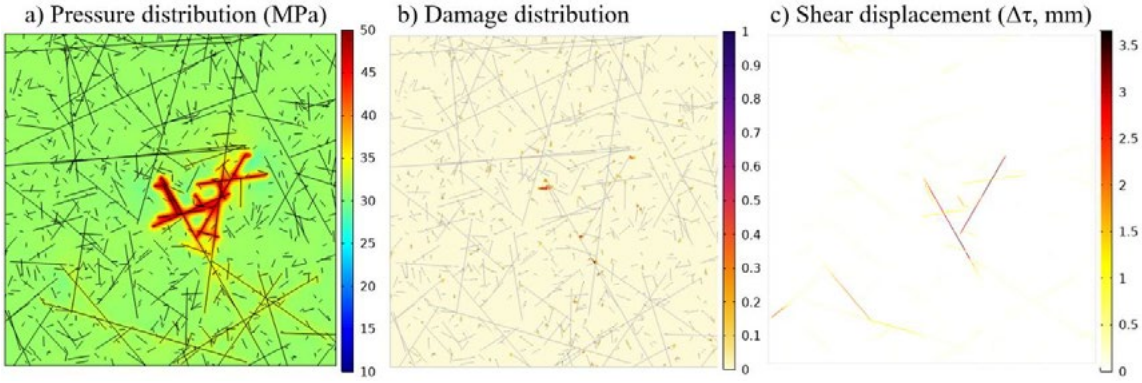

Fig. 1: Spatial distribution of pressure (a), damage (b), and shear displacement difference (c) in a model with power law length exponent a=2, fracture density d=0.4, and percolation parameter p=13.07. Here, we show just one discrete fracture network as illustration.

4. Conclusion

Our study highlights the influence of fracture network structure on the spatiotemporal characteristics of injection-induced seismicity. The insights underscore the importance of considering fracture network distribution in the assessment of seismic risks associated with subsurface fluid injections.

5. References

Keranen, K. M., & Weingarten, M. (2018). Induced Seismicity. *Annual Review of Earth and Planetary Sciences*, *46*(Volume 46, 2018), 149–174. https://doi.org/10.1146/annurev-earth-082517-010054

Lei, Q., Gholizadeh Doonechaly, N., & Tsang, C.-F. (2021). Modelling fluid injection-induced fracture activation, damage growth, seismicity occurrence and connectivity change in naturally fractured rocks. *International Journal of Rock Mechanics and Mining Sciences*, *138*, 104598. https://doi.org/10.1016/j.ijrmms.2020.104598

Mignan, A., Broccardo, M., Wiemer, S., & Giardini, D. (2017). Induced seismicity closed-form traffic light system for actuarial decision-making during deep fluid injections. *Scientific Reports*, *7*(1), 13607. https://doi.org/10.1038/s41598-017-13585-9

Norbeck, J. H., McClure, M. W., & Horne, R. N. (2018). Field observations at the Fenton Hill enhanced geothermal system test site support mixed-mechanism stimulation. *Geothermics*, *74*, 135–149. https://doi.org/10.1016/j.geothermics.2018.03.003

Accelerating Earthquake Simulations via Nonsmooth Mechanics and Reduced-Order Modeling

David Riley[1] and Ioannis Stefanou[1]

[1] IMSIA, CEA, CNRS, EDF, ENSTA Paris, Institut Polytechnique de Paris, Palaiseau, France
E-mail:david.riley@ensta.fr, ioannis.stefanou@ensta.fr

Keywords: earthquakes, poroelastodynamics, nonsmooth dynamics, model order reduction

1. Introduction

Deep geothermal energy, carbon capture and storage, and hydrogen storage involve injecting fluids into the Earth's crust, potentially inducing or triggering earthquakes [1]. Effective mitigation strategies require simulating fault dynamics and fluid injection from wells, typically through computationally demanding poroelastic dynamic equations. To efficiently address this challenge, we propose combining nonsmooth friction laws and model order reduction techniques. Specifically, nonsmooth friction ensures accurate adherence to Coulomb friction criteria and allows efficient implicit time integration [2]. At the same time, model order reduction intelligently decreases spatial degrees of freedom, significantly enhancing computational speed without compromising accuracy [3]. This approach provides a practical, accurate framework for exploring earthquake controllability and optimizing seismic risk management.

2. Methodology

Traditional poroelastodynamic earthquake simulations typically involve solving equations in complex 3D domains. Here, we simplify the computational challenge by focusing solely on the fault interfaces, disregarding elastic wave propagation into the bulk. Adopting the approach from previous works [4,5], we solve a reduced-order interface model governed by linear momentum expressed in a compact state-space representation:

$$\begin{bmatrix} M & 0 & 0 \\ 0 & I & 0 \\ 0 & 0 & I \end{bmatrix} = \begin{bmatrix} -H & K & 0 \\ I & 0 & 0 \\ 0 & 0 & I \end{bmatrix} \begin{bmatrix} v \\ \delta \\ |v| \end{bmatrix} + \begin{bmatrix} Hv_\infty - Kv_\infty + F_r(t,s,|v|) \\ 0 \\ 0 \end{bmatrix}, \quad (1)$$

Here $K \in \mathbb{R}^{N\times N}$ represents the elastic stiffness matrix, $H \in \mathbb{R}^{N\times N}$ is the viscosity matrix, $v_\infty \in \mathbb{R}^N$ is the far-field loading velocity, $\delta \in \mathbb{R}^N$ is the fault displacement, and $F_r \in \mathbb{R}^N$ denotes frictional resistance. Coulomb friction constraints form a nonsmooth, convex set:

$$C = \{(F_r, q) \in \mathbb{R}^N \times \mathbb{R}_+^N \mid |F_r| \le q\}, \quad (2)$$

where $q = \mu(t,s,|v|)A\sigma_n'$ with friction coefficient $\mu(t,s,|v|)$ defined by a slip-weakening law [6]:

$$\mu(t,s,|v|) = \mu_d + \Delta\mu e^{-\frac{s}{d_c}}, \quad (3)$$

with μ_d being the dynamic friction, $\Delta\mu$ the friction drop, s the time-integrated absolute value of velocity (slip), and d_c the characteristic slip distance. As an additional layer of

complexity, we generate gaussian random fields of $\Delta\mu$ and d_c to induce spatial heterogeneities. In this work, numerical integration is efficiently achieved using variational inequality solvers that robustly handle the nonmsooth friction conditions, a novel application in earthquake modelling that greatly enhances computational speed.

3. Results

In Fig. 1, we display the results of the simulation of the scenario discussed in the previous section from the point of instability. Notably, this implementation accurately simulates the true stick-slip behavior of earthquake faults, as demonstrated in Fig. 1 (a) and (c). Furthermore, after a large slipping event, the entire system clearly returns to sticking, as indicated by the plateau in Fig. 1 (b). Moreover, despite the spatial complexity of such a problem the variational inequality solution yields a solution that can produce up to a 5x speed improvement over an equivalent regularized formulation.

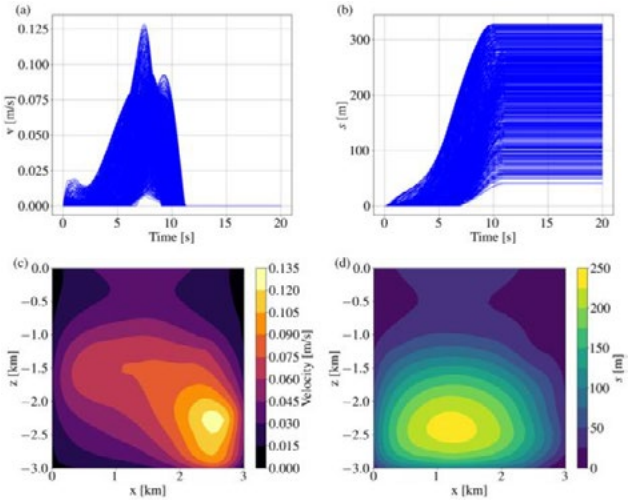

Fig. 1: Results from nonsmooth a simulation. (a) Velocities against time, (b) slip against time, (c) velocity contours and (d) slip contours in space at time = 7.3 s.

4. Conclusions

Herein, we introduced a streamlined computational framework combining nonsmooth frictional mechanics with model order reduction for earthquake simulations. By focusing computations directly on the fault interface and leveraging variational inequalities for friction dynamics, we achieve significant computational efficiency gains. The presented approach paves the way for practical, high-speed simulations making it particularly useful for real-time control applications [5].

5. References

[1] Ellsworth, W. L., 'Injection-Induced Earthquakes', Science, 341, 1225942 (2013).
[2] Acary, V., and Brogliato, B., Numerical Methods for Nonsmooth Dynamical Systems: Applications in Mechanics and Electronics, Springer, Heidelberg (2008).
[3] Antoulas, A. C., Approximation of Large-Scale Dynamical Systems, SIAM, Philadelphia (2005).
[4] Tzortopoulos, G. and Stefanou, I., Preventing instabilities and inducing controlled, slow-slip frictionally unstable systems, JGR: Solid Earth, 127, 7, *e2021JB023410 (2022).*
[5] Gutierrez-Oribio, D., Stefanou, I., and Plestan, F., Passivity-based control of underactuated mechanical systems with coulomb friction: Application to earthquake prevention, 165, 111661 (2024)

Hysteresis and Strain Memory in Deformable Porous Media under External Stress

Satyaki Kundu and Yaniv Edery*

Abstract

Hysteresis in porous media critically influences the mechanical stability and efficiency of subsurface operations such as CO_2 sequestration, hydrogen storage, and geothermal energy extraction. Yet, conventional models often treat hysteresis as an emergent bulk property, neglecting the microscale deformation processes that govern it. Our study aims to establish a systematic link between local-scale deformation mechanisms—such as localized shear failure and compaction bands—and global stress-strain responses observed during fluid pressurization cycles. Rather than treating hysteresis loops as phenomenological curves, we develop a mapping between loop characteristics (shape, asymmetry, memory) and the physical mechanisms that drive them.

In this work, we develop a transparent rock-like synthetic medium to directly observe the origin of hysteresis in fluid-induced deformation. The sample is formed by sintering Poly-Methyl-Methacrylate (PMMA) beads of sand-grain size, mimicking the mechanical behavior of sandstone at lower pressures. To enable internal strain tracking, approximately 1% of the particles are replaced with fluorescent microspheres, which are solidified into the structure during sintering. The sample is saturated with an index-matched oil, rendering the bulk material optically transparent while preserving the visibility of the fluorescent tracers. Fluid is then injected cyclically using the same oil, allowing precise control over pore pressure. The embedded fluorescent particles move with the solid matrix and are tracked using a high-speed camera, capturing real-time deformation during each pressure cycle. Particle Image Velocimetry (PIV) is used to analyze these displacements and extract spatially resolved strain fields. This experimental approach enables us to connect microscale deformation processes to macroscopic hysteresis behavior, providing detailed insight into the rate- and history-dependent response of porous media.

We systematically explore how hysteresis characteristics—such as loop shape, width, and memory effects—depend on pressure sweep rate and hold time. Our experiments reveal that faster sweep rates widen the hysteresis loops in accordance with power-law scaling. In addition to sweep-rate dependence, we study different kinds of memory effects, such as return point memory and the Kovacs effect, which manifest during cyclic loading and encode the system's response history. These memory effects serve as diagnostic markers for the evolution of metastable configurations and localized deformation zones within the medium. Moreover, we study how strain relaxes under constant effective stress by holding the pressure at selected intermediate levels. In many viscoelastic or poroelastic systems, constant stress does not ensure constant strain. Instead, the strain exhibits time-dependent relaxation governed by material-specific timescales. In our experiments, the relaxation behavior follows exponential or power-law decay, providing insight into how the material responds to long-term loading and how it distributes and dissipates stress over time.

Understanding how pore-scale deformation mechanisms give rise to macroscopic hysteresis behavior allows us to build a predictive framework that moves beyond empirical observations. This multiscale perspective reveals key features such as energy dissipation, strain localization, and failure precursors—elements that are essential for modeling the coupled Thermo-Hydro-Mechanical-Chemical (THMC) processes that govern subsurface systems.

*Civil and Environmental Engineering, Technion – Israel Institute of Technology, Haifa 32000, Israel. *kundusatyaki@campus.technion.ac.il*, *yanivedery@technion.ac.il*

Artificially intelligent subsurface coupled modelling, an energy industry perspective

Vincenzo De Gennaro[1]

[1] SLB New Energy Technology - Industrial Decarbonisation, Pau, France
E-mail: vdegennaro@slb.com

Keywords: THMC, modelling, CCS, deep learning

Abstract

New energy applications, such as CCS, hydrogen storage, and geothermal energy, can greatly benefit from the oil and gas industry's expertise in subsurface measurements, characterization, and modelling. However, there are many fields of investigation and methodologies in subsurface modelling, including thermo-hydro-mechanical-chemical (THMC) coupling, that are unfamiliar to traditional oil and gas approaches. Siloed domains schemes are among the main factors that have often hindered the adoption process, slowing down integration. Additionally, the intrinsic difficulty in finding a balance between complexity, typical of science driven activities, and straightforwardness, typical of business-driven activities, has also substantially contributed to increase the gap between theories and applications.

Simulations-driven approaches are ubiquitous nowadays. Examples of applications in science and engineering are numerous in domains like physics, biology, chemistry, civil engineering, mechanical engineering, environmental science. Adoption of numerical analyses to solve multiphysical processes is also a vital part of subsurface geoscience. For all these fields of applications, in recent years, artificial intelligence and more specifically deep learning advancements have resulted in remarkable accomplishments.

Embracing these new methodologies is crucial for advancing current practices of the energy industry into more sophisticated and efficient solutions. It is essential for future simulation systems to integrate both classical numerical techniques and AI methods. Moreover, AI introduces stimulating new opportunities in areas that have been difficult for traditional numerical methods, such as handling complex distributions and uncertainty in simulations. These areas are often the “black hole” where the above quoted balance between complexity and straightforwardness gets loss, widen the divide between theories and applications.

This keynote lecture will showcase some examples from CCS and discuss how the energy transition also represents a shift in the mindset of geoscientists and engineers.

Geologic storage of carbon in serpentinized ultramafics: advances and setbacks

Pouyan Asem[1], Bojan Guzina[1], Joseph Labuz[1], Juerg Matter[2], John Rudnicki[3], Vaughan Voller[1], Emmanuel Detournay[1]

[1]Department of Civil, Environmental, and Geo- Engineering, University of Minnesota, MN 55455, USA; [2] School of Ocean and Earth Science, University of Southampton, SO14 3ZH, UK; [3]Department of Civil and Environmental Engineering, Northwestern University, IL 60208, USA

Keywords: Infiltration; Diffusion; Geochemical-hydromechanical processes

1. Introduction

Storage of anthropogenic carbon dioxide as thermodynamically stable carbonate minerals [1] or by carbonate alkalinity production has gained interest in recent years. In short, the process consists of injection of low pH, carbon-bearing fluids in ultramafic formations. As the matrix of most ultramafics has undergone serpentinization to various degrees, with nanodarcy permeability and low reactive surface area, fluid access to reactive sites and evolution of fluid composition allowing for mineralization or alkalinity production are the rate limiting processes. Therefore, the fractures that serve as fluid pathways are also credited for most of the evolution in water chemical composition.

As carbon-bearing fluids interact with fracture walls, their chemical composition evolves to Type I waters that are characterized by their Mg-HCO_3^{1-} signature. This fluid continues to react with fracture walls or possibly infiltrates into cavities residing in the porous matrix of a polymineralic serpentinized rock, characterized by poromechanical and geochemical signatures (Fig. 1) and eventually evolve into Type II, Ca-OH^{1-} waters. The infiltration stage will create an interconnected fluid phase allowing for diffusion of chemical species within the matrix and between the matrix and fracture network. These hydromechanical-geochemical processes constitute a feedback loop and are coupled [2], with an increase concentration of alkaline earth metals and carbonate alkalinity. The combination of these two factors will solubilize CO_2 and under ideal conditions result in precipitation of carbonate or hydrated carbonate minerals, as observed in ultramafic formations around the world. In this paper, we provide an overview of work that aims to understand parameters that will lead to, or limit, carbon storage in ultramafic rocks.

2. Methodology

The experimental framework consists of intact specimens of serpentinized harzburgite interacting, under closed conditions, with a fluid based on Type I waters. The specimens are instrumented with strain gages to monitor volumetric changes if and when mineralization takes place. Frequent water sampling affords tracking chemical composition, carbonate alkalinity, and fluid pH. Analysis of the rock itself using wavelength dispersive spectroscopy (WDS) allows for determining mineral chemical compositions and solid solutions in evolution of fluid composition. Analysis of fluid chemical composition using geochemical codes provides an evolution of saturation indices with respect to carbonate and phyllosilicate minerals.

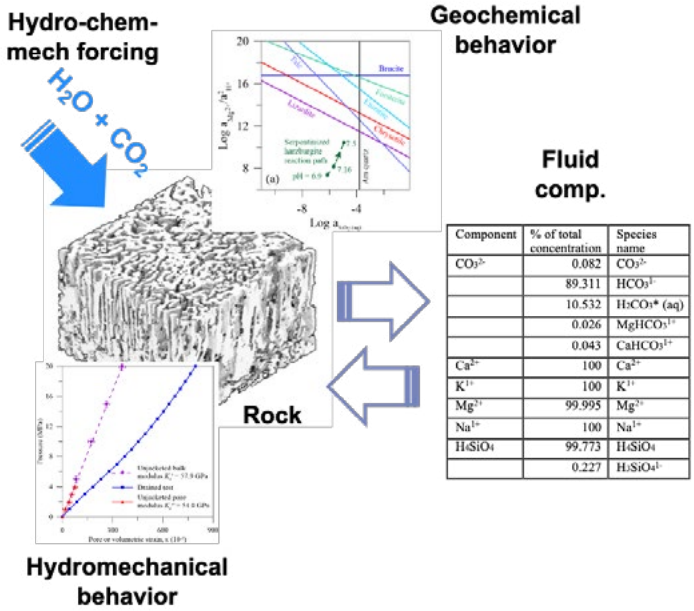

Fig. 1: Approach to understanding hydromechanical-geochemical couplings in serpentinized rock.

3. Main results

Experiments on interactions of intact matrix and the reactive fluid demonstrated (i) pH increased from 5.9 to 7.5 over 31 weeks; (ii) carbonate alkalinity remained constant pointing to the ability of the rock to maintain pH > pKa1 of the carbonate system and to solubilize CO_2; (iii) dissolution was incongruent with respect to Mg and Si, favoring Si release at pH > 6; (iv) increased reactive surface area creates improved dissolution and facilitated carbonate alkalinity production; and (v) aqueous phase was undersaturated with respect to carbonate and hydrous minerals due to low reactive surface area of the matrix caused by precursor serpentinization reactions.

4. Conclusions

While much has been learned in recent years about the hydromechanical-geochemical couplings in serpentinized rocks, critical aspects of their behavior remain unknown. A thorough understanding of these processes is needed before the feasibility of carbon storage by mineralization can be assessed. What is clear from the results presented is that the rate limiting parameter is the low reactive surface area associated with the matrix. The existence of fractures will increase the reactive surface area and reaction rates, which can facilitate faster carbonate and total alkalinity production. Therefore, the focus will be on the creation of new fractures and development of engineered mechanisms (*e.g.* fluid compositions) that prevent passivation effects of the fracture walls and hence allow for sustainable geological host formations for storage of CO_2.

5. References

[1] Kelemen, P.B. and J. Matter. "In situ carbonation of peridotite for CO_2 storage." Proceedings of the National Academy of Sciences of the United States of America, 2008, 105(45).

[2] Asem, P., J. Matter, J.T. Mitchell, C. Neil and J.F. Labuz. "Geochemical-hydromechanical couplings during water-serpentinized harzburgite interactions at 20°C and 30 bars." Chemical Geology, 2024, 670: 122413.

Introducing a novel scale for studying geological CO_2 storage

Eleni Stavropoulou[1], Dario Sciandra[1], Lyesse Laloui[1]

[1]*Ecole Polytechnique Fédérale de Lausanne (EPFL), Laboratory for Soil Mechanics (LMS), EPFL-ENAC-LMS, Station 18, CH-1015 Lausanne, Switzerland*
E-mail: eleni.stavropoulou@epfl.ch, dario.sciandra@epfl.ch, lyesse.laloui@epfl.ch

Keywords: geological CO_2 storage, physical model, hydromechanical modelling

1. Introduction

Geological CO_2 storage (GCS) is an efficient way to store large volumes of captured CO_2 to meet the stringent climate goals. GCS involves a broad range of coupled THM phenomena that manifest differently depending on the spatial and temporal scales and geomaterials. Current efforts for representative modelling are hindered by the sparse data from field-scale measurements, limited spatial resolution from well-logging techniques and the relevance of representative elementary volumes and time scales in lab testing [1]. This work aims to contribute to upscaling of GCS by introducing a novel intermediate scale of observation that will serve as a missing link between the lab and the field.

2. Methodology

A metre-scale physical model of the entire reservoir/caprock system has been designed to simulate field conditions for CO_2 storage (Fig. 1a). This original testbed aims to enable high resolution measurements while taking into account spatial variability and distribution. The hydromechanical setup consists of a cylindrical cell in which a synthetic reservoir layer (cemented sand) at the bottom and a synthetic caprock layer (recompacted shale) above will be compacted and saturated with water at stress and pore pressure levels representative of 800 m depth (180 bar and 80 bar, respectively), before CO_2 injection in the reservoir layer.

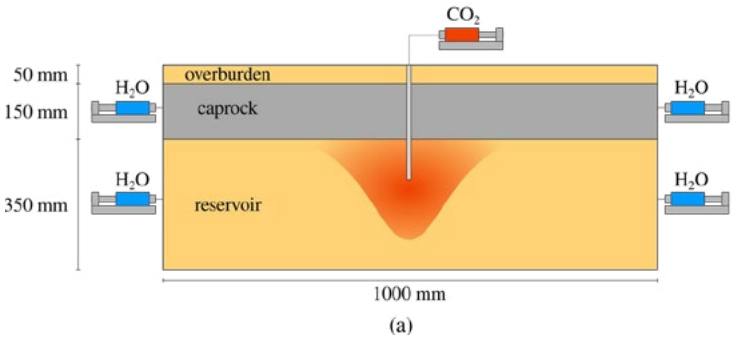

(a)

	recompacted shale	cemented sand
porosity	16 %	28 %
permeability	$1.3 \cdot 10^{-19}$ m^2	$2.1 \cdot 10^{-13}$ m^2

(b)

Fig. 1: (a) Physical model for GCS, (b) hydraulic properties of the recompacted synthetic geomaterials

3. Results

The hydromechanical behaviour of the used geomaterials (Fig. 1b) has been studied in the lab and the main hydraulic properties, such as porosity, water permeability and CO_2 entry pressure, have been acquired. High porosity and permeability were measured for

the reservoir material (see Fig. 1b), with values relevant to natural reservoir materials such as sandstones [2]. In the case of the caprock material, of particular importance is the sealing capacity. The preliminary results showed low permeability values (in the order of 10^{-19} m²) and high CO_2 breakthrough pressure (1-2 MPa), comparable to those of a natural caprock [3].

Based on the acquired experimental results, the metre-scale campaign has been designed with numerical simulations. Different resaturation and CO_2 injection strategies (e.g. injection pressure and duration) were evaluated with the aid of a fully coupled FE hydromechanical model, aiming to reproduce boundary conditions relevant to the field, and optimise the duration of the campaign. Water saturation was performed from bottom to top (Fig. 2a) and the results suggested an optimised 2 month duration for compaction and water saturation of the entire system (reservoir and caprock) before CO_2 injection. Simulations of gaseous CO_2 injection at different constant rates revealed that at this scale CO_2 propagation is dominated by diffusion phenomena, thus injection under constant pressure (Fig. 2b) shall be preferred to study multi-phase flow as expected in the field.

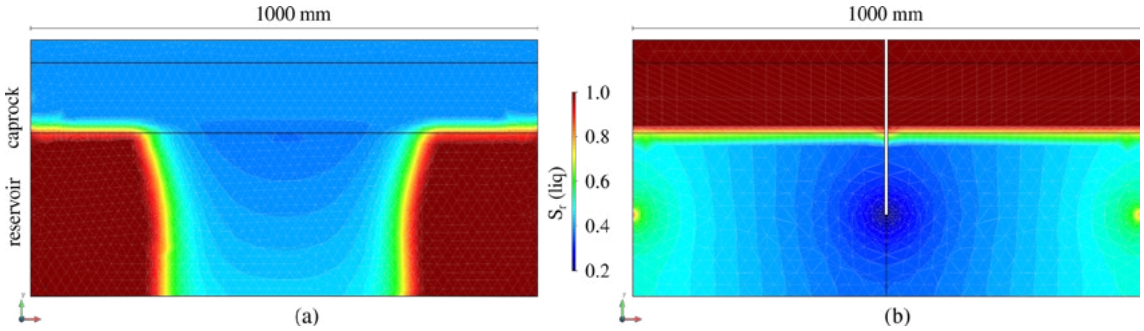

Fig. 2: Liquid saturation after (a) 26h of water resaturation, (b) 24h of CO_2 injection at constant pressure

4. Conclusions

An original metre-scale physical model has been designed to study the coupled processes in GCS. The setup considers the entire reservoir/caprock system and targets CO_2 injection under conditions similar to the field. Lab-scale results showed that the hydromechanical properties of the used geomaterials are comparable to natural caprock and reservoir materials. Numerical modelling of the metre-scale campaign suggested CO_2 injection under constant pressure to priviledge advection-dominated CO_2 flow.

5. References

[1] Ma, X., Hertrich, M., Amann, et. al. Multi-disciplinary characterizations of the BedrettoLab-a new underground geoscience research facility. Solid Earth, 13(2), 301-322, 2022.

[2] Delle Piane, C., & Sarout, J. Effects of water and supercritical CO2 on the mechanical and elastic properties of Berea sandstone. International Journal of Greenhouse Gas Control, 55, 209-220, 2016.

[3] Stavropoulou, E., & Laloui, L. Evaluating CO2 breakthrough in a shaly caprock material: a multi-scale experimental approach. Scientific Reports, 12(1), 10706, 2022.

Hydro-mechanical modelling of swelling in clayey host rocks for subsurface energy applications

Michelangelo Cardin[1], Alessio Ferrari[1,2]

[1] *Engineering Department, University of Palermo, Palermo, Italy*
[2] *EPFL, Ecole Polytechnique Fédérale de Lausanne, Lausanne, Switzerland*
E-mail: michelangelo.cardin@unipa.it, alessio.ferrari@epfl.ch

Keywords: Double-structured porosity, Swelling behaviour, Host rocks

1. Introduction

The increasing demand for sustainable energy solutions has led to a growing interest in subsurface storage technologies, including nuclear waste disposal, CO2 and hydrogen H2 storage, and deep geothermal energy systems. These applications often involve deep clay formations, commonly referred to as host rocks, which are selected for their low permeability and hydro-mechanical properties. Among the various host rocks studied in this context, Opalinus Clay Shale (OPA) is a well-characterized claystone, primarily associated with nuclear waste disposal. Its mechanical and hydraulic features make it a relevant case study for understanding the hydro-mechanical behaviour of compacted clay-rich formations under subsurface conditions. Experimental observations [1–2] suggest that intact OPA is characterized by a single dominant porosity, associated with the voids between clay particles (microporosity), with characteristic sizes of approximately 10–30 nm. However, when subjected to loading/unloading or imbibition/drying cycles, an additional macroporosity may develop along bedding planes, with larger pores in the range of tens to hundreds of micrometers. These complex porosity interactions are not unique to OPA but are observed in several host rocks, especially under THMC conditions. This study presents a double-structured hydro-mechanical model based on the Barcelona Expansive Model (BExM) [3], adapted to capture the porosity evolution in clayey host rocks. The model is validated against experimental tests, demonstrating its capability to reproduce the stress-dependent swelling behaviour observed in laboratory conditions.

2. Model

To accurately describe the swelling behaviour of clayey host rocks, a double-structured hydro-mechanical model has been developed. The constitutive relationships are formulated using a separate stress variable approach, distinguishing the effects of net stress and suction. Regarding the elastic behaviour, in this model it is attributed exclusively to the microstructure, meaning that the evolution of induced macroporosity is treated as a purely plastic deformation. For the plastic response, the model follows the classical framework of the BExM model with three main yield surfaces defined in the p – s plane: (i) the Suction Decrease (SD), (ii) the Suction Increase (SI) and (iii) the Loading Collapse (LC) yield surfaces. The model parameters were calibrated using experimental results from oedometer swelling tests conducted on specimens of Opalinus Clay Shale,

considered here as a representative clayey host rock. Two of these tests, in which resaturation was performed under constant load, are shown in Fig. 1, along with the corresponding model predictions.

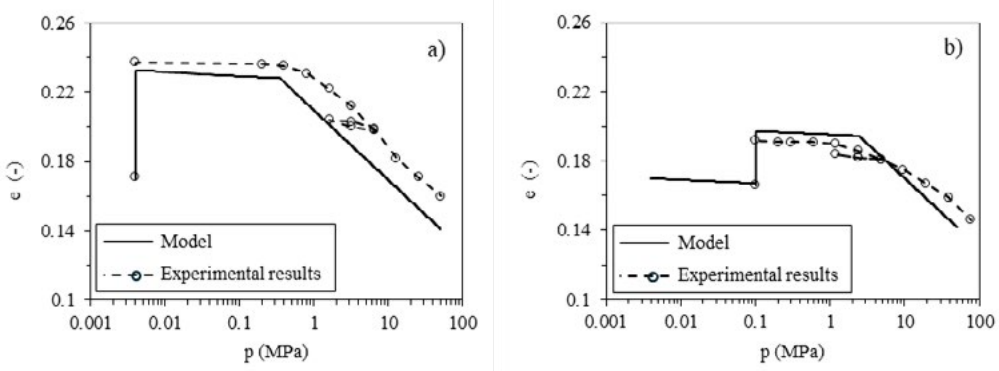

Fig. 1: Oedometric tests with (a) a swelling phase under a constant stress of 0.004 MPa and (b) 0.1 MPa.

From Fig. 1, it can be observed that swelling deformations are significantly influenced by the applied load, leading to a constitutive response that is highly dependent on the stress path. Moreover, the amount of swelling allowed during the resaturation phase has a direct impact on the preconsolidation stress during the subsequent reloading phase. In particular, greater swelling leads to a more pronounced reduction in preconsolidation stress, which may be attributed to the development of induced macroporosity along the bedding planes. These aspects, the stress-path dependency of swelling behaviour and the evolution of yield stress due to plastic swelling, are successfully captured by the elasto-plastic constitutive model developed in this study.

3. Conclusion

This study investigates the swelling behaviour of clayey host rocks through a double-structured hydro-mechanical model based on the BExM. By providing a framework capable of predicting stress-dependent swelling in deep clayey formations, the proposed model contributes to a better understanding of the hydro-mechanical response of these geomaterials. These insights are valuable for applications such as underground energy storage and waste disposal, where the behaviour of expansive clay formations is a key factor in system performance. Ongoing work is focused on enhancing this version of the model to account for the influence of temperature and aqueous solution composition, thus developing a THMC model.

References

[1] E. Crisci, Study of hydro-mechanical behaviour of clay shales under controlled environmental conditions, PhD Thesis, Faculté de l'environnement naturel, architectural et construit, EPFL, Lausanne (2019).

[2] A. Minardi, Experimental investigation of the hydro-mechanical behaviour of argillaceous rocks, PhD Thesis, Faculté de l'environnement naturel, architectural et construit, EPFL, Lausanne (2018).

[3] E.E. Alonso, J. Vaunat, A. Gens, Modelling the mechanical behaviour of expansive clays, Engineering Geology, 54, 173–183 (1999).

Influence of carbon dioxide on micro-cracking: insights from nanoscale investigation

Fanyu Wu[1], Manman Hu[1, *]

[1] *Department of Civil Engineering, The University of Hong Kong, Hong Kong, Hong Kong SAR*
E-mail: fywu@connect.hku.hk; mmhu@hku.hk

Keywords: Subcritical cracking; CO_2 environment; Fluid-crack interaction; Molecular dynamics.

1. Introduction

Geological carbon storage in porous reservoirs, as a promising large-scale carbon reduction technique, has been playing a crucial role in the Climate Change mitigation efforts. Carbonate minerals (e.g., calcite) are ubiquitously presented in candidate formations suitable for geological Carbon Capture and Storage (CCS). The dynamic process of chemically induced alteration on carbonate-rich reservoirs due to the injection of supercritical CO_2 holds paramount importance for achieving an economic injectivity, an overall structural integrity, as well as the long-term safety of the subsurface process. How the carbonate rock undergoes chemical deterioration in the presence of CO_2 has its roots in how microcracks interact with the reactive environment, which remains largely unknown. In this study [1], we employ a powerful tool of reactive force field (ReaxFF) molecular dynamics (MD) simulation, investigating into the impact of representative CO_2 environments on Mode I tensile crack propagation in calcite at micro-scale. Our simulation results provide new insights on the process of subcritical calcite cracking induced by a reactive environment via carbon dioxide injection and hence sheds light also on the future integration of the "Utilization" aspect into CCS.

2. Methodology

The ReaxFF MD simulations were performed using the large atomic/molecular massively parallel simulator (LAMMPS) [2]. Calcite samples with dimensions of 100 Å × 12 Å × 196 Å were created. Mode I loading was applied perpendicular to the calcite (104) cleavage plane. A representative CO_2 condition was examined to illustrate the influence of reactive environments on crack propagation in calcite. In the base case, the pre-notched calcite sample was placed in a vacuum condition. In the second scenario, a "CO_2-H_2O Mixture" bath with dimensions of 40 Å × 12 Å × 196 Å was created by evenly mixing CO_2 and H_2O molecules, with each component occupying half of the total volume of the reservoir. The reservoir was connected to the calcite sample under the same mechanical loading condition. The density of liquid-like CO_2 was set to 0.6 g/cm^3, simulating a supercritical state. During the process of crack propagation, fluid molecules from the reservoir diffused into the calcite matrix from the crack lips, interacting with the

stressed solid. The fluid reservoir was enclosed by reflective walls to prevent molecules from escaping and to maintain the initial density and volume.

3. Main Results

With a constant strain rate, the stress of calcite increases linearly with the strain in both scenarios. Calcite loaded in a vacuum environment achieves a higher yield stress of 5.66 GPa. In comparison, the yield stress of calcite in the CO_2-H_2O mixture significantly decreases to 4.98 GPa, indicating a pronounced chemo-mechanical weakening effect due to the presence of both H_2O and CO_2 molecules in the subcritical regime. Furthermore, calcite samples experience catastrophic failure earlier in CO_2-H_2O condition at a strain of 6.22 %, while the failure in the vacuum condition occurs at a strain of 7.45 %. This observation supports the argument that the combined action of chemical and mechanical loads accelerates calcite failure more than the pure mechanical load setting. Our simulation results also indicate that the calcite loaded in the vacuum environment exhibits a fracture toughness of 0.75 $MPa \cdot m^{1/2}$. However, in a mixed CO_2-H_2O environment, the fracture toughness of calcite decreases to 0.66 $MPa \cdot m^{1/2}$, which is 12 % lower than the reference case. Additionally, we observe a slow crack propagation characterizing a subcritical growth phase, followed by a fracturing phase where the crack velocity surges by orders of magnitude. In the subcritical-growth regime, the crack tip advances slowly although the stress intensity factor is below the critical value. In the presence of a mixed CO_2-H_2O environment, this critical value is reached earlier than in the vacuum case due to the significant reduction in fracture toughness of calcite caused by the crack-fluid interaction. It is noted that in the subcritical-growth regime, the calcite sample in the CO_2-H_2O condition propagates faster with a sharper shape than the vacuum case.

4. Conclusion

This study provides an atomistic-scale investigation into the influence of environmental conditions on the subcritical crack propagation in calcite, with a focus on the scenarios at the near-wellbore region in CO_2 geological storage. Utilizing ReaxFF MD simulations, we examined the complex interactions between Mode I crack propagation in calcite and its surrounding chemical environment. The main findings are listed as follows: (a) Calcite sample exposed to CO_2-H_2O mixture exhibits a significant reduction in the yield stress with a lower accumulated strain at yield. (b) In mixed CO_2-H_2O environment, a lower fracture toughness of calcite is obtained at 0.66 $MPa \cdot m^{1/2}$, which is 12 % lower than that in the vacuum condition. (c) Analysis of the crack length and tip radius propagation suggests that the pre-existing crack extends faster and with a smaller radius of curvature in the CO_2-H_2O environments than in vacuum.

5. References

[1] Wu, F., and Hu, M. Influence of carbon dioxide on micro-cracking in calcite: An atomistic scale investigation. Journal of Geophysical Research: Solid Earth, 130, e2024JB030896. (2025).
[2] Plimpton, S. Fast parallel algorithms for short-range molecular dynamics. Journal of Computational Physics, 117(1), 1–19. (1995).

Hydro-Mechanical Coupled Simulation for Assessing Deep Seismic Risk in Geological CO_2 Storage

Kenji Furui[1], Aya Katsuta[1], Satomi Kamada[1], Hung Vo Thanh[2]

[1] *Department of Earth Sciences, Resources and Environmental Engineering, Waseda University, Tokyo, Japan*
E-mail: furui@waseda.jp, aya.katsuta867@moegi.waseda.jp, s.kamada@akane.waseda.jp
[2] *Waseda Research Institute for Science and Engineering, Waseda University, Tokyo, Japan*
E-mail: hungvothanh@aoni.waseda.jp

Keywords: finite element analysis, joint element, induced seismicity, geological CO_2 storage, hydro-mechanical process

1. Introduction

A major challenge in Carbon Capture and Storage (CCS) is assessing the risk of induced seismicity from underground CO_2 storage since, currently, there is no established technology that can accurately predict earthquakes. This study simulates geological CO_2 storage using a hydro-mechanical model to assess fault stability and propose a structured approach to injection-induced seismic risk assessment.

2. Methodology

This study presents a three-dimensional poroelastic finite element model with joint elements [1] to calculate fault slip displacement. CO_2 injection into a reservoir is simulated using a commercial flow simulator, providing saturation and pore pressure distributions as inputs for stress analysis (i.e., one-way coupling). Pre-existing strain distribution in formations is established based on initial stress and pore pressure gradients. Fault stability is assessed, and mechanical parameters are adjusted if instability occurs. After force equilibrium is achieved, pore pressure changes from CO_2 injection are applied, and resulting stress variations, slip displacement, and seismic moment are calculated for seismic risk assessment.

3. Main Results

Assuming that CO_2 is injected into a relatively shallow aquifer, a geological model is constructed with layers representing the surface, seal, reservoir, and deep basement rock. The fault plane is modeled as extending from the surface layer to the basement rock and is set to a critically stressed state. Additionally, this study assumes no hydraulic connectivity between the reservoir and the fault. When the pore pressure in the reservoir was increased by 1 MPa, calculations of Coulomb stress change and seismic moment upon fault failure indicated that larger seismic moments occurred in the upper part of the basement rock rather than at the reservoir depth (Fig. 1). This finding aligns with induced seismic characteristics observed in some field studies [2, 3, 4].

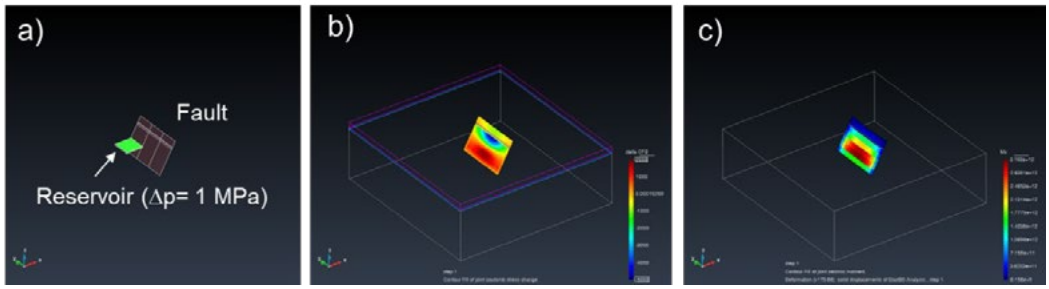

Fig. 1: a) Location of the fault and reservoir, b) Coulomb stress change, and c) seismic moment intensity for assessing seismic risk of the known fault.

In some cases [3, 4], earthquakes have been reported on previously unidentified faults. This study assessed the seismic risk of such faults using elastic strain energy density and Formation Robustness Index (FRI). The simulation results showed that regions with negative FRI change and high elastic strain energy density near the CO_2 injection area had a higher likelihood of induced-seismic activity.

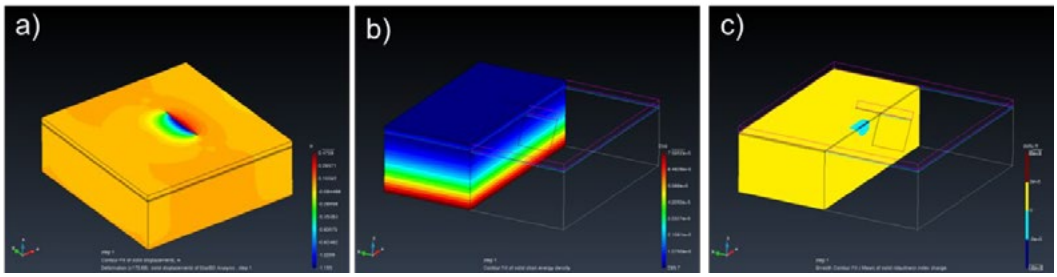

Fig. 2: a) Vertical displacement, b) Elastic strain energy density, and c) formation robustness index for assessing seismic risk of unmapped faults.

4. Conclusion

The study highlights that rock strength variations, initial stress, and pore pressure significantly influence induced-seismicity risk during CO_2 injection. Observed events in unidentified faults suggest the need for formation stability indicators to assess seismic risks beyond known faults. These insights help engineers define monitoring requirements and improve CCS project safety.

5. References

[1] Beer, G.,'An Isoparametric Joint/Interface Element For Finite Element Analysis', International Journal for Numerical Methods in Engineering, Vol 21, 585-600 (1985).
[2] Weingarten, M., B., 'On the Interaction Between Fluids and Earthquakes in Both Natural and Induced Seismicity', Ph.D dissertation, University of Colorado (2015).
[3] Gaite, B., Ugalde, A., Villasenor, A., and Blanch, E., 'Improving the location of induced earthquakes associated with an underground gas storage in the Gulf of Valencia (Spain)', Physics of the Earth and Planetary Interiors, Vol 254, 46-59 (2016).
[4] Zhou, P., Yang, H., Wang, B., and Zhuang, J., 'Seismological Investigations of Induced Earthquakes Near the Hutubi Underground Gas Storage Facility', Journal of Geophysical Research: Solid Earth, Vol 124, 8753-8770 (2019).

Poro-elasto-visco-plastic behaviour of claystone for deep radioactive waste disposal

Junfeng Ren[1], Philipp Braun[1], Siavash Ghabezloo[1], Carlos Plúa[2], Minh-Ngoc Vu[2]

[1] *Laboratoire Navier, Champs-sur-Marne, France*
E-mail: philipp.braun@enpc.fr
[2] *Andra, Châtenay-Malabry, France*

Keywords: claystone; hydro-mechanical coupling; triaxial testing; time-dependency

1. Introduction

The Callovo-Oxfordian (COx) claystone, serving as the host rock for the potential deep geological repository for the disposal of the most highly radioactive waste in France, is expected to experience thermal loading up to 90 °C due to the decay heat of radioactive nuclides [1]. This study investigates the transversely isotropic poro-elasto-visco-plastic properties of COx claystone after thermal loading. In this study, the rock behavior is characterized experimentally and modelled through a combination of constitutive features. The model is readily implemented in a finite element simulation framework allowing for parameter calibration and site-scale simulation.

2. Methodology

Samples of COx claystone, previously subjected to in-situ heating tests at the Andra Underground Research Laboratory in Meuse / Haute-Marne, were extracted for laboratory investigation. These samples were resaturated under stress conditions close to in-situ state, and deviatoric stress was applied either parallel or perpendicular to the bedding planes, following different stress paths until failure. Additionally, an isotropic compression test was conducted. The drained and undrained behaviors of the samples were investigated by pseudo-undrained rapid loading and drainage phases. Drained elastic and plastic strains were decomposed through mechanical loading cycles, allowing the determination of a set of drained elastic parameters and identifying the plasticity onset. The constitutive law was implemented in the finite element solver FEniCSx [2] using the MFront tool [3].

3. Main Results and Conclusions

The measured failure characteristics of the samples were similar to non-heated samples, and different stress paths showed no significant effect of the temperature on their critical state. The experimental results were used to develop and calibrate a poro-elasto-visco-plastic constitutive law. Asymmetric Cam Clay (ACC) model was used, coupled with a non-uniform scaling method to account for anisotropic plasticity, and the overstress model was incorporated for visco-plastic behavior. This numerical simulation tool can be used to analyse the thermo-hydromechanical response of the COx at various scales.

Finally, 2D and 3D simulations of tested samples under various loading conditions were conducted to successfully calibrate constitutive parameters.

4. References

[1] Andra, 'Evaluation of the feasibility of a geological repository in an argillaceous formation', Report Dossier 2005 Argile (2005).

[2] Baratta, I., A., Dean, J., P., Dokken, J., S., Habera, M., Hale, J., S., Richardson, C., N., Rognes, M., E., Scroggs, M., W., Sime, N., Wells, G., N., 'DOLFINx: The next generation FEniCS problem solving environment', doi.org/10.5281/zenodo.10447666 (2023).

[3] Helfer, T., Michel, B., Proix, J.,-M., Salvo, M., Sercombe, J., Casella, M., 'Introducing the open-source mfront code generator: Application to mechanical behaviours and material knowledge management within the PLEIADES fuel element modelling platform', Computers & Mathematics with Applications, 70:994–1023 (2015).

Sustainable exploitation of mafic rock quarry waste for carbon sequestration

Ioannis Ioannou[1], Theodora Kyratsi[2], Ioannis Rigopoulos[1], Loucas Kyriakou[1]

[1] *Department of Civil and Environmental Engineering, University of Cyprus, Nicosia, Cyprus*
E-mail: ioannou.ioannis.1@ucy.ac.cy, rigopoul@ucy.ac.cy, kyriakou.loucas@ucy.ac.cy
[2] *Department of Mechanical and Manufacturing Engineering, University of Cyprus, Nicosia, Cyprus*
E-mail: kyratsi.theodora@ucy.ac.cy

Keywords: CO_2 storage, Mineral carbonation, Renders

1. Introduction

Mineral carbonation is a carbon capture and storage (CCS) technology that was initially proposed by Seifritz [1]. This includes the reaction of CO_2 with rocks containing Ca- and/or Mg-silicate minerals to form stable carbonate minerals, such as calcite ($CaCO_3$), dolomite ($CaMg(CO_3)_2$) and magnesite ($MgCO_3$).

Ultramafic and mafic lithologies are amongst the most promising rocks for the mineralization of CO_2. Such lithologies are abundant globally and respective quarries produce aggregates for the construction industry. These quarries, however, also produce considerable fine waste material that may be used as feedstock for mineral carbonation.

This paper discusses the potential of using waste material (quarry fines) from mafic rock quarries for the safe storage of CO_2. This is achieved through the addition of such a waste material in lime-based composite building materials that may be used to sequester CO_2 directly from the atmosphere during their lifetime.

2. Methodology

A dolerite quarry waste sampled from the outskirts of the Troodos ophiolite complex in Cyprus, which is one of the most well-preserved ophiolite complexes in the world, was used in this study. The sample was first subjected to XRD analysis to determine its mineralogical composition. It was then ball-milled in wet conditions to reduce its size to the nanoscale and thus enhance its reactivity with CO_2. The ball-milled material (NW) was used at either 5% or 15% w/w in partial replacement to CL80-S hydrated lime binder to produce renders in the laboratory. Unmilled waste material (UMW) from the same quarry was also used for comparison purposes. The renders were designed with a constant binder/aggregate ratio (1/3) and workability (165±5 mm). Their physico-mechanical properties in the hardened state were determined after 7, 28 and 90 days of curing.

3. Results

The mineralogical composition of the dolerite quarry waste sample included augite, anorthite, chlorite, actinolite, epidote, albite, quartz, calcite and magnetite. Among these minerals, augite and anorthite are rich in the divalent cations Ca^{2+}, Mg^{2+} and Fe^{2+}, which are essential for mineral carbonation [2]. Ball milling did not alter the mineralogical composition of the sample; nevertheless, XRD demonstrated a structural disordering of the constituent silicate minerals, which is important for the enhancement of carbonation reactions [3].

The results of the experiments for the determination of the physical properties of the hardened end-products clearly showed an enhancement of the carbonation process in the composites with the waste material, compared to the reference composite. This was quantified using the ratio of calcium hydroxide ($Ca(OH)_2$) to calcite ($CaCO_3$), estimated via thermal analyses.

Besides the enhancement of the carbonation reaction kinetics, the addition of the ball-milled dolerite quarry waste material to the lime composites also led to a denser and more homogeneous microstructure. This was confirmed through SEM observations.

Regarding the mechanical properties, an enhancement of both the compressive strength and dynamic modulus of elasticity was observed in the composites with the ball-milled dolerite quarry waste. This was attributed to a filler effect and the enhancement of carbonation reactions. On the other hand, a generally inferior mechanical performance was observed in the composites with the unmilled dolerite.

4. Conclusions

The results revealed that the mafic rock quarry waste may be successfully used by the construction industry as additive, in replacement to the binder, to produce environmentally friendly composite materials. The enhancement of the carbonation reactions in the latter could contribute to the sequestration of CO_2 at ambient conditions, as well as to the development of building materials with improved engineering properties. It is important to note that mafic rocks are abundant worldwide. In addition, it should be underlined that similar applications could be proposed for quarry fines generated from ultramafic rock quarries, which also show global abundance and contain higher contents of Mg-silicate minerals. Hence, the proposed approach could have a considerable impact on the decarbonization of the construction sector, along with a great positive economic and environmental impact on the quarrying and building industries worldwide.

5. References

[1] Seifritz, W., 'CO_2 disposal by means of silicates', Nature, 345, 486-490 (1990).
[2] Lackner, K.S., Wendt, C.H., Butt, D.P., Joyce Jr., E.L., Sharp, D.H., 'Carbon dioxide disposal in carbonate minerals', Energy, 20, 1153-1170 (1995).
[3] Rigopoulos, I., Petallidou, K.C., Vasiliades, M.A., Delimitis, A., Ioannou, I., Efstathiou, A.M., Kyratsi, T., 'On the potential use of quarry waste material for CO_2 sequestration', Journal of CO_2 Utilization, 16, 361-370 (2016).

Thermo-Hydro-Mechanical modeling for CCS geomechanical applications: a zero-thickness approach

Adrià Pérez[1], José Alvarellos[1], Enric Ibañez[1], José María Segura[1], Daniel Garolera[2], Lucía Barandiaran[2] and Ignacio Carol[3]

[1] *Repsol Technology Lab, Madrid, Spain*
E-mail: adria.perez@repsol.com, jose.alvarellos@repsol.com, enric.ibanez@repsol.com, josemaria.segura@repsol.com
[2] *DRACSYS, S.L., Barcelona, Spain*
E-mail: daniel.garolera@dracsys.com, lucia.barandiaran@dracsys.com
[3] *Department of Civil and Environmental Engineering, Technical University of Catalonia, Barcelona, Spain*
E-mail: ignacio.carol@upc.edu

Keywords: CCS, multiphase flow, THM Coupling, Zero-thickness interfaces, Joule-Thomson Effect

1. Introduction

As the energy sector intensifies efforts to reduce greenhouse gas emissions, carbon capture and storage and, particularly, the injection of CO_2 into subsurface geological formations, has emerged as a fundamental component of decarbonization strategies.

However, accurately modeling CO_2 behavior in the subsurface requires more than conventional geomechanical modeling techniques. The injection process involves intricate multiphase flow dynamics, thermal variations, geochemical reactions, and all its potential geomechanical impacts. These factors demand the use of specialized numerical models capable of capturing the coupled processes that govern CO_2 injection, migration and long-term storage integrity.

Thus, this article presents a thermo-hydro-mechanical fully coupled numerical model with CO_2 dissolution and Joule-Thomson effects, in a context of a dual-porosity system, where fractures (natural and induced) are explicitly represented by means of zero-thickness interface elements.

2. Methodology

A fully coupled thermo-hydro-mechanical (THM) multiphase numerical model has been developed to simulate both continuum and zero-thickness interface elements. The model captures the behaviour of supercritical CO_2 flow within a deformable porous medium, including the presence of discontinuities, under non-isothermal conditions.

The model incorporates mechanical deformation, thermal processes (advective and conductive heat transport), and multiphase flow in porous media. It accounts for key physical phenomena such as the Joule–Thomson effect, CO_2 dissolution, and fracture mechanics. The governing equations for the deformable porous medium are based on the formulations proposed by [1,2]. Additionally, the thermodynamic behaviour of CO_2 is described using the Peng–Robinson equation of state [3].

The methodology is based on a dual-porosity approach that accounts for fluid flow within both the fracture network and the continuous pore matrix. To accurately represent fracture propagation —whether naturally or induced— zero-thickness interface elements are incorporated. These elements are governed by a mechanical constitutive law based in fracture mechanics and fracture energies [4].

3. Main results

The described model has been applied in multiple CO_2 injection studies, with a specific focus on 2D near-wellbore simulations. Figure 1 presents the results of a thermally induced fracture generated during the injection process, after 20 and 60 days of injection. As shown in the figure 1, a cooling effect is induced by the Joule-Thomson mechanism, which leads to the opening of the fracture in the direction of the maximum principal stress.

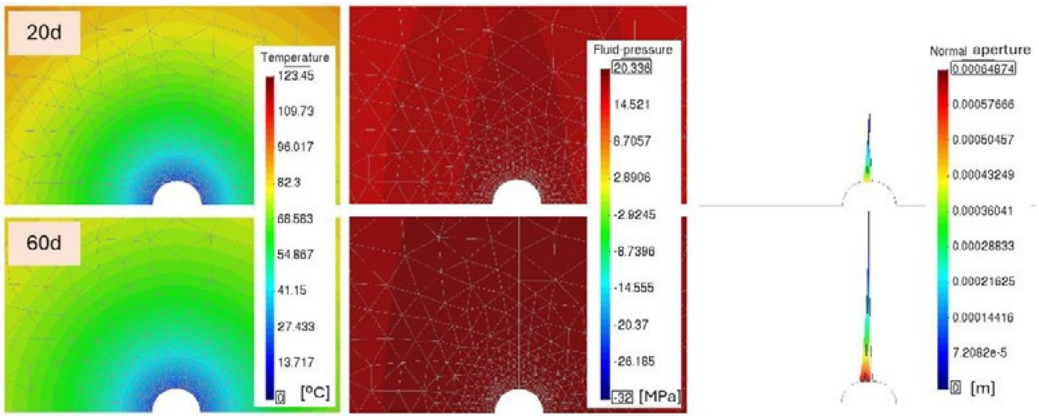

Fig. 1: Cooling effect and fracture aperture after 20 and 60 days of injection.

4. Conclusions

One of key strengths of the presented numerical model is the ability to detect the onset of thermal fractures and assess their potential impact on reservoir containment, caprock integrity, and nearby fault systems —which is critical for minimizing the risk of induced seismicity—, enhancing the safety and effectiveness of CCS operations.

This modeling approach supports strategic decision-making by improving well placement based on predicted fracture behavior in a discrete manner, tracking changes in injectivity over time, and simulating the temporal evolution of fractures. Overall, it is a powerful tool for optimizing injection strategies and ensuring long-term storage integrity.

5. References

[1] Lewis & Schrefler, The Finite Element Method in the Static and Dynamic Deformation and Consolidation in Porous Media, Wiley & Sons (1998).

[2] Li & Laloui (2016) 'Coupled multiphase thermo-hydro-mechanical analysis of supercritical CO2 injection: Benchmark for the In Salah surface uplift problem.' International Journal of Greenhouse Gas Control. Vol 51, 394-408 (2016)

[3] Peng & Robinson, 'A New Two-Constant Equation of State', Industrial & Engineering Chemistry Fundamentals, Vol 15 (1), 59-64 (1976)

[4] Carol, I., Prat, P. & Lopez, C., 'Normal/shear cracking model: application to discrete crack analysis'. Journal of engineering mechanics, Vol 123(8), 765-773 (1997)

Rock hydrothermal alteration and fluid composition controls fault frictional healing in the continental crust

Rodrigo Gomila[1], Wei Feng[1], Barbara Cantucci[2], Alessandra Sciarra[2], Giulio Di Toro[1,2]

[1] *Dipartimento di Geoscienze, Università degli Studi di Padova, Padua, Italy*
E-mail: r.gomilaolmosdeaguilera@unipd.it
[2] *Sezione Roma 1, Istituto Nazionale di Geofisica e Vulcanologia, Rome, Italy*

Keywords: Fluid-Rock Interaction; Fault Frictional Healing; Fluid Chemistry; Atacama Fault System; Seismogenic Fault

The process of fault frictional healing, which refers to a fault's capacity to restore its strength over time between seismic events, is a critical factor influencing the seismic cycle [1]. After a fault experiences rupture during an earthquake, this frictional healing enables the surrounding rocks to accumulate elastic energy, which will subsequently be released in the following earthquake.

It is widely accepted that fault frictional healing (or static friction) increases over time and is influenced by the specific rock type or mineralogy of the fault. Nevertheless, the majority of existing research on frictional healing has been conducted under conditions that do not accurately reproduce the environment found at seismogenic depths. In these deeper settings, deformation—whether resulting from natural processes or human activities—occurs in the presence of hot and pressurized hydrothermal fluids. These fluids significantly affect the strength and frictional characteristics of faults by promoting or inhibiting various chemical reactions [2].

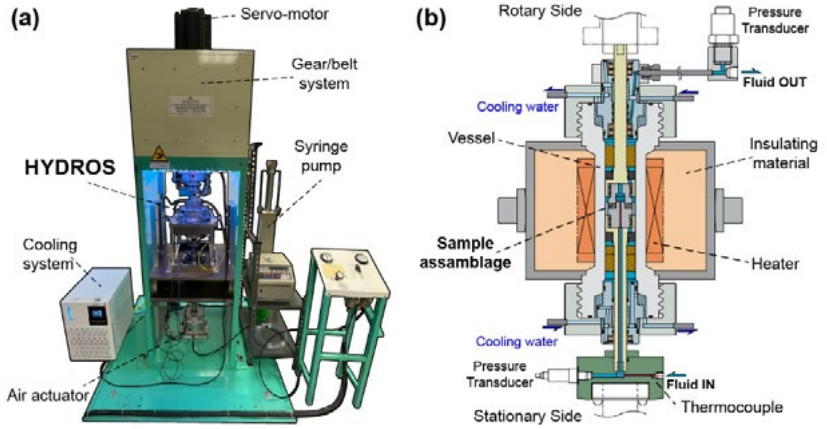

Fig. 1: Detailed schemes of the experimental set-up. (a) Rotary Shear Apparatus (ROSA). (b) the hydrothermal pressure vessel (HYDROS).

In this study, we present the findings derived from an innovative experimental setup (Fig. 1) that consists of a rotary shear apparatus (ROSA; Fig. 1a) and a specialized hydrothermal vessel (HYDROS; Fig. 1b). The integration of these two systems facilitates the simulation of the loading conditions and large slip displacements characteristic of natural faults, along with environmental parameters representative of

seismogenic depths, featuring hot and pressurized fluids. The natural case study pertains to an ancient seismogenic fault within the Atacama Fault System in Chile, comprised of altered rock types (specifically chlorite- and epidote-rich cataclasites) situated within a continental crystalline basement of non-altered granodiorite (Fig. 2a). Experimental results from week-long experiments on powdered samples reveal that, in the non-altered granodiorite, fault frictional healing does not increase over time as typically expected and observed in the cataclasites. Instead, granodiorite exhibits a decrease with time. However, initial fluid chemistry plays a fundamental role in the fault frictional healing response, showing a dramatic change in the non-altered rocks in the presence of equilibrated fluids with a different chemistry (Fig. 2b).

This decrease in fault frictional healing and how fluids change during the evolution of faults, can have significant implications for the recurrence intervals of earthquakes and magnitude (increasing and decreasing, respectively) and the dynamics of the seismic cycle for both natural and human-induced earthquakes.

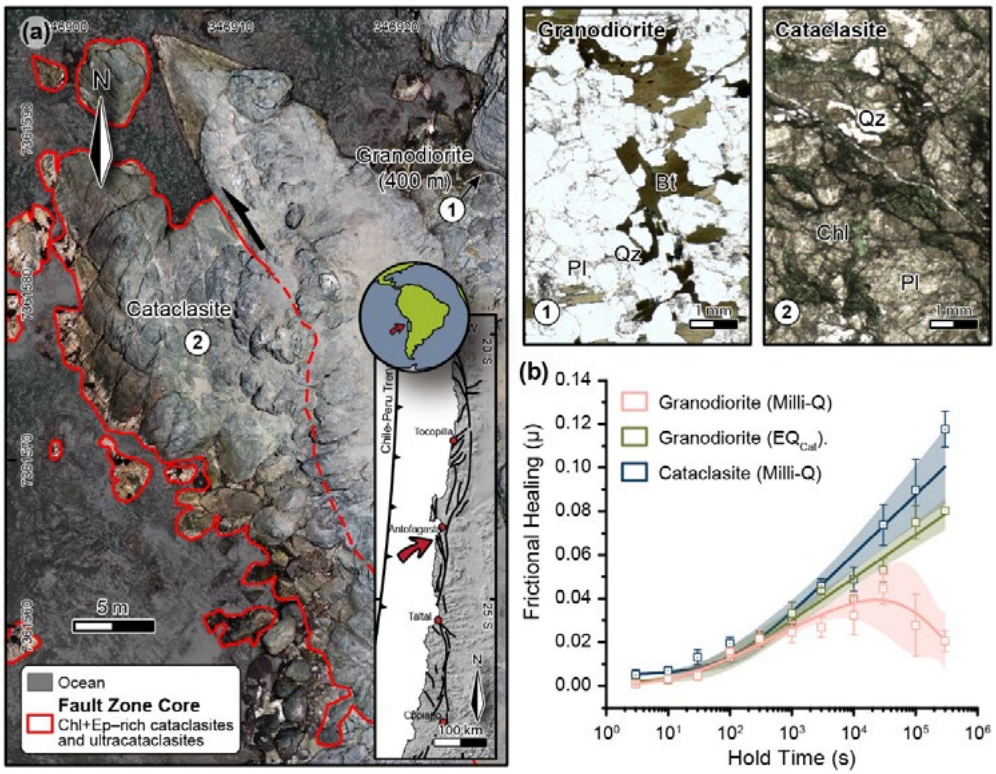

Fig. 2: (a) Samples locations within the Atacama Fault System, outlined areas in red are the fault-core, and thin sections of the granodiorite and cataclasite. (b) Dependence of fault frictional healing with hold time for non-altered granodiorite and the cataclasite with both pure Milli-Q water and in equilibrium with the cataclasite. Best fitting curves for the average values (standard error shown); shaded areas 95% best fitting curves confidence band.

References

[1] Dieterich, J. H. Time-dependent friction in rocks. J. Geophys. Res. 77, 3690–3697 (1972).

[2] Mironenko, M. V. & Zolotov, M. Y. Equilibrium-kinetic model of water-rock interaction. Geochemistry Int. 50, 1–7 (2012).

Thermo-poro-elastoplastic Rock Response in Enhanced Geothermal Systems

D. Nicolas Espinoza and Matthew L. McLean

Hildebrand Department of Petroleum and Geosystems Engineering, The University of Texas at Austin, Austin, USA
E-mail: espinoza@austin.utexas.edu, matthewmclean@utexas.edu

Keywords: EGS, short-circuit, destressing, poromechanics

1. Introduction

The large-scale deployment of geothermal energy can assist with the transition away from fossil fuels. Two promising designs for expanding geothermal capacity are hydraulic fracture-enhanced geothermal systems (Fig. 1) and closed-loop multi-well systems. However, several technical challenges remain, including reducing the uncertainties associated with multistage hydraulic fracturing, ensuring high flow rates as well as distribution, and minimizing the risk of induced seismicity and well mechanical failure. This paper explores how heat depletion impacts reservoir geomechanics.

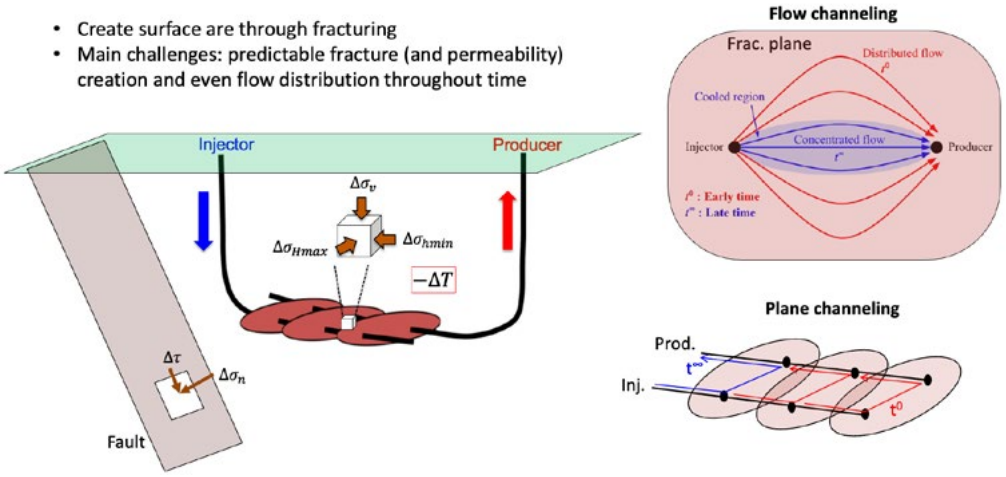

Fig. 1: Schematic of an Enhanced Geothermal System (EGS) and possible geomechanical implications: fault reactivation, thermal short-circuits (flow and plane channeling)

2. Methodology

We solve 3D coupled solid equilibrium, mass balance, and energy balance equations to capture the bulk reservoir response to non-isothermal fluid injection. The methodology employs coupled thermo-mechanical-hydraulic (THM) numerical simulation solved with the Finite Element Method (FEM) under the Fenicsx platform [1]. The main novelty of our approach is including mass balance in wellbores and multiple fractures and rock effective nonlinear and inelastic response [2,3]. Hydraulic fractures and wellbores are simplified to 2D and 1D elements embedded in a 3D domain. Unlike most geothermal work, we also considered undrained thermo-poromechanical response.

3. Results

The results indicate that the response of EGS and closed-loop multi-well systems can be significantly affected by thermal de-stressing. EGS systems can develop flow and plane channeling due to thermal de-stressing and fracture opening [2-3]. Figure 2 shows an example comparison of EGS fracture response to cooling considering linear elastic and elasto-plastic responses. The likelihood of short-circuiting depends on rock nonlinear elastic properties, strength, initial effective stress and temperature change. Closed-loop designs can also develop geomechanical risks. Aggressive heat extraction combined with high rock mass stiffness can cause the reservoir rock to reach its yield surface near wells [4]. Rock properties are highly influenced by pre-existing natural fractures, hence, these should thoroughly characterized and incorporated in models through effective rock models or discrete fracture networks if computational cost is available.

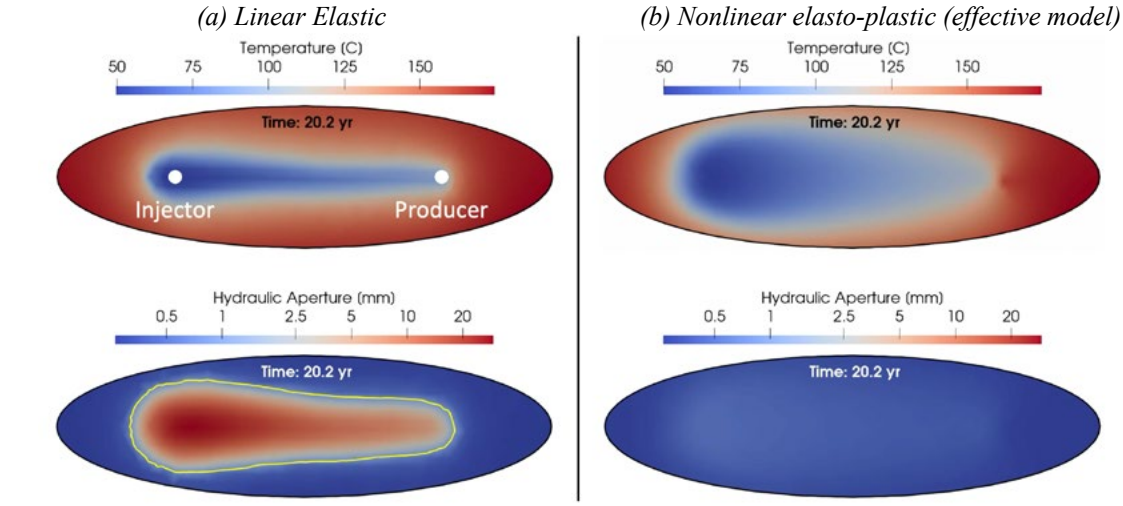

Fig. 2: Results of flow channeling in an EGS fracture considering different constitutive models.

4. Conclusions

Geomechanical events can limit the geothermal heat recovery factor. This recovery factor depends on the system's geometric configuration, temperature variations, rock stiffness and strength, and the local stress field.

5. References

[1] McLean, M. L., & Espinoza, D. N. (2023). "An open source FEM code for solving coupled thermo-poroelastoplastic processes". Open Geomech, 5, 1-9.
[2] McLean, M. L., & Espinoza, D. N. (2023). "Thermal destressing: Implications for short-circuiting in enhanced geothermal systems". Renewable Energy, 202, 736-755.
[3] McLean, M. L., Espinoza, D. N., & Ahmmed, B. (2024). "The impact of effective fractured rock mass properties on development of flow channeling in enhanced geothermal systems". Renewable Energy, 237, 121592.
[4] McLean, M. L., & Espinoza, D. N. (2024). "Thermo-poromechanical rock response around operating deep closed-loop geothermal wellbores". Rock Mechanics and Rock Engineering, 57(10), 8759-8775.

Unique Lithium Genesis: Hydro-Mechano-Chemical Pathways in the Cooper Basin

Yongqiang Chen[1*], Klaus Regenauer-Lieb[1*]

[1] *WA School of Mines: Minerals, Energy and Chemical Engineering, Curtin University., Perth 6102, Australia.*

E-mail: Yongqiang Chen yqzchen@gmail.com,Klaus Regenauer-Lieb klaus@curtin.edu.au

Keywords: Reaction-cross-diffusion modelling, Lithium-rich fluid generation, Granite reservoirs, Stress-triggered fluid generation, Fluid generation-driven fracturing

1. Introduction

The Cooper Basin, a prime target for lithium extraction, presents a striking anomaly: While volcano-sedimentary and crystalline basins in hydrothermal settings normally drive high Na-release (Fig. 1), the low salinity of the Cooper Basin presents an extreme endmember. Na/Li thermometry [1]indicates low-temperature Li release. We attribute this to the fast uplift of the granite shortly after its emplacement 300 Myrs [2], juxtaposed with evidence of relatively recent reactivation in a high-temperature (230°C+) regime. This reactivation, indicated by geothermal well data and high lithium concentrations (200+ ppm), suggests that the previously established fluid pathways are now being influenced by a new, hotter fluid flow. We hypothesise that tectonic stress during the basin's initial uplift released lithium from granite sheet silicates, creating these pathways via hydro-mechano-chemical instabilities (Fig. 2c). The preservation of these fluids through subsequent burial, coupled with this recent high-temperature reactivation, by plate collision less than 10 Myrs ago, potentially explains the persistent Na/Li ratios, which may reflect ongoing fluid-rock interactions under the current thermal conditions.

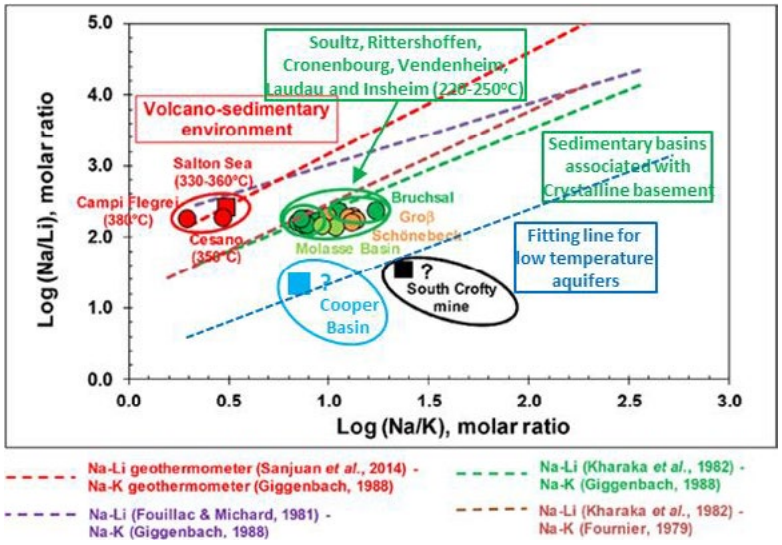

Fig. 1. Log (Na-Li) versus Log (Na-K), with molar ratios, for deep Li-rich fluids (integrated data from Cooper basin and Sanjuan et al. [1])

2. Methodology and Expected Results

A deformation band enabled by chemical fluid release [3] is proposed here for the breakdown of granite (Fig. 2): (a) schematic process of mechano-geochemical fluid release and deformation band generation; (b) mechano-geochemical fluids migrating through the grain-boundary network; (c) the critical situation for fluid focussing into deformation band is reached when the matrix compacts faster than fluid percolation.

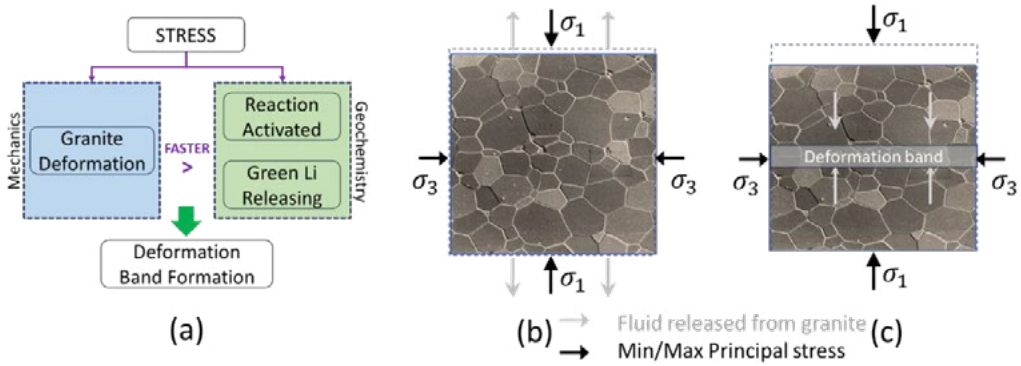

Fig. 2. Illustration for two Li migration scenarios in tight granite.

The following is a reaction-cross-diffusion model to characterise fluid generation and rock deformation under stress. Eq. 1 describes the diffusion of rock deformation. Eq. 2 describes the diffusion of internal fluid in rock. The relative evolution rates between these two processes control the generation of deformation bands. p_s and p_f are stress on solid and fluid. d_M, D_M, D_H, and d_H are the diffusion coefficients. R_1 and R_2 are the reaction terms for stress and fluid releasing, respectively.

$$\frac{\partial p_s}{\partial t} = D_M \frac{\partial^2 p_s}{\partial x^2} + d_H \frac{\partial^2 p_f}{\partial x^2} + R_1 \qquad \text{Eq. 1}$$

$$\frac{\partial p_f}{\partial t} = d_M \frac{\partial^2 p_s}{\partial x^2} + D_H \frac{\partial^2 p_f}{\partial x^2} + R_2 \qquad \text{Eq. 2}$$

3. Acknowledgements

This work is funded by the Australian Research Council Discovery Early Career Researcher Award (ARC DECRA) No. DE250100674.

4. References

1. Sanjuan, B., et al., *Lithium-rich geothermal brines in Europe: An up-date about geochemical characteristics and implications for potential Li resources.* Geothermics, 2022. **101**.
2. Gravestock, D.J., *Stratigraphic frameworks for correlation*, in *The petroleum geology of South Australia*, D.I. Gravestock, Hibburt, J.E. & Drexel, J.F. , Editor. 1998, Primary Industries and Resources SA: Adelaide. p. 117–128.
3. Alevizos, S., et al., *A Framework for Fracture Network Formation in Overpressurised Impermeable Shale: Deformability Versus Diagenesis.* Rock Mechanics and Rock Engineering, 2017. **50**(3): p. 689-703.

Modeling water inflow and temperature variations around a freezing tunnel in fractured rock

Jia-Jing Lin[a], Chuanyin Jiang[a], Chin-Fu Tsang[a,b], Auli Niemi[a], Patrik Vidstrand[c], Qinghua Lei[a]

[a] *Department of Earth Sciences, Uppsala University, Uppsala, Sweden*
[b] *Lawrence Berkeley National Laboratory, Berkeley, USA*
[a] *Rock Engineering Research Foundation, Stockholm, Sweden*
E-mail: jia-jing.lin@geo.uu.se

Keywords: freeze-thaw cycle, groundwater flow, heat transfer, multi-physics coupling, fracture network

1. Introduction

Infrastructure development in cold regions presents significant geotechnical challenges due to freeze-thaw cycles [1, 2]. The frost zone gradually develops at the walls of the tunnel that is open to the surface as the tunnel temperature drops below freezing, with water influx towards the tunnel accelerating ice formation and contributing to tunnel wall failure. The present study employs a 2D coupled thermo-hydro (TH) model to investigate the low-temperature zone propagation around the tunnel.

2. Methodology

The coupled TH model is solved using the finite element method. Fluid flow is governed by mass balance equations formulated separately for the rock matrix and fractures:

$$\rho_{\mathrm{w}}\left(S_{\mathrm{m}}\frac{\partial p}{\partial t}+\alpha_{\mathrm{B}}\frac{\partial \varepsilon_{\mathrm{v}}}{\partial t}\right)-\nabla\cdot\left(\rho_{\mathrm{w}}\mathbf{u}_{\mathrm{m}}\right)=0,\ \mathbf{u}_{\mathrm{m}}=-\frac{\kappa_{\mathrm{m}}}{\mu}\left(\nabla p-\rho\mathbf{g}\right) \tag{1}$$

$$b\rho_{\mathrm{w}}S_{\mathrm{f}}\frac{\partial p}{\partial t}+\rho_{\mathrm{w}}\frac{\partial b}{\partial t}-\nabla_{\tau}\cdot\left(b\rho_{\mathrm{w}}\mathbf{u}_{\mathrm{f}}\right)=\rho_{\mathrm{w}}\left(f_{\mathrm{up}}+f_{\mathrm{bottom}}\right),\ \mathbf{u}_{\mathrm{f}}=-\frac{\kappa_{\mathrm{f}}}{u}\left(\nabla_{\tau}p-\rho\mathbf{g}\right) \tag{2}$$

where, ρ is the density, S is the storage coefficient, μ is the dynamic viscosity of water, p is the pressure, t is time, ε_v is the volumetric strain, $\mathbf{u}$ is the velocity vector, b is aperture, f is the fluid exchange term between fractures and matrix, with subscripts 'up' and 'bottom' denoting the up or bottom matrix block at either side of the fracture, and κ is the permeability; the subscripts w, m, and f denote water, matrix, and fractures, respectively. Notably, permeability is assumed invariant under freeze-thaw cycles, as this study focuses on fluid-thermal interactions rather than mechanical deformation.

Similarly, heat transfer is described by energy balance equations for both domains:

$$(\rho C)_{\mathrm{eff}}\frac{\partial T}{\partial t}+\rho_{\mathrm{w}}C_{\mathrm{w}}\mathbf{u}_{\mathrm{m}}\cdot\nabla T-\nabla\cdot\left(\lambda_{\mathrm{eff}}\nabla T\right)=0 \tag{3}$$

$$b\rho_{\mathrm{w}}C_{\mathrm{w}}\frac{\partial T}{\partial t}+b\rho_{\mathrm{w}}\mathbf{u}_{\mathrm{f}}C_{\mathrm{w}}\nabla_{\tau}T-\nabla_{\tau}\cdot\left(b\lambda_{\mathrm{w}}\nabla_{\tau}T\right)=e_{\mathrm{up}}+e_{\mathrm{bottom}} \tag{4}$$

where, C is the specific heat capacity, λ is the thermal conductivity, T is the temperature, and e is the energy exchange term between fractures and matrix.

In this study, we develop a model to simulate water inflow and temperature variations around a 4 m-diameter circular tunnel within a 16 m × 16 m square domain. The fracture network follows a power-law distribution with the fracture intensity P_{21} = 2.5 m^{-1}. The water table is fixed at the top boundary, while the initial domain temperature is uniformly 10°C. All other outer boundaries are impermeable and adiabatic. The tunnel boundary is at atmospheric pressure and experiences diurnal sinusoidal temperature fluctuations between -2°C and 2°C over three months. A stationary hydraulic analysis is initially conducted, followed by time-dependent TH coupling to assess temperature effects.

3. Preliminary Results and Discussion

The hydraulic head distribution exhibits significant spatial variations due to the presence of fractures (Fig. 1a), with interconnected fractures dominating the fluid flow (Fig. 1b). The low-temperature zone initiates at the tunnel wall and gradually propagates into the fractured rock (Fig. 1c). In regions with closely spaced fractures, heat transfer is enhanced, accelerating thermal advection. The frost zone is found to progress at a slower rate within fractures compared to the matrix.

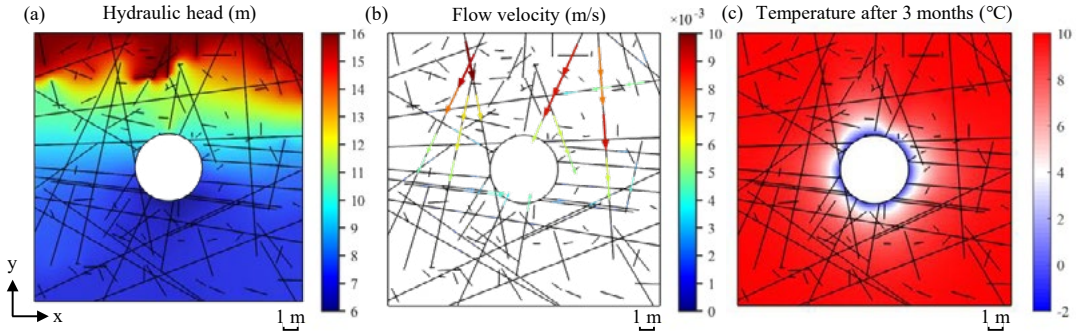

Fig. 1: Spatial distribution of (a) hydraulic head, (b) flow velocity, and (c) temperature

To sum up, this study shows that cyclic thermal variation could drive the gradual expansion of the frost zone, with significant implications for assessing frost risks to underground infrastructure in cold regions. Further studies are underway to include additional factors and arrive at quantitative estimate of frost zone growth and development.

Acknowledgement

Funding support by the Rock Engineering Research Foundation (BeFo project 524) is gratefully acknowledged.

References

[1] Grossi C.M., Brimblecombe P., and Harris I., 'Predicting long term freeze–thaw risks on Europe built heritage and archaeological sites in a changing climate.' Science of The Total Environment, 377(2):273–281. (2007).

[2] Zhang S.J., Lai Y.M., Zhang X.F., Pu Y.B., and Yu W.B., 'Study on the damage propagation of surrounding rock from a cold-region tunnel under freeze–thaw cycle condition.' Tunnelling and Underground Space Technology, 19(3), 295–302. (2004).

Water-rock interaction experiments to assess environmental effects in the Geothermal Laboratory in the Crystalline Basement (GeoLaB)

Harald Milsch, Fiorenza Deon, Maximilian Dietze,
Ulrike Hoffert, Ingo Sass

GFZ Helmholtz Centre for Geosciences, Geoenergy, Potsdam, Germany
milsch@gfz.de

Keywords: water-rock interactions; dissolution; environment; underground laboratory

1. Introduction

The GeoLaB (Geothermal Laboratory in the Crystalline Basement) is a planned research infrastructure in Germany funded by the Helmholtz Association with the aim of researching the use of geothermal resources at the meso-scale. It is a collaboration between the GFZ Potsdam, Karlsruhe Institute of Technology, TU Darmstadt, UFZ Leipzig and the German Federal Company for Radioactive Waste Disposal (BGE).

The aim of the project are scientific findings to develop utilization strategies for geothermal energy production from crystalline rocks. Experiments are to be carried out directly on the rock formation, forcing fluids into the rock under high pressure. The underground laboratory is to be excavated in fissured, crystalline rock with defined overburden at some suitable site. GeoLaB is currently in the planning and exploration phase. Potential targets are the crystalline basement rocks in the Black Forest or Odenwald whereas for the Odenwald, the area around the so called Tromm is of great relevance.

2. Methodology

To support the permitting process of the planned laboratory, potential environmental effects of water-rock interactions need to be investigated. For this purpose, natural water sampled from local springs was pumped through rock samples of Tromm granite collected from the Streitsdöll quarry for seven days at temperatures of 50 °C, 100 °C and 150 °C using a flow-through apparatus. Before, the cylindrical rock samples were submitted to a Brazilian Disc Test to obtain one single fracture along the flow direction. The fluid used was analyzed for its cationic and anionic hydro-chemical components before and after the experiment using ion chromatography (IC) and mass spectroscopy (ICP-MS). The granite samples were examined geochemically using X-ray diffraction (XRD) and X-ray fluorescence (XRF) analysis.

3. Results

In order to investigate the dissolution behavior of the rock and water samples, the substance concentrations of the input and output fluids were compared with each other. No general dependence on temperature was found. Calcium was the only element whose dissolution behavior was dependent on temperature in all test series. It was also

found that magnesium, strontium and bromine tend to adsorb to the rock, while potassium and fluorine, chromium, manganese, nickel, copper, arsenic, rubidium, molybdenum, silver, tin, cesium and lead tend to dissolve. The numerical modeling of a cation exchange using PhreeqC did not provide any reliable information on the dissolution behavior of the chemical components, so that several simultaneous processes, such as surface complexation, can be assumed to control the dissolution behavior.

4. Conclusions

Possible environmental effects were examined to determine whether the dissolved chemical components could have an impact on groundwater quality during future use of the Tromm site. The limit values of the German Drinking Water Ordinance were compared with the values of the fluids that flowed through the rock sample. The limit values for arsenic and chromium were exceeded but only in one sample each and only slightly. Within the experimental limits it can thus be assumed that water-rock interactions would likely not yield groundwater contamination.

Effects of pore fluid properties on Fault Weakening and Thermo-Hydro-Mechanical Processes in the Groningen Gas Reservoir

Chien-Cheng Hung[1*], André R. Niemeijer[1]

[1]*Department of Earth Sciences, Utrecht University, Utrecht, The Netherlands*
E-mail: c.hung@uu.nl

Keywords: Dynamic friction; Fluid viscosity; Thermal-mechanical pressurization; Fault-zone permeability; Principal slip zone

The slip behavior of faults in subsurface reservoirs is critically controlled by the multiscale, coupled Thermo-Hydro-Mechanical (THM) processes that govern frictional weakening during seismic slip. One key mechanism is thermal pressurization (TP), where frictional heating causes pore fluid expansion, reducing effective stress and promoting slip. The efficiency of TP is highly dependent on the thermal and hydraulic properties of the in-situ pore fluid [1, 2]. While previous experiments on water-saturated faults containing Groningen gas reservoir sandstone gouges have demonstrated significant weakening [3, 4], the in-situ pore fluid is more complex, comprising brine or brine-gas mixtures (mostly methane and nitrogen) with distinct viscosity (η) and thermal pressurization factor (Λ) where the latter is defined by [1] as:

$$\Lambda = \frac{\lambda_f - \lambda_n}{\beta_f + \beta_n} \quad (1)$$

where λ_f and λ_n are the thermal expansivities of the fluid and pores, respectively, and β_f and β_n are the compressibilities of the fluid and pores, respectively.

To investigate the role of pore fluid properties on induced seismicity, we conducted rotary-shear friction experiments at medium slip velocity (5 cm/s) on simulated Slochteren sandstone fault gouges, systematically varying pore fluid composition (DI water, in-situ brine, 1 cSt, and 5 cSt silicone oil) under drained and undrained conditions. Our results confirm that TP is the dominant weakening mechanism across all fluids, yet brine-saturated gouges exhibit the least effective TP (Figure 1). Additionally, microstructural analyses shows that fluids with higher viscosity limit grain size refinement within the principal slip zone, leading to higher frictional heating. Grain size refinement and localization affect permeability and this permeability evolution needs to be incorporate into the slip-on-plane model [1] to yield stress drop and temperature predictions more consistent with our experimental data.

By improving our understanding of coupled THMC processes in faulted reservoir rocks, this work contributes to refining rupture models and constraining the maximum potential moment magnitude of future induced earthquakes.

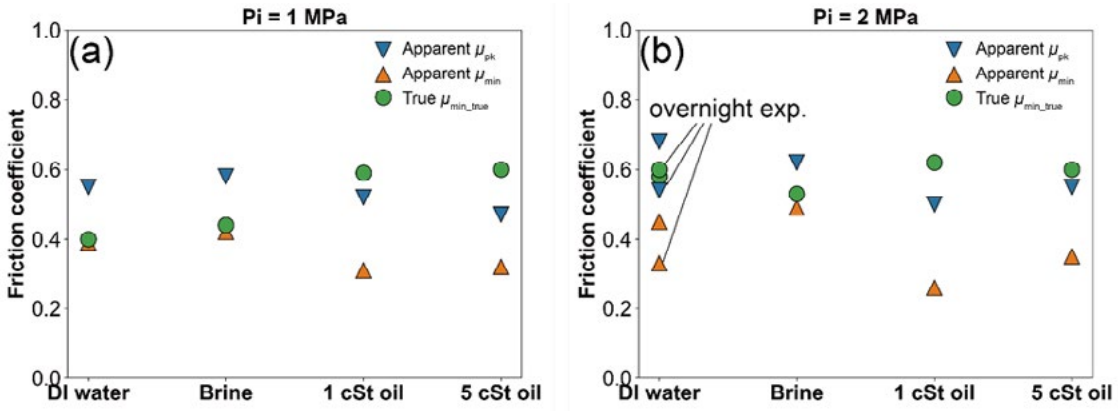

Fig. 1: Experimental data of apparent peak friction μ_{pk} (defined as $\tau_{pk} / (\sigma_n - P_i)$, where P_i is the initial fluid pressure), apparent minimum friction μ_{min} (defined as $\tau_{min} / (\sigma_n - P_i)$), and true minimum friction μ_{min_true} (defined as $\tau_{min} / (\sigma_n - P_f)$, where P_f is the instantaneous fluid pressure change) for all four pore fluids. Panels (a) and (b) correspond to experiments conducted at P_i = 1 MPa and P_i = 2 MPa, respectively. Overnight experiments refer to tests with a holding time (the duration between the end of the conditioning stage and the start of the main slip stage) exceeding 15 hours, whereas the remaining tests had a holding time of less than 2 hours.

References

[1] Rice, J. R. (2006). Heating and weakening of faults during earthquake slip. Journal of Geophysical Research: Solid Earth, 111(B5).

[2] Cornelio, C., Passelègue, F. X., Spagnuolo, E., Di Toro, G., & Violay, M. (2020). Effect of fluid viscosity on fault reactivation and coseismic weakening. Journal of Geophysical Research: Solid Earth, 125(1), e2019JB018883.

[3] Chen, J., Hunfeld, L. B., Niemeijer, A. R., & Spiers, C. J. (2023). Fault weakening during short seismic slip pulse experiments: The role of pressurized water and implications for induced earthquakes in the Groningen gas field. Journal of Geophysical Research: Solid Earth, 128(2), e2022JB025729.

[4] Hunfeld, L. B., Chen, J., Niemeijer, A. R., Ma, S., & Spiers, C. J. (2021). Seismic slip-pulse experiments simulate induced earthquake rupture in the Groningen gas field. Geophysical research letters, 48(11), e2021GL092417.

An experimental apparatus to investigate fluid-assisted long-term recovery of fractured rocks

Michele Fondriest[1], Ismay Vénice Akker[1]

[1]Department of Geosciences, University of Padova, Padova, Italy

Seismological observations show that earthquakes produce significant changes in the elastic and transport properties of active fault zones, with co-seismic drops in seismic wave velocities consistently followed by a slow post-seismic recovery, over months to few years. This suggests the existence of a damage-recovery cycle with the recovery phase possibly driven by a range of fluid-assisted re-strengthening (healing-sealing) mechanisms in the fractured medium and/or stress relaxation. The mechanical-chemical processes of fault zone healing-sealing are therefore crucial in understanding many aspects of fault zones behavior, such as earthquake recurrence and rupture dynamics. Such processes do not only play an important role in understanding unconventional seismicity, such as 'slow and low frequency earthquakes' as observed at active plate boundaries, but are also pivotal for the application of deep geothermal energy, CO_2 sequestration and the underground storage of radioactive waste. In the upper crust, fractures are dominantly sealed through mineral precipitation from supersaturated fluids that are chemically out of equilibrium with the host rock. Fracture sealing through mineral precipitation can either occur under high fluid availability during advective transport or can be controlled at small-scale by self-sealing diffusive processes (e.g., dissolution-precipitation). In order to improve the understanding of the damage-recovery cycle of fractured rocks we investigate how transport mechanisms (advection vs. diffusion) and fracture sealing rates are coupled. To do so, we use a "percolation cell" apparatus recently installed at Department of Geosciences of the University of Padua (Fig. 1).

The "percolation cell" apparatus was designed to run long-term fluid flow experiments under hydrostatic conditions up to 100 MPa confinement, 100 MPa pore fluid pressure and 250°C temperature. It is equipped with two syringe pumps and a back-pressure regulator that allow to monitor permeability evolution through time and a set of high-temperature P- and S- piezoelectric transducers to track changes of rock elastic properties in-situ. In addition, the pore fluid inlet circuit can flow into a stirred autoclave to pump solutions with controlled chemistry up to 20 MPa pore pressure and 200°C temperature through an externally heated pipe. Such an experimental setup allows to study both diffusion- and advection-dominated regimes within conditions representative for the upper crust. In order to quantitatively document the sealing process, the selected rock samples are analyzed by X-ray microtomography before and after the experiments. In addition, optical as well as scanning electron microscopy is applied to document the mechanical-chemical processes of fracture sealing. To study the fluid chemistry over time, fluids are analysed through ICP-MS.

A first series of experiments has been started to investigate the mechano-chemical recovery of fractures in carbonates at upper crustal conditions. Two preliminary long-term flow tests were performed with de-ionized water at 25°C through rock cylinders of micritic limestones with mated and non-mated single fractures under 20 MPa confining pressure and 5 MPa pore pressure. Time evolution of permeability were monitored together with the fluid-chemistry at the outlet. In addition, X-ray microtomography and SEM analyses were performed. Further experiments will be conducted on pre-fractured carbonates containing (i) a single un-mated fracture (e.g. saw-cut or displaced tensile fracture) and (ii) multiple microfractures with preferred vertical orientation produced in

dynamic loading experiments with a Split Hopkinson Pressure Bar (SHPB) (Aben et al., 2017a, b). This approach will allow us to investigate the role of the initial (micro)fracture network, the effect of the initial chemistry of the injected fluid and the effect of temperature on the sealing processes.

This work will advance our knowledge about the damage-recovery cycle in fractured carbonates through the investigation of sealing processes active at different timescales using a unique experimental approach.

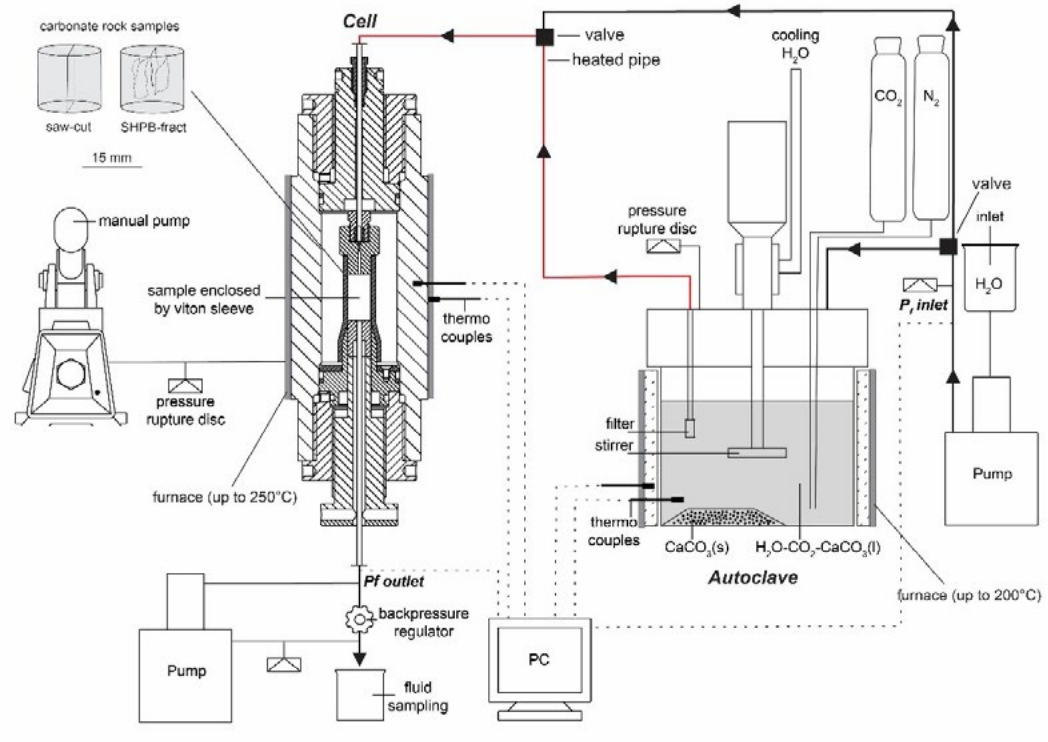

Figure 1. Fluid percolation cell as is currently installed at the University of Padova. Two samples types will be used (saw cut and SHPB fractured).

References

Aben, F., Doan, M. L., Gratier, J. P. & Renard, F. Experimental postseismic recovery of fractured rocks assisted by calcite sealing. *Geophysical Research Letters* **44**, 7228-7238 (2017a).

Aben, F. M., Doan, M.-L., Gratier, J.-P., & Renard, F.. Coseismic damage generation and pulverization in fault zones: Insightsfrom dynamic Split-Hopkinson Pressure Bar experiments. In M. Y. Thomas, H. S. Bhat, & T. M. Mitchell (Eds.), Evolution of fault zone properties and dynamic processes during seismic rupture (pp. **47–80**). Washington, DC: John Wiley & Sons, (2017b).

Hydrogen-Induced Alterations in Clay Micromechanics: Assessing Caprock Integrity for Underground Storage

P. Cheng[1], T. Mishra[2], C.P. Zhang[3], J.M. Miocic[1]

[1] *Energy and Sustainability Research Institute Groningen, University of Groningen, Nijenborgh 6, 9747 AG, Groningen, The Netherlands*
E-mail: p.cheng@rug.nl, j.m.miocic@rug.nl
[2] *Surface Technology and Tribology, Faculty of Engineering Technology, University of Twente, 7500 AE, Enschede, The Netherlands*
E-mail: t.mishra@utwente.nl
[3] *State Key Laboratory of Coal Mine Disaster Dynamics and Control, School of Resources and Safety Engineering, Chongqing University, Chongqing, 400044, China*
E-mail: lszcp1485@cqu.edu.cn

Keywords: Underground hydrogen storage; Caprock integrity; Clay; Nanoindentation; Micromechanics

1. Introduction

Underground hydrogen storage (UHS) has emerged as a promising solution to address the intermittency of energy supply and demand, playing a crucial role in the transition to a sustainable energy system [1, 2]. The effectiveness of UHS depends on the integrity of the overlying caprock [3], which acts as a natural barrier to prevent hydrogen migration and ensure long-term containment. Clay minerals are fundamental components of low-permeability caprocks such as shales, mudstones, and claystones, contributing significantly to their sealing capacity [4]. The primary clay minerals, including illite, smectite, and chlorite, exhibit distinct micromechanical properties that may be altered upon exposure to hydrogen [5]. Therefore, investigating the micromechanical behavior of clay minerals before and after hydrogen exposure is essential. A deeper understanding of these changes will provide valuable insights into the mechanical stability of clay-rich caprocks, ultimately supporting the safe and efficient implementation of UHS.

2. Methodology

To gain a comprehensive understanding of the behavior of clay minerals in UHS, a high-pressure and high-temperature (HPHT) cell is utilized to simulate subsurface conditions. The experimental design incorporates a range of pressures, temperatures, clay mineral types, and treatment fluids to systematically evaluate their influence on clay behavior under hydrogen exposure.

This study focuses on three key aspects of clay mineral alteration: mineralogical composition, pore system characteristics, and micromechanical properties. To achieve a thorough assessment, a suite of advanced analytical techniques is employed. X-ray powder diffraction (XRD) is used to analyze mineralogical changes, while low-pressure gas adsorption (LGA) characterizes pore structure and surface area. Scanning electron microscopy (SEM) provides high-resolution imaging of microstructural modifications, and nanoindentation quantifies micromechanical properties at the microscale. These

investigations will offer critical insights into the mechanical behavior of clay minerals and the fundamental mechanisms governing their response to hydrogen exposure, ultimately contributing to a deeper understanding of caprock integrity in UHS applications.

3. Main Results

While our experiments are currently ongoing, we expect the following results:

(i) Mineralogical changes

Hydrogen exposure is expected to cause minimal changes in illite, with possible swelling in smectite, particularly in water or brine. Chlorite may undergo slight alterations due to redox reactions in hydrogen-rich environments. These changes could impact the long-term stability of clay-rich caprocks in UHS.

(ii) Pore system modifications

Hydrogen exposure is anticipated to increase smectite porosity and surface area, especially in water-H_2 or brine-H_2 conditions. Illite is expected to remain stable in pore structure, while chlorite may show minor pore changes due to redox effects. These modifications may affect the sealing efficiency of caprocks.

(iii) Micromechanical property variations

Hydrogen exposure may weaken smectite mechanically, particularly in water or brine, due to swelling. Illite should retain its mechanical strength, while chlorite may experience slight weakening from redox reactions. These changes could influence the caprock's long-term sealing capacity.

4. Conclusion

The combined effects of mineralogical, pore system, and micromechanical changes are expected to directly influence the integrity of clay-rich caprocks in UHS. A comprehensive understanding of these responses is crucial for assessing the safety and effectiveness of hydrogen storage in subsurface formations.

5. References

[1] Miocic, J.M., Alcalde, J., Heinemann, N., Marzan, I. and Hangx, S., 'Toward energy-independence and net-zero: The inevitability of subsurface storage in Europe', ACS Energy Letters, 7(8), 2486-2489 (2022).

[2] Sambo, C., Dudun, A., Samuel, S.A., Esenenjor, P., Muhammed, N.S. and Haq, B., 'A review on worldwide underground hydrogen storage operating and potential fields', International Journal of Hydrogen Energy, 47(54), 22840-22880 (2022).

[3] Zivar, D., Kumar, S. and Foroozesh, J., 'Underground hydrogen storage: A comprehensive review', International Journal of Hydrogen Energy, 46(45), 23436-23462 (2021).

[4] Ugarte, E.R. and Salehi, S., 'A review on well integrity issues for underground hydrogen storage', Journal of Energy Resources Technology, 144(4), 042001 (2022).

[5] Labus, K. and Tarkowski, R., 'Modeling hydrogen – rock – brine interactions for the Jurassic reservoir and cap rocks from Polish Lowlands', International Journal of Hydrogen Energy, 47(20), 10947-10962 (2022).

THM Investigation of Frost Heave in Freezing Soils

Hoong Hao Yap[1], Federico Lattuada[1], Ferdinando Marinelli[2], Sebastià Olivella[3]

[1] *Department of Engineering, University of Cambridge, Cambridge, United Kingdom*
E-mail: hhy26@cam.ac.uk, fnl20@cam.ac.uk
[2] *Department of Civil, Architectural and Environmental Engineering, University of Naples Federico II, Naples, Italy*
E-mail: ferdinando.marinelli@unina.it
[3] *Department of Civil and Environmental Engineering, Universitat Politècnica de Catalunya, UPC Campus Nord, Barcelona, Spain*
E-mail: sebastia.olivella@upc.edu

Keywords: Frozen Soil, Frost Heave, Finite Element Method

1. Introduction

Frost heave is a major concern in cold-region geotechnics, driven by coupled thermo-hydro-mechanical (THM) processes where water migration to freezing fronts forms ice lenses, causing ground displacement. Its severity depends on soil properties like permeability and water retention, as well as boundary conditions such as overburden pressure and thermal gradients. While advances in numerical modelling have improved understanding of frozen ground behaviour, predictive capabilities for transient effects under complex conditions remain limited. This study evaluates a THM model's performance against experimental data for a Kaolin clay – LBS fraction E sand mixture under controlled thermal, hydraulic and mechanical conditions *[1]*.

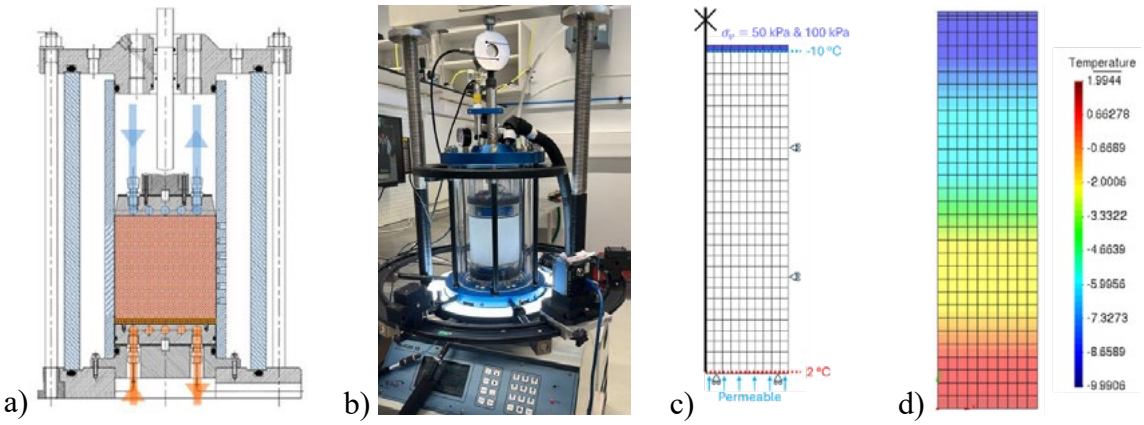

Fig. 1: a) FHA cross section diagram showing the cold and warm bath fluid direction [1], b) Kaolin - Sand soil sample ready to be tested in the FHA [1], c) Mesh and boundary conditions of the numerical model, d) Variation in temperature after 40 hours of freezing.

2. Methodology

This study investigates frost heave mechanisms through a combination of experimental and numerical analysis under a vertical stress of 50 kPa and 100 kPa. The experimental tests were conducted using a Frost Heave Apparatus (FHA) (Fig. 1a-b). The

apparatus maintained a temperature of -10°C at the top using a chilled metal plate, while the base was kept at 2°C with a continuous water supply, creating a one-dimensional freezing front that allows water to migrate from the warm end to the cold end. Displacements of the top plate were measured to capture the frost heave response. A two-stress variable constitutive model by *[2]*, implemented in CODE_BRIGHT, was used in the numerical analysis. The finite element model accounts for the various THM boundary conditions in the experimental setup (Fig. 1c). Calibration was performed through parametric studies, confirming mesh independence by systematically refining material parameters and boundary conditions (Fig. 1d).

3. Main Results

The results demonstrate an agreement between experimental and numerical predictions of frost heave at 50 kPa and 100 kPa (Fig. 2a-b). As the vertical stress increases, both volume change and water influx decrease, reflecting the expected behaviour of frozen soils. Initially, a brief period of water expulsion occurs due to volumetric expansion, followed by water migration into the soil sample. This process is consistent with premelting mechanisms that drive water movement toward the freezing front. Sensitivity analysis highlights intrinsic permeability as a key factor influencing frost heave, with higher permeability facilitating greater water migration and increased heave (Fig. 2c). These findings validate the predictive capability of the coupled THM framework and emphasize the importance of accurately determining intrinsic permeability for reliable THM modelling of freezing soils.

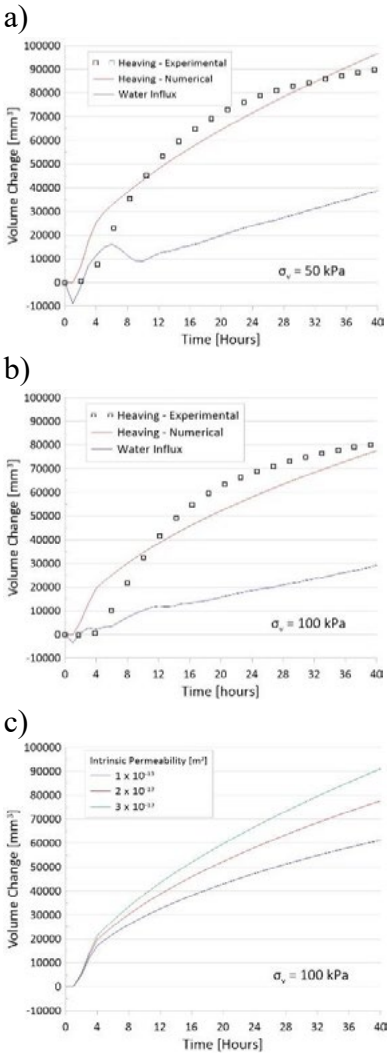

Fig. 2: Frost-heave responses of soil under varying conditions: (a) Experimental and numerical comparison at 50 kPa, (b) Experimental and numerical comparison at 100 kPa, and (c) Influence of intrinsic permeability on frost-heave behaviour.

4. References

[1] Lattuada, F., 2024. Experimental investigation of soil volume changes during freezing and thawing [PhD thesis, University of Cambridge]. Apollo - University of Cambridge Repository. https://doi.org/10.17863/CAM.115778

[2] Nishimura, S., Gens, A., Olivella, S. and Jardine, R.J., 2009. THM-coupled finite element analysis of frozen soil: formulation and application. Géotechnique, 59(3), pp.159-171.

A mechanical melt localization instability in partially molten rock with a pressure-generating feedback loop

Qingpei Sun[1,2], Klaus Regenauer-Lieb[1], Manman Hu[2]

[1] *WASM:Minerals, Energy and Chemical Engineering, Curtin University, Perth, Australia*
E-mail: qpsun@connect.hku.hk, klaus@curtin.edu.au
[2] *Department of Civil Engineering, The University of Hong Kong, Hong Kong*
E-mail: mmhu@hku.hk
Keywords: Melt segregation, Turing instability, Pattern formation

1. Introduction

Partially molten rocks, crucial in Earth's dynamics, show complex melt migration patterns through high-pressure melt bands (Fig. 1). Traditional models suggest melt (Leucosomes in Fig. 1) moves via filter pressing through grain boundaries [1,2] while melt accumulation in ductile compaction bands under high pressure remains not fully explained [3]. In this study, we propose a novel framework that relaxes the local equilibrium assumption from previous works. This framework not only provides a compelling explanation for enigmatic melt band patterns but also illuminates the crucial role of high melt pressures in shaping melt migration within the Earth's interior.

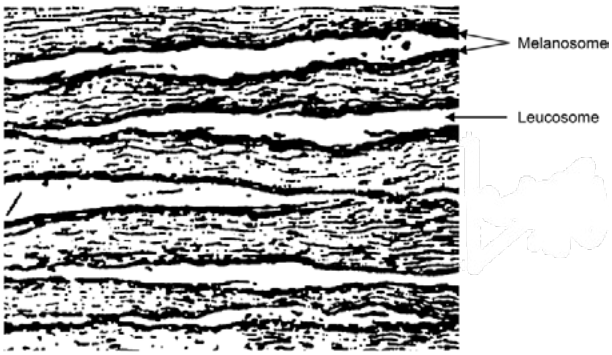

Figure 1 Melt segregation into light- (Leucosomes) and dark-coloured (Melanosomes) bands in granitic rocks [1].

2. Reaction-cross-diffusion formulation for hydro-mechanical system

To model the behaviours of a hydro-mechanically coupled system, we relax the restriction of local equilibrium conditions between melt and matrix implicit in the concept of effective pressure, deriving a minimum set of two reaction-cross-diffusion (RXD) equations in terms of the normalised solid viscous-plastic overstress $\tilde{p}_s = \bar{p}_s/p_{ref}$ and pore fluid pressure $\tilde{p}_f = p_f/p_{ref}$, together with the normalisation $\tilde{x} = x/l_0$, $\tilde{t} = \dot{\varepsilon}_0 t$

$$\frac{\partial \tilde{p}_s}{\partial \tilde{t}} = \tilde{D}_M \nabla^2 \tilde{p}_s + \tilde{d}_H \nabla^2 \tilde{p}_f + \tilde{a}_{11}\tilde{p}_s + \tilde{a}_{12}\tilde{p}_s^2 + \tilde{a}_{13}\tilde{p}_s^3 + \tilde{a}_{14}\tilde{p}_f \quad (1)$$

$$\frac{\partial \tilde{p}_f}{\partial \tilde{t}} = \tilde{d}_M \nabla^2 \tilde{p}_s + \tilde{D}_H \nabla^2 \tilde{p}_f + \tilde{a}_{21}\tilde{p}_s + \tilde{a}_{22}\tilde{p}_f \quad (2)$$

The nonlinear terms in Eq. (1) are associated with the rheological behaviours of the solid matrix (3rd order power law adopted here) while the linear reaction terms represent the fluid/solid pressure source.

3. Stability analysis and numerical simulation results

Based on the linear stability analysis, various instabilities can be revealed for the RXD system [4]. This study primarily investigates the quasi-static Turing instability by

numerically solving Eqs. (1-2) with the Fourier spectral method. The simulation results in Fig. 1 demonstrate that although the system initially starts in a disordered state, spatially ordered patterns spontaneously emerge over time, leading to localised channels within both the solid matrix and fluid melt. This temporal-spatial evolution indicates that the RXD model can create a positive feedback loop: pressure waves in the solid rock matrix expel melt, which then gathers in high-pressure bands and further elevates during melt channelling instabilities.

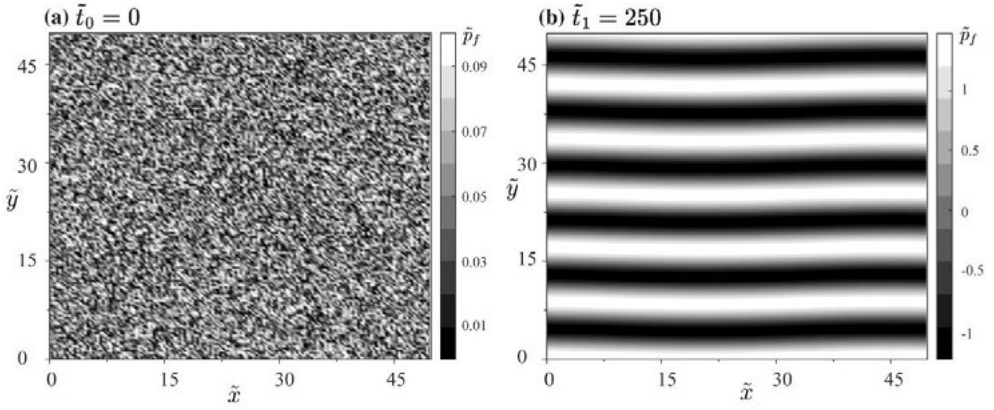

Fig. 1: 2D Numerical simulation of Turing instability: (a)Initial state with random perturbations (b)Localized channels induced by Turing instability

4. Conclusion

This work presents a reaction-cross-diffusion approach to model melt segregation processes in partially molten rocks. The theoretical and numerical analysis shows that the compaction of the rock matrix, coupled with its nonlinear viscosity, can lead to an instability that increases fluid pressure and expels the melt into adjacent channels. The finding highlights the complex interplay between melt, matrix, and viscosity in controlling fluid dynamics on Earth. It opens new avenues for understanding geological processes, potentially shifting the focus towards internal instabilities as a driver for high melt pressures.

5. References

[1] Mehnert, K. R. (1969). " Migmatites and the Origin of Granitic Rocks." Geological Magazine 106(2): 222-223.

[2] McKenzie, D., 'The generation and compaction of partially molten rock', Journal of Petrology, 25, 713-76 (1984).

[3] Veveakis, E., Regenauer-Lieb, K., & Weinberg, R., 'Ductile compaction of partially molten rocks: the effect of non-linear viscous rheology on instability and segregation', Geophysical Journal International, 200, 519-523 (2015)

[4] Sun, Q., Regenauer-Lieb, K., & Hu, M., 'A Reaction-cross-diffusion formulation for the evolution of compaction bands', Journal of Geophysical Research: Solid Earth, 130, (2025)

Micromechanical analysis of Fluid injection in unconsolidated formations using the FEM with zero-thickness interfaces.

Daniel Garolera[1], Charalampos Konstantinou[2], Ignacio Carol[3], Panos Papanastasiou[2]

[1]DRACSYS, S.L., Barcelona, Spain. Email: daniel.garolera@dracsys.com
[2] Department of Civil and Environmental Engineering, U. of Cyprus , Nicosia, Cyprus
[2] PHAETHON Centre of Excellence, U. of Cyprus, Nicosia, Cyprus
Email: konstantinou.charalampos@ucy.ac.cy, panospap@ucy.ac.cy
[3]Department of Civil and Environmental Engineering, UPC, Barcelona Spain
Email: ignacio.carol@upc.edu

Keywords: Finite Element Method, Zero-thickness interfaces, fracture mechanics, fluid injection in unconsolidated formation

1. Introduction

Numerous applications in hydrogeology, geo-environmental and geo-energy engineering require the injection of a fluid into the formation. The interaction between the soil or rock matrix and the selected fluids is pivotal for each application, and relevant parameters in the design must be adjusted accordingly. Such designs must also prioritize safety, operational effectiveness, and the minimization of potential environmental impacts and infrastructure failure risks. Given that these weak materials have different hydraulic and mechanical properties compared to competent rocks, their infiltration and fracturing response remains largely unknown. This study focuses on modelling the results of a series of experimental tests that were carried out on artificially cemented porous media which were generated via microbially induced carbonate precipitation (MICP), a process that results in the cementation of silica particles [1]. The cores were subjected to an anisotropic triaxial stress state, and a prescribed fluid injection along a central small-diameter axial perforation. Depending on the flow rate, degree of cementation and stress intensity and anisotropy, the fluid caused radial fractures of various configurations in the samples.

2. Methodology

The modelling has been undertaken with the FE code DRAC, based on the FEM with multi-phase multi-physics features and zero-thickness interface elements (also known as cohesive elements). These elements are inserted in between standard continuum elements to represent the effect of existing or potential fractures, not only in the mechanical behavior but also flow or diffusion-wise. From the mechanical viewpoint, these elements are equipped with constitutive laws incorporating fracture mechanics principles including fracturing parameter G_f. For the numerical simulation of the lab tests, the sample geometry includes the representation of individual grains generated randomly by Voronoi Tesselation, separated from each other by interface elements. The anisotropic confinement stresses are applied on the outer boundary while the injection is applied on a central circle (experimental perforation). The fracture parameters are adjusted to the

cementation level, and the fluid flow along inter-grain interfaces follows the cubic law. A summary of the approach can be found in [2].

3. Main Results

The paper presents a sample of the results obtained, illustrated in Fig. 1. The figure shows a comparable fracture pattern between the experimental and numerical simulations. The displayed images correspond to an intermediate cementation level case (6%-7%) [1] conducted under low confining stress conditions (σ_H = 400 kPa and σ_h = 300 kPa) and fluid flow at a rate of 100 ml/min. Both figures display the primary cracks, which are aligned approximately with the maximum principal stress direction (y-axis). Additionally, the numerical model reveals a significant zone of micro-cracking, which correlates with the important leak-off observed in the experimental tests.

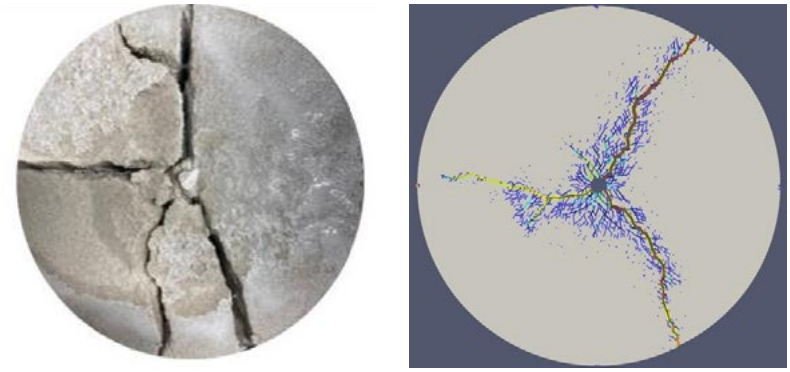

Fig.1: Comparison between experimental and numerical simulation results. Left) Microphotograph captured at the end of the experiment. Right) Numerical simulation result showing fracture energy dissipation (Wcr/GfI) at the end of the simulation (60s injection) displayed on the deformed mesh (x5).

4. Conclusions

The results obtained exhibit realistic fracture values and fracture patterns as compared to experiments. The conclusion is that the approach used seems to be a valid approach to model the fracture of weakly consolidated sandstone samples subjected to fluid injection. The developed micro-scale model can be used in applications where fluid flow in porous media serves as the underlying mechanism.

5. Acknowledgements

Funding was provided from the European Regional Development Fund and the Republic of Cyprus through the Research Promotion Foundation (Cyprus RPF, RESTART 2016–2020 PROGRAMMES, Project H2StorEMed, BILATERAL/ISRAEL (MOST)/0224/0039. The contribution of the UPC team was also supported in part by projects PID2023-149724NB-I00 from MCIN/MCINU (Madrid), which includes FEDER funds from the European Union, and 2021SGR00610 from Generalitat de Catalunya (Barcelona)

6. References

[1] C. Konstantinou, R. K. Kandasami, G. Biscontin, and P. Papanastasiou, "Fluid injection through artificially reconstituted bio-cemented sands," Geomechanics for Energy and the Environment, p. 100466, Apr. 2023, DOI: 10.1016/j.gete.2023.100466.

[2] Garolera, D. , Carol, I. and Papanastasiou, P, 'Micromechanical analysis of sand production', Int J Numer Anal Methods Geomech. 2019;43:1207–1229.

Ground response during short-term borehole thermal energy storage operation

Irfan Ahmad Shah[1], Prasenjit Basu[1], Santiram Chatterjee[2]

[1] *Dept. of Civil Engineering, Indian Institute of Technology Bombay, Mumbai, India*
E-mail: shahirfan@iitb.ac.in, pbasu@civil.iitb.ac.in, sc@civil.iitb.ac.in

Keywords: borehole, thermal energy storage, Finite element analysis, clay

1. Introduction

Borehole Thermal Energy Storage (BTES) technology employs subsurface soil and rock formations as medium for storage of excess thermal energy and recovery of the same during the period of high demand. Thermal energy storage in compacted soil is advantageous to reduce thermal losses [1]. Coupled thermo-hydro-mechanical (THM) disturbances in soil surrounding a thermally active borehole (BH) may potentially compromise borehole stability and operational life of a BTES facility. This research employed an anisotropic thermoplastic soil constitutive model [2] in finite element analyses (FEAs) that investigate ground response during borehole-soil heat exchange and quantify thermal performance of a borehole heat exchanger. FEAs account for the influence of heating on generation of excess pore-water pressure (PWP) and subsequent soil deformation during dissipation of thermally induced PWP.

2. Finite Element Analysis

Figure 1a shows a finite element model developed to examine short-term (one year) response of a BHE with length L = 40m and diameter D = 0.15m. Material properties of the soil domain (Kaolin) were adopted from Shah et al. [3]. Fluid (water) injection into the borehole at a constant mass flow rate of 0.3 kg/sec was simulated. The representative inlet fluid temperature [Figure 1b] is average monthly ambient temperature of Rajasthan, India, as recorded in 2024 [4].

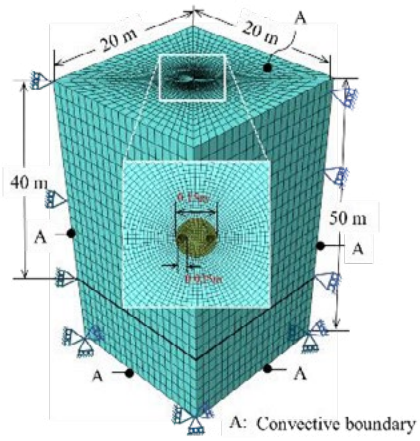

Fig. 1(a): Finite element model of geothermal heat exchanger.

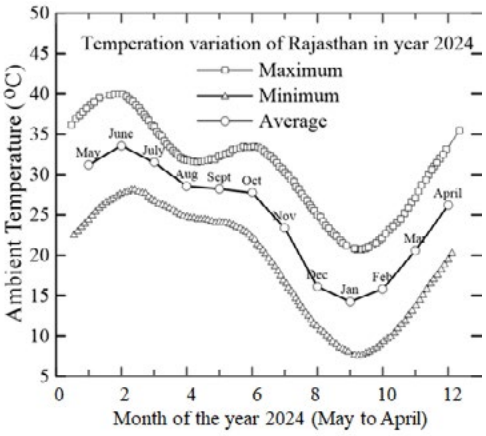

Fig. 1(b): Ambient temperature profile of Rajasthan, India in year 2024

3. Results and Discussion

Figure 2 shows power output and average BH surface temperature over one-year operational cycle (May to April). The maximum power output (=13.5 W/m) occurred in the peak of summer in May, followed by a steady decline until October. From October to mid of January, BH extracts thermal energy from soil formation. However, energy is stored during the remaining months for extraction during peak demand period. Figure 3 demonstrates temperature and excess PWP distribution within the soil domain during BHE operation. The plots were derived at six normalized distances d/D (= 0, 4, 6, 8, 10) from the borehole surface. Heat gradually dissipates into the ground and heat storage concentrates within a narrow zone within $10D$ from the borehole center. Due to THM coupling, PWP develops as a response to thermal loading. Such response results in the drop of mean effective stresses in the soil domain. For the temperature profile used in this study, the maximum evolution of excess PWP was observed at the BH-soil interface with values ranging between +1.5 and –0.5 kPa.

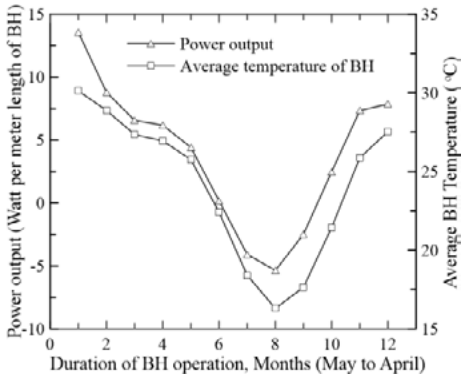

Fig. 2: Power output and average temperature of borehole

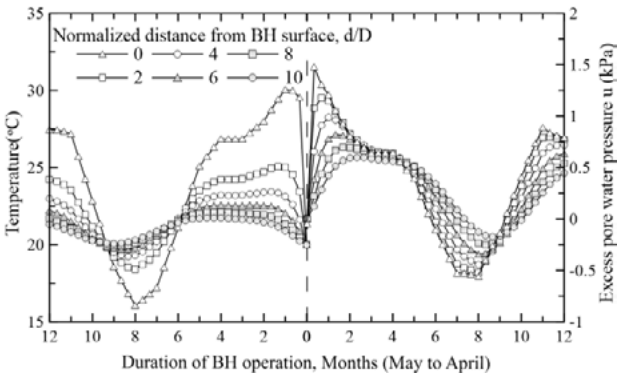

Fig. 3: Distribution of temperature and excess pore water pressure in soil during borehole operation

4. Conclusions

This study investigated ground response to short-term BHE operation in India. An anisotropic thermoplastic material model was used to simulate the soil behaviour. A peak power output of 13.5 W/m was recorded in May. Heat transfer in the soil resulted in the evolution of excess PWP (δu) and a corresponding drop in mean effective stress ($\delta p'$). The $\delta u/\delta p'$ ratio was observed to peak at the borehole-soil interface reaching a maximum value of 0.16 in the month of May. However, peak ground heave occurred in October, with a value of 2mm recorded to the top surface of the model. Due to the THM coupling, the peak in excess PWP did not align with the peak in ground deformation.

5. References

[1] Xu, J., Wang, R. Z., and Li, Y., 'A review of available technologies for seasonal thermal energy storage', Solar energy, 103, 610-638 (2014).

[2] Shah, I.A., Dastider, A.G., Basu, P., and Chatterjee, S.,'A thermoplastic clay constitutive model with temperature dependent evolution of stress anisotropy', Geomechanics for Energy and the Environment, 38, 100568 (2024).

[3] Shah, I.A., Chatterjee, S., and Basu, P., 'Coupled thermo-hydro-mechanical analysis of undrained uplift capacity for seabed pipelines buried in soft clays', Under Review

[4] www.weatherspark .com, accessed: February 24 2025.

Time-dependent constitutive model based on the damage evolution law

Mohammadreza Aghajanzadeh[1], Hossein Masoumi[1]

[1] *Department of Civil Engineering, Monash University, Melbourne, Australia*
Reza.Aghajanzadeh@monash.edu, Hossein.Masoumi@ monash.edu

Keywords: Creep, Time-dependent deformation, Viscoelastic-Viscoplastic, Damage evolution.

1. Introduction

Many undergrounds and surface rock engineering structures (e.g., tunnels, dams, underground energy storage sites, and mines) have long service life, spanning decades. Stability of these structures is very important to ensure their sustainable and safe operation over a long period [1, 2]. Deformation of such structures may last for decades, and failure of surrounding rocks subjected to long-term loading may occur after several years or decades. This can compromise integrity of structures on or within rock masses leading to high maintenance costs [3, 4].

This study introduces a comprehensive constitutive model designed to predict the time-dependent mechanical behaviour of brittle and quasi-brittle rocks under prolonged loading conditions. The model was experimentally validated using Gosford sandstone samples, with creep tests performed under various stress ratios. Material parameters for each model component were calibrated using iterative optimization methods.

2. Methodology

The proposed model incorporates elastic, viscoelastic, viscoplastic, and damage components to characterize rock deformation across all three creep stages: primary, secondary, and tertiary. The elastic response models immediate, reversible deformation using Hooke's law, based on isotropic linear elasticity. The primary creep stage is captured by the Kelvin-Voigt viscoelastic model, which combines spring and dashpot elements to describe time-dependent, reversible deformation under constant loading. The secondary stage, defined by a steady deformation rate, is modelled using the Norton creep law, a power-law formulation calibrated with a stress exponent and fluidity parameter to reflect long-term creep behaviour. Viscoplastic behaviour is incorporated through the Perzyna model with a non-associated flow rule, enabling realistic simulation of irreversible strain under prolonged or high stress. To capture the accelerating deformation of the tertiary creep stage, the model includes a damage evolution law originally proposed by Kachanov, accounting for microcrack development and its effect on rock integrity.

3. Main Results

Comparison between the experimental data and the model outputs shows in Figure 1 at various creep stress ratios, where the experimental data represented by continuous lines and the model's results are represented by the dashed lines. The alignment between the model outputs and experimental data is remarkably precise, underlining the robustness and relevance of the proposed model. Additionally, the results highlight that the model accurately predicts the tertiary creep region.

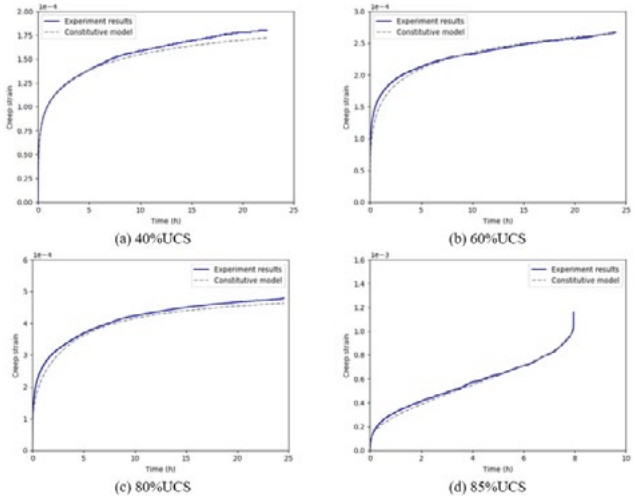

Fig. 1: An example figure showing the conference logo

4. Conclusion

The findings from this study indicate that the proposed model provides a significant improvement in predicting the long-term strength and failure of rock materials under high stress conditions. By accurately depicting the entire creep curve and recognizing the critical transitions between different creep stages, the model offers substantial advancements over existing models. These improvements have practical implications for the design and safety evaluations of rock structures, enabling more accurate assessments of their long-term stability and integrity.

5. References

1. Lajtai, E., R. Schmidtke, and L. Bielus. *The effect of water on the time-dependent deformation and fracture of a granite*. in *International Journal of Rock Mechanics and Mining Sciences & Geomechanics Abstracts*. 1987. Elsevier.
2. Martin, C. and N. Chandler. *The progressive fracture of Lac du Bonnet granite*. in *International journal of rock mechanics and mining sciences & geomechanics abstracts*. 1994. Elsevier.
3. Heap, M., et al., *Time-dependent brittle creep in Darley Dale sandstone.* Journal of Geophysical Research: Solid Earth, 2009. **114**(B7).
4. Pan, X., F. Berto, and X. Zhou, *Investigation of creep damage mechanical behaviors of red sandstone considering temperature effect.* Fatigue and Fracture of Engineering Materials and Structures, 2022. **45**(2): p. 411-424.

Investigation of a thermal energy storage sand battery

Imad El-Chiti[1], Shadi Najjar[1*], Joseph Zeaiter[2], Salah Sadek[1], Siba Haidar[1], Clara El-Sayegh[1]

[1] *Department of Civil and Environmental Engineering, American University of Beirut, Beirut, Lebanon*
[2] *Baha and Walid Bassatne Department of Chemical Engineering and Advanced Energy, American University of Beirut, Beirut, Lebanon*

**E-mail: shadi.najjar@aub.edu.lb*

Keywords: Thermal energy storage, sensible heat, energy geotechnics, sand battery

1. Introduction

Sensible seasonal thermal energy storage (STES) technologies consisting of insulated storage tanks filled with water, sand, or rock are finding applications in water and space heating in residential communities. There is a need for experimental and numerical investigations to understand the performance of these systems with respect to the impact of tank size, filler material, and heat transfer fluid (HTF) characteristics on efficiency and cost. A laboratory-scale testing program is implemented to investigate the thermal performance of a storage tank where the nature and porosity of the filler and HTF type are varied. The experimental data is used to calibrate a numerical finite element model in COMSOL to be used in future work to predict heat transfer mechanisms and efficiency in full scale STES tanks. This research contributes to a deeper understanding of STES systems, enabling their optimization for specific heating demands.

2. Methodology

The storage tank is shown in Figure 1. The tank (diameter = 30cm, height = 135cm) includes silica sand as the main storage filler and oil as the heat transfer fluid (HTF). Oil circulates through 55 steel pipes (diameter = 16mm) to inject and extract thermal energy from the tank, with the oil temperature controlled with a thermal control unit. The Thermal Energy Storage (TES) unit is designed to accommodate a storage capacity of 3 kWh of thermal energy. The instrumentation consists of 16 thermocouples connected to the center and edge pipes at different depths, within the sand at adjacent locations, and at the top and bottom oil collectors to measure the inlet and outlet temperature. The TES unit is insulated with two layers of 5cm rockwool with a density of 65 kg/m³. Table 1 summarizes the parameters that were varied in different experiments. In parallel to the lab experiments, a numerical 3D model of the tank was built in COMSOL as shown in Figure 1. The model was used to compare experimental and numerical results.

Table 2. Efficiency of TES unit for different operational conditions

Experiment	HTF Flow Rate	Filler Density (kg/m^3)	HTF Type	T_H (°C)	T_L (°C)	Efficiency
1	200 g/min	1450	Texatherm	130	20	67.4%
2	400 g/min	1450	Texatherm	130	20	44.0%
3	200 g/min	1450	Sunflower	130	20	68.1%
4	200 g/min	1550	Sunflower	130	20	67.7%

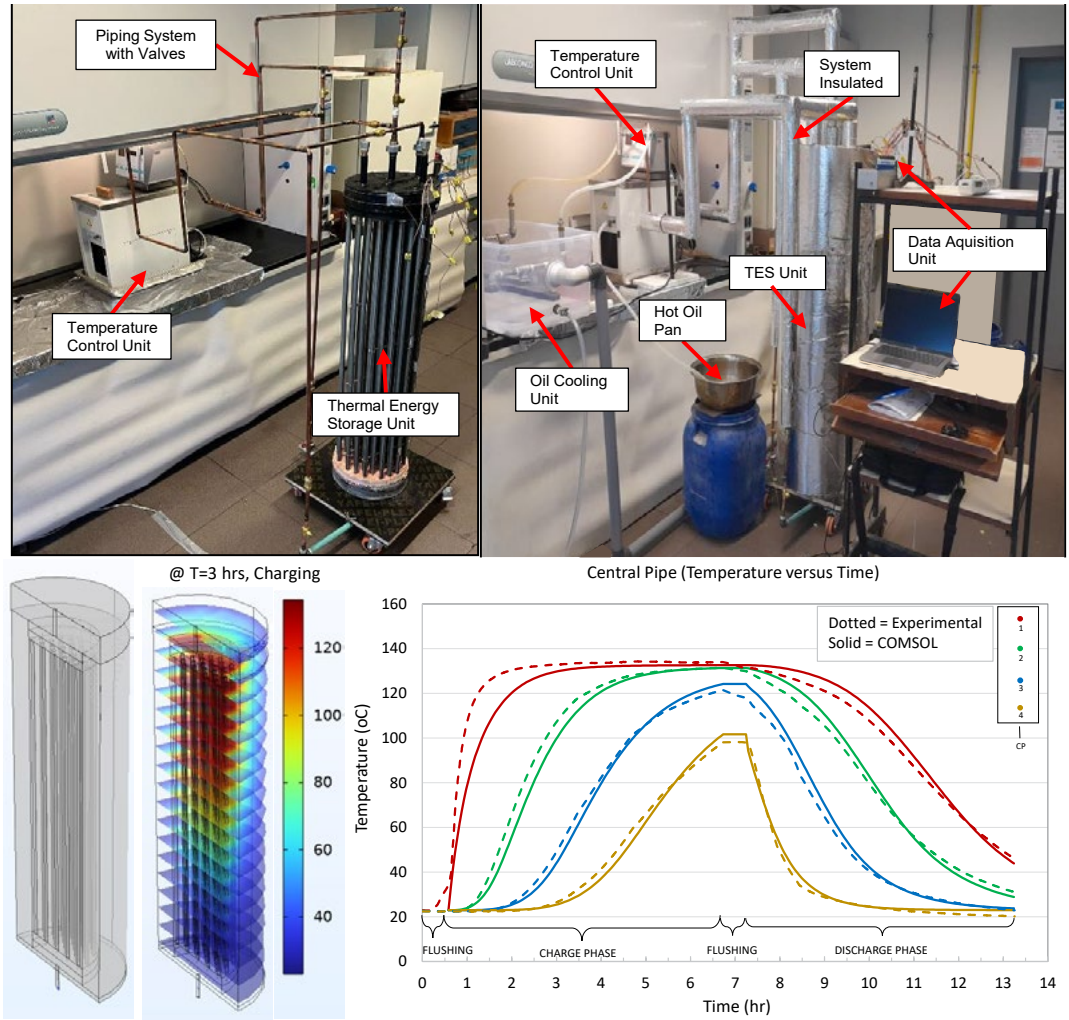

Fig. 1: Experimental and numerical models with results for temperature variation (charge and discharge)

3. Main Results

The thermal efficiencies (Li et al. 2012) of the TES units are presented in Table 1 and reached a high value of 68% for a flow rate of 200 g/min (irrespective of filler density and oil type), and 44% for a flow rate of 400 g/min. Results from the COMSOL simulation (Fig. 1) indicate an ability to accurately predict the temperature variations observed during the charging and discharging phases of the experimental tests.

4. Conclusions

The experimental and numerical results presented in this paper for a laboratory-scale thermal energy storage tank are promising and pave the way for a realistic investigation of the thermal performance of full-scale thermal energy storage tanks in future studies.

5. References

Li, W., Van Lew, J., Chan, L., Karaki, W., Stephens, J., O'Brien, E., 'Similarity and generalized analysis of efficiencies of thermal energy storage systems', Renewable Energy, 39, 388–402, (2012).

Geomechanics at extreme conditions: how do we model tightly coupled process across the scales?

Manolis Veveakis[1]

[1] Department of Civil and Environmental Engineering, Duke University, USA
E-mail: manolis.veveakis@duke.edu

Keywords: Coupled processes, Porous Microstructure, Minkowski functionals

1. Introduction

Human Civilization is facing the challenges of ensuring sustainability of water and energy resources, handling environmental concerns through safe disposal of energy waste (nuclear, CO2 storage etc), as well as safety of the urban areas with respect to natural hazards (earthquakes, landslides). Suggested solutions include engineering at extreme conditions of temperature, pressure, fluid composition, chemical reactions, and involve understanding their interaction and influence on the mechanical response of geomaterials at loadings that can span several time scales, from a few seconds to millions of years. However, the response of materials in any of these conditions is not deeply understood, making the engineering design in such conditions a formidable challenge.

2. Methodology

A key element in meeting these challenges is to develop a modeling framework that is able to incorporate a variety of physical processes typically met in these conditions (Thermal-Mechanical-Hydraulic-Chemical), incorporate info that can be constrained at laboratory conditions and factor in the geometric and mineralogical complexity of the porous microstructures that geomaterials commonly exhibit. To do so, we rely on concepts of integral geometry expressed through Hadwiger's theorem [1] to have a mathematically complete description of the porous microstructure through Minkowski functionals that can be selected as the primary geometric morphometers Mi. Hadwiger's theorem states that d + 1 Minkowski functionals can effectively characterize the geometric shape and composition of a microstructure, with d representing the dimension of the geometric system. All other descriptors that are additive, motion-invariant and conditionally continuous are a linear combination of the above functionals. In the case of a 3D system, the four Minkowski functionals of the domain formed by the grains of the microstructure Ω are the total volume of grains (i.e. porosity), the total grain surface area, their mean curvature (mean grain size) and their Gaussian curvature. When the mechanical laws are homogenized over these morphometers, the hypothesis is that they are able to capture a mathematically complete description of the mechanical evolution of the microstructure and link together the different physical processes affecting the various morphometers independently.

3. Main Results

We have utilized a variety of approaches to test different aspects of how coupled processes and geometry can be homogenized together. Through coupled chemo-mechanical degradation, modelled via phase field directly on digitized CT-scan samples [2], we can obtain the yield stress of the material to scale exponentially with the morphometers as $\sigma_Y = \sigma_0 e^{\sum a_i M_i}$. When this is generalized to triaxial loading [3], we can recover the entire yield envelope commonly met at geomaterials and assess the effect of processes like cementation on the strength of the material (Fig. 1). These results can be further used to inform machine-learning frameworks to be able to forecast the response of geomaterials given their microstructure under certain mechano-physical loading [4], but also to design optimal porous microstructures for desired performance under a given required strength [5].

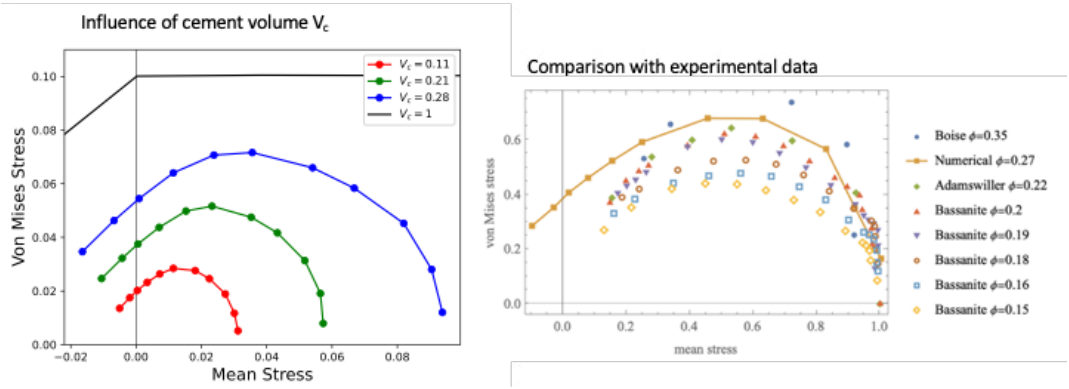

Fig. 1: Left: Influence of increasing cementation volume on the yield surface of a porous material; Right: Comparison between yield surfaces obtained experimentally for Bassanite and sandstone and a yield surface obtained numerically in our study.

4. Conclusion

Based on the results of this work, tightly coupled processes across the scales can be homogenized at the porous microstructure level, resulting into a non-additive dissipative expression with respect to the morphometers. This in turn allows predicting and designing the response of geomaterials under coupled processes and loadings.

5. References

[1] Aboulhassan, A., Hadwiger, M. & Wodo, O. 2020. Extracting topology, shape and size from heterogenous microstructure. Comput. Mater. Sci. 173, 109402.

[2] Guevel, A., H. Rattez, E. Veveakis, 2022. Morphometric description of strength and degradation in porous media Int. J. Solid Struct., 241, 111454

[3] Lesueur M., E. Veveakis, and H. Rattez 2022. Influence of cementation on the yield surface of rocks numerically determined from digital microstructures, Int. J. Plas., 103338

[4] Lindqwister W.,J. Peloquin, L. E. Dalton, K. Gall and M. Veveakis, 2025. Predicting the Mechanical Response Profile of Porous Materials via Microstructure-Informed Neural Networks, Nature Communications- Engineering, 4, 73

[5] Tian, Q., W. Lindqwister, M. Veveakis, L. E. Dalton. 2025. "Learning Latent Hardening (LLH): Enhancing Deep Learning with Domain Knowledge for Material Inverse Problems." Philosophical Transactions A (In Press). https://doi.org/10.1098/rsta.2024.0043

Fracture closure in pure quartz sandstone at low stress and temperature

Harald Milsch[1], Chaojie Cheng[1, 2], Renchao Lu[3],
Haibing Shao[3], Olaf Kolditz[3, 4]

[1] *GFZ Helmholtz Centre for Geosciences, Geoenergy, Potsdam, Germany*
[2] *KIT Karlsruhe Institute of Technology, Applied Geosciences, Karlsruhe, Germany*
[3] *Helmholtz Centre for Environmental Research - UFZ, Leipzig, Germany*
[4] *Technical University Dresden, Dresden, Germany*
milsch@gfz.de

Keywords: fluid-rock interactions; sandstone; pressure solution; fracture permeability

1. Introduction

Within the Earth's upper crust, rock fractures are important structural features as they permit effective fluid transport. Fluid-rock interactions proceeding therein may provoke time-dependent deformation associated with permeability changes. Mechanistically and in the presence of fluids, changes in fracture aperture are mainly governed by three grain-scale processes, i.e., pressure solution, free face dissolution (and/or precipitation), and stress corrosion cracking, which constitute a complex coupling of hydraulic, thermal, mechanical, and chemical (HTMC) mechanisms.

2. Methodology

The purpose of this contribution is to report on the outcome of a continuous long-term flow-through experiment conducted on a single-fractured pure quartz sandstone (Fontainebleau) at 60 °C. Changes in effective pressure (1, 17, and 29 MPa) and pore fluid composition (deionized water and Si-rich solution) were sequentially imposed to investigate their respective effect on time-dependent fracture closure. Complementary analyses of the effluent Si concentration (ICP-OES) and microstructure (fracture surface scanning, µCT, SEM) were performed.

3. Results

The results of this experiment evidence that even at comparatively low temperatures and effective pressures fractures in dense quartz-rich sandstones can undergo substantial closure (i.e., by 50 % in hydraulic aperture) within 4 months (Fig. 1, open squares), with strong implications for fracture permeability. Compared to natural settings, this may have been favored by the use of deionized water as the pore fluid, but a significant contribution to the overall aperture decline was also observed when the pore fluid was close to saturation with respect to Si during stage III.

Concurrent effluent analyses for Si concentration evidence transients with reaction time as well as trapping of Si-enriched fluid within asperity contacts (Fig. 1, blue triangles). SEM-imaging reveals both dissolution features and brittle processes at

asperities. µCT-imaging clearly demonstrates an increase in total contact area of the two fracture halves after the experiment.

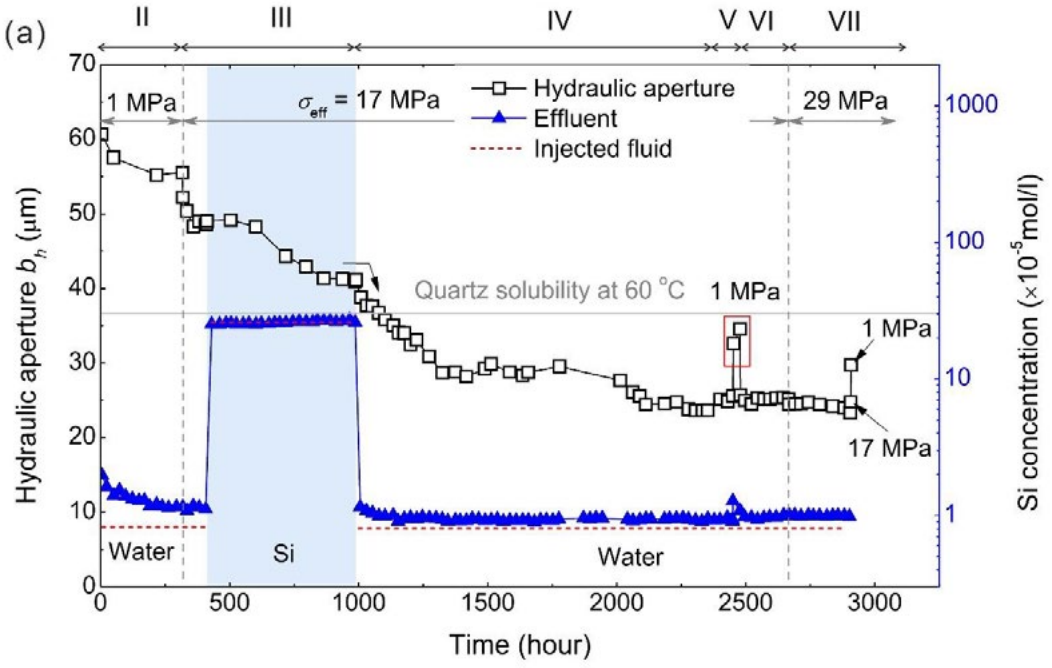

Fig. 1: Hydraulic aperture (open squares) and effluent Si concentration (blue triangles) measured as a function of time for the full duration of the experiment. Stages II to VII relate to specific effective pressure and fluid conditions aiming to decipher their relative effect on hydraulic aperture evolution.

4. Conclusions

In combination with the chemical and microstructural investigations performed it is suggested that, depending on the imposed conditions and the evolutionary state of fracture morphology, overall fracture deformation is controlled by a complex succession and/or combination of pressure solution, stress corrosion cracking, and free face dissolution. To become activated, stress corrosion cracking appears to require a higher effective pressure than pressure solution at a comparable contact area ratio.

At some point, as both the total contact area and the diffusion path length within the asperity interfaces increase with time, both pressure solution and stress corrosion cracking halt and the dynamics of fracture closure then is controlled exclusively by free face dissolution without signs of reactivation of the former mechanisms within the experimental effective pressure limits. This implies that the deformation mechanisms that are driven by diffusion and/or stress (i.e., pressure solution and stress corrosion cracking) may deactivate, yielding a significant decrease in the fracture closure rate.

The role fluid plays in crack interaction

Jing Chen[1], Manman Hu[1]

[1] Department of Civil Engineering, The University of Hong Kong, Hong Kong
E-mail: jing2511@connect.hku.hk, mmhu@hku.hk

Keywords: Crack interaction, Fluid-driven fracture, Analogue experiment

1. Introduction

Interaction between neighboring cracks is essential to the understanding of crack network formation. While fluid-driven crack interaction is ubiquitous in nature and frequently encountered in geo-engineering applications, the process remains largely unknown due to its inherent complexity when fluid is involved [1]. In particular for a pair of fluid-driven cracks, how the injected fluid infiltrates into the rock matrix from the near-tip region of one crack, meanwhile being affected by the dynamic infiltration occurring around the other crack tip, remains barely explored.

Here we investigate into this process with 2-D analogue experiments [2] using a Hele-Shaw cell. By probing the system behavior in response to fluid injection, a repulsion-attraction relationship during different phases of macroscopic crack pair interaction is revealed. Meanwhile, we illustrate the dynamic interplay between the infiltrating fluid and the deforming hydrogel around the propagating crack tips where stress concentrates.

2. Experimental setup

A Hele-Shaw cell with fixed external boundaries was constructed for examining the dynamic interaction between an EP crack pair [3,4] driven by fluid injection under plane strain conditions (Figure.1a). The transparent alginate hydrogel was used as an analogue for low-permeability host formation [2] confined in the cell. Two acrylic tubes were symmetrically mounted into the cell, each featuring a perforation hole (diameter of approximately 1 mm) in the side walls to direct the flow direction of the injected fluid (Figure.1a), such that two hydro-cracks approach to each other towards the center (Figure.1b). A constant flow rate of 10 ml/min was applied to drive the water injection via a dual-channel syringe pump. And Rhodamine 6G was selected as the fluorescent dye for injection to visualize the interacting fluid-infiltration zones.

3. Repulsion-attraction of fluid-driven crack pair

The experimental results demonstrate an archetypal three-stage behavior as shown in Figure.1b. The fluid-driven crack pair first advance along their initial colinear path when relatively far apart, after which they undergo a repulsive growth. Upon the two tip points approaching the horizontal separation of $\Delta x \approx 3$ mm, their vertical distance Δy reaches the maximum value, after which the growth of the crack pair switches to a mutual attraction. Besides, the uncertainty arises in the fringe patterns of the fluid-infiltration zones around the propagating tips (Figure.1d-f) indicating a tight coupling between the fluid motion and matrix deformation during the crack interaction. The moment when the two fluid-infiltrating zones undergo initial coalescence (Figure.1e) corresponds to point ``c'' in Figure.1c where the interacting cracks transit to slow down their repulsion and prepare for a mutual attraction.

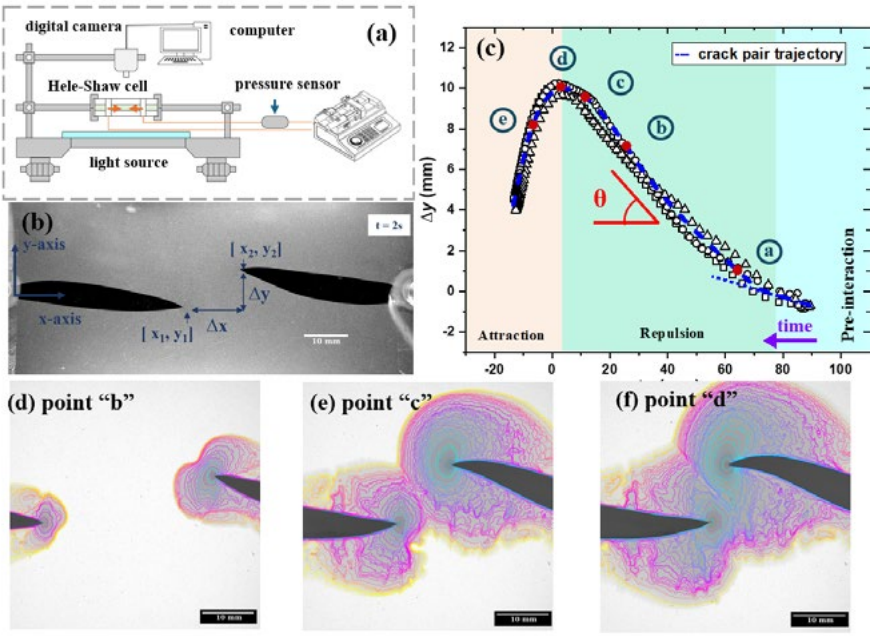

Fig. 1: Repulsion-attraction behavior of a pair of fluid-driven crack (a)Experimental setup; (b) Fluid-driven crack in the analogue rock material; (c)Crack pair trajectory; (d-f) Evolution of fluid-infiltration zones around the crack tips

4. Conclusion

This work presents an experimental investigation into the interacting behavior of a fluid-driven crack pair using a Hele-Shaw setup. The growth path of the crack pair undergoes a remarkable transition from an initial repulsion to mutual attraction upon a critical proximity. By illuminating the evolution of the fluid-infiltration zones around the advancing crack tips, we show that this repulsion-attraction transition is enabled by the coalescence of the two fluid-infiltrating process zones, where the important role of fluid pressurization and its tight coupling with the deforming solid matrix is highlighted, characterizing the dynamic interplay of the crack pair system. The presented study advances the understanding of adjacent crack interaction and probes the dynamics of crack network formation, which is of paramount importance to a wide range of industrial practices concerning fluid injection into the subsurface.

5. References

[1] Murphy, Hugh D., Jefferson W. Tester, Charles O. Grigsby, & Robert M. Potter., 'Energy extraction from fractured geothermal reservoirs in low-permeability crystalline rock', Journal of Geophysical Research: Solid Earth 86, no. B8 (1981)

[2] Chen, Jing, & Manman Hu., 'Single fluid-driven crack propagation in analogue rock assisted by chemical environment.', Geomechanics for Energy and the Environment 37 (2024)

[3] Fender, Melissa L., Frédéric Lechenault, & Karen E. Daniels., 'Universal shapes formed by two interacting cracks.' Physical Review Letters 105, no. 12 (2010): 125505.

[4] Dalbe, Marie-Julie, Juha Koivisto, Loïc Vanel, Amandine Miksic, Osvanny Ramos, Mikko Alava,& Stéphane Santucci., 'Repulsion and Attraction between a Pair of Cracks in a Plastic Sheet.', Physical review letters 114, no. 20 (2015): 205501.

A Fully Coupled XFEM Model for Simulating a Vertical Fluid-Driven Fracture Breaching Caprock in Anisotropic Layered Formation

Ernestos Sarris[1*,3], Elias Gravanis[2], Loizos Papaloizou[3]

[1]*School of Geology, Department of Minerology-Petrology-Economic Geology, Aristotle University of Thessaloniki (AUTH), Greece*
E-mail: esarris@geo.auth.gr
[2]*Department of Civil Engineering and Geomatics, Cyprus University of Technology Limassol, CY-3036, Cyprus*
E-mail: elias.gravanis@cut.ac.cy
[3]*Department of Engineering, Civil and Environmental Engineering Program, University of Nicosia, Nicosia, CY-1700, Cyprus*
E-mail: papaloizou.lo@unic.ac.cy

Keywords: $ScCO_2$ fracturing, XFEM simulation, Caprock breach, K-dominated regime

1. Introduction

A significant challenge in CO_2 storage operations is managing and predicting vertical fracture growth caused by CO_2 injection. This is crucial because uncontrolled vertical fractures can extend into overlying rock layers (caprocks), leading to serious operational issues and potential irreversible damage to the storage formation. The orientation of hydraulic fractures depends on the in-situ stress regime and propagate perpendicular to the direction of the minimum principal stress or in a parallel direction with the maximum principal stress. If the vertical stress is larger than the plane horizontal stresses, fractures are expected to grow vertically into the caprock unless adequately contained. Geological formations consist of layered rocks with varying mechanical properties and anisotropic stress fields, creating stress contrasts between layers. When a hydraulic fracture encounters a formation with varying fracture toughness, either weaker or stronger, the propagation behavior is influenced by the non-local characteristics of the hydraulic fracture, affecting pressure distribution and fracture geometry. These unwanted fractures pose a significant risk to caprock integrity in CO_2 sequestration applications [1-3].

2. Methodology

In this study, we utilize the Extended Finite Element Model (XFEM) within a fully coupled hydro-mechanical framework to analyze fluid-driven vertical fractures. These fractures propagate through two-layered permeable formations by injecting an incompressible viscous fluid at the fracture inlet, assuming plane strain conditions. Fluid flow within the fracture is modeled using lubrication theory ignoring leak-off effects, while pore fluid movement in the porous formation is governed by Darcy's law. The coupling is based on Biot's theory, and fracture propagation is modeled using a fracture criterion in the spirit of cohesive based damage mechanics. Numerical simulations with FEM are conducted to evaluate fracture opening, length, and propagation pressure over time but also as a function of length [3-5].

3. Results

The focus of the study was to examine fracture containment within reservoirs, particularly when fractures propagate through layered formations. The computational model's accuracy was validated against the toughness-dominated regime parametric space without leak-off. Numerical results are presented for layered formations with heterogeneous stress conditions and varying mechanical properties, ranging from hard (shale) to soft (evaporite) caprock formations, to assess fracture containment as shown in fig.1

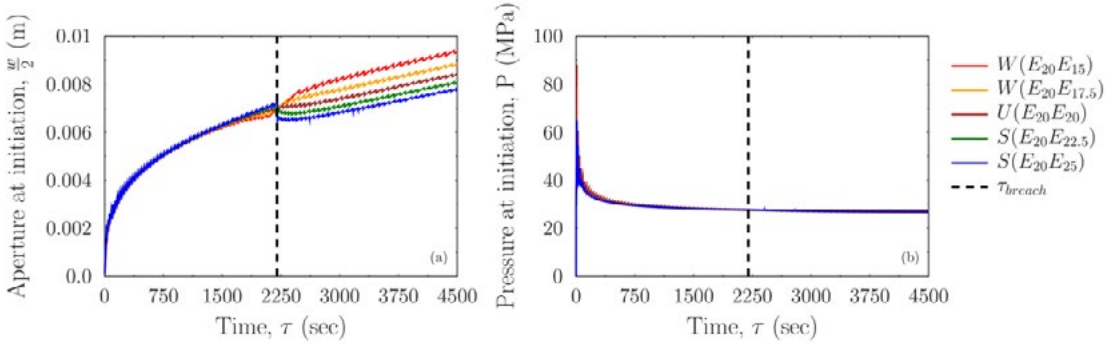

Fig. 1: Numerical solution of the fluid driven fracture. (a) aperture at onset point with time and (b) pressure at onset point with time. Fracture breaches the caprock at 2250 sec

4. Conclusions

The numerical simulations revealed that caprock breach results in wider fractures in soft evaporites and narrower ones in hard shales, with pressure profiles remaining the same at the initiation point Stress anisotropy was found to affect the apertures and the pressure at initiation point. Finally, the formation pressure was found to also affect the aperture and pressure. With increasing formation pressure, wider fractures are created with larger pressure.

5. References

[1] Sarris, E., Gravanis, E., & Papanastasiou, P., 'Investigation of self-similar interface evolution in carbon dioxide sequestration in saline aquifers', Transport in porous media, 103(3), 341-359, (2014).

[2] Sarris, E. &Gravanis, E., 'Flow regime analysis of the pressure build-up during CO_2 injection in saturated porous rock formations', Energies, 12(15), 2972, (2019).

[3] Papanastasiou, P., & Sarris, E.,'Cohesive zone models', In Porous rock fracture mechanics, Woodhead Publishing (2017).

[4] Vahab, M., & Khalili, N., 'X-FEM modeling of multizone hydraulic fracturing treatments within saturated porous media'. Rock Mechanics and Rock Engineering, 51, 3219-3239, (2018).

[5] Yang, L., & Chen, B. 'Extended finite element-based cohesive zone method for modeling simultaneous hydraulic fracture height growth in layered reservoirs'. Journal of Rock Mechanics and Geotechnical Engineering. 16,(8), 2960-2981,(2024).

Stress-dependent permeability decline in a chalk reservoir

Euripides Papamichos[1,2], Michalis Kattis[3]

[1] *Aristotle University of Thessaloniki, Greece*
epapamic@civil.auth.gr
[2] *SINTEF Industry, Trondheim, Norway*
[3] *NTNU Norwegian University of Science and Technology, Trondheim, Norway*
michael.kattis@ntnu.no

Keywords: chalk, pore collapse, permeability, constitutive model

1. Introduction

Depleted chalk reservoirs in the North Sea may experience a decline in permeability during waterflooding for pressure maintenance. In this work we look at the permeability decline due to pore collapse of the weak and water sensitive reservoir chalk. An elastoplastic model was developed to model the mechanical behavior of the chalk and was coupled to a stress-dependent permeability model to approximate the permeability decline during pore collapse. Results from waterflooding simulations are presented for a reservoir element that is subjected to depletion and waterflooding.

2. Chalk mechanical model for pore collapse and water sensitivity

Chalk exhibits high porosity ϕ but low permeability k. For example, ϕ = 41-46% and k = 2-3 mD for the Mons chalk we studied which is an analogue of the high porosity sections of North Sea chalk reservoirs. Chalk is also susceptible to pore collapse and shows water/brine sensitivity of its strength and stiffness. The elastoplastic behavior of chalk was modeled through a water sensitive single yield surface modified Drucker-Prager model to include a pressure cap. It addresses both shear and compaction failure with one yield and one plastic potential surface. In the past, a single yield surface model was used to model the Pietra Leccese chalk [1], [2], and the model was later enhanced to include destructured chalk as well [3]. Here a modified version of this model is used. The process of rock destructuration builds on ideas introduced by Lagioia and Nova [4] for the case of mechanical destructuration of a calcarenite. The chalk model was calibrated on triaxial and hydrostatic tests on oil and brine saturated specimens of Mons.

3. Stress-dependent permeability model

Permeability results from hydrostatic and oedometric compression tests in Mons show that until pore collapse permeability decreases slowly with increasing stress due to volumetric compaction and porosity reduction. The experiments also show that pore collapse fundamentally changes the rock structure by destructuration which causes a sharp decrease in permeability [5]. This requires a post pore collapse modification of the porosity dependent Kozeny-Carman formula for the permeability. The proposed modification includes a stress-dependent pore collapse term to account for the permeability decline due to pore destructuration.

4. Results

We calculated the permeability decline in a reservoir element upon depletion from the original in situ stresses, followed by repressurization with simultaneous exchange of the saturation fluid from oil to brine and finally depressurization to the depleted state. Oedometric conditions and no arching of the vertical stress were assumed. Figure 1 plots the total vertical and horizontal stresses, the reservoir pressure, the water saturation and the normalized with the initial permeability during the various phases of the simulation. A decline of permeability to ca 40% of the original is predicted.

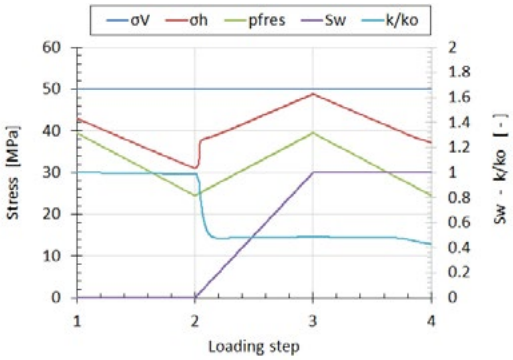

Fig. 1. Total vertical σV and horizontal σh stress, reservoir pressure pfres, water saturation Sw and normalized permeability k/ko.

5. Conclusions

Pore collapse in chalk is a mechanism that causes a sharp decline in permeability. The permeability decline at pore collapse was modeled with a modified Kozeny-Carman model that is not only porosity dependent but it is coupled to the stresses. The simulation of depletion and water injection and the permeability decline was demonstrated by representing the reservoir as a single element under initially in situ stresses and pore pressure followed by depletion, and then repressurization and water flooding.

6. Acknowledgments

This work has been supported by the research project “Chalk influx and solids production mitigation in the North Sea” funded by the Research Council of Norway, Aker BP, and ConocoPhillips Norway (Petromaks 2 program, Project # 306106, 2020).

7. References

[1] *Papamichos E, Brignoli M, Santarelli FJ (1997). An experimental and theoretical study of a partially-saturated collapsible rock. Mechanics of Cohesive-Frictional Materials 2, 3, 251-278.*

[2] *Papamichos E (1998). Chalk production and effects of water weakening. Intl Journal for Rock Mechanics and Mining Sciences 35, 4-5, 529-530.*

[3] *Papamichos E, Flatebø R, Stenebråten JF (2009). A model for destructured and water sensitive chalk. In Computational Geomechanics ComGeo I - 1st Intl Symposium on Computational Geomechanics, S Pietruszczak et al (eds), 81-94, Juan-les-Pins, France. Invited Lecture.*

[4] *Lagioia R, Nova R (1995). An experimental and theoretical study of the behaviour of a calcarenite in triaxial compression. Géotechnique 45, 4, 633-648, doi: 10.1680/geot.1995.45.4.633.*

[5] *Papamichos E, Berntsen AN, Flatebø RE, Kristiansen TG, Vejbæk O, Omdal E (2023). Coupled mechanical and permeability model for grain crushing and pore collapse. ARMA23-718, 57th US Rock Mechanics/Geomechanics Symp, Atlanta, GA, USA.*

Coupled effect of hydrate saturation and confinement pressure on geomechanical response of gas hydrate bearing sediments

Mahima S Rao[1], Sahil Wani[1], Ramesh Kannan Kandasami[1]

[1] *Department of Civil Engineering, Indian Institute of Technology Madras, Chennai, India*

E-mail: 5mahimasrao5@gmail.com, shlwn76@gmail.com, rameshkk@civil.iitm.ac.in

Keywords: geomechanical response, deviatoric stress, dilation, strain-softening

1. Introduction

Gas hydrates are a promising alternate unconventional energy resource due to their abundant existence, high energy density, and relatively low carbon footprint. However, methane extraction from hydrate-bearing sediments (HBS) poses significant geohazards due to phase transitions occurring within sediment pores [1]. Thus, understanding the geomechanical characteristics of HBS is crucial. The current study experimentally investigates the strength, stiffness and volumetric deformations of HBS accounting for variations in hydrate saturation and effective confinement pressure. The volumetric fraction of hydrates (hydrate saturation) influences the geomechanical response by binding sediment grains, bridging gaps between them, or filling pores. Additionally, the confining pressure is examined as it indirectly represents the depth at which HBS occurs, influencing its mechanical response. The experimental analysis of the coupled effect of hydrate saturation and effective confinement pressure carried out in the present study revealed their combined influence on the mechanical behaviour of HBS, aiding in the realistic assessment of reservoir stability and response under in-situ conditions. Additionally, a recent and advanced gas hydrate hypoplastic constitutive model [2] is calibrated using the current experimental results. Following the model validation, several numerical experiments are conducted for various hydrate saturations (0, 5, 10, 15, 20, 30, 35, 40 %) and confining pressures (0.5, 0.75, 1, 1.25, 1.5, 1.75, 2, 2.25 MPa), offering a cost-effective and time-efficient alternative to extensive experimental testing.

2. Methodology

The experiments were conducted using an advanced high-pressure, temperature and gas-controlled triaxial apparatus. The hydrates were formed in host sand via the excess gas method [3], targeting hydrate saturation (S_h) levels: 0%, 20%, and 40%. Triaxial experiments were performed under effective confining pressures (σ_3') of 1, 2, and 3 MPa. The obtained experimental data were used to calibrate and validate the recent hypoplastic constitutive model [2]. The model predictions were compared with experimental results to assess its efficacy.

Results

The series of consolidated drained triaxial compression experiments (Fig. 1) suggest that the maximum deviatoric stress (q_{max}) increases with σ_3' across all hydrate saturations (S_h = 0%, 20%, 40%). Further, for a given σ_3', q_{max} also rises with S_h, however the increase is negligible upto S_h = 20% at σ_3' = 2 and 3 MPa. Stress-strain analysis indicates a transition from strain-softening to hardening and volumetric response shifts from dilation to contraction with higher σ_3', especially at higher S_h. Further, the stress-strain response obtained from the calibrated hypoplastic model was compared with experimental results (Fig. 2) and the model closely matched with the observed data.

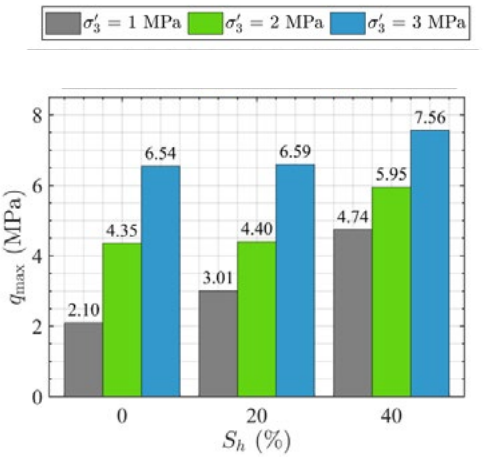

Fig. 1: Maximum deviatoric stress obtained for the specimens at different σ_3'

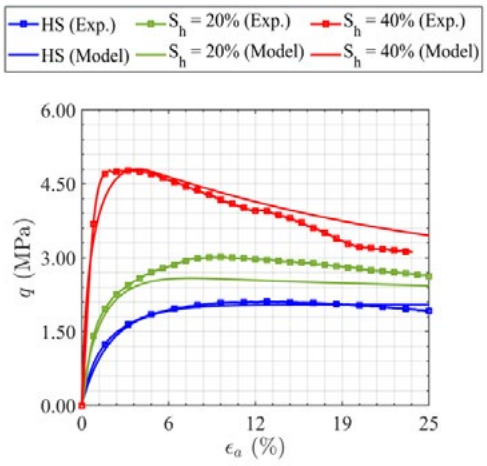

Fig. 2: Comparison of model prediction with experimental findings at σ_3' = 1 MPa

3. Conclusion

The experimental study on HBS revealed that at greater depths, lower hydrate volume fractions contribute less to the geomechanical strength. In contrast, higher hydrate fractions significantly improve strength even at deeper sediment layers. Additionally, the study confirmed that an advanced hypoplastic constitutive model effectively captures the geomechanical response of HBS with reasonable accuracy.

4. References

[1] Wani, Sahil, Rahul Samala, Ramesh Kannan Kandasami, and Abhijit Chaudhuri. 'Positioning of horizontal well-bore in the hydrate reservoir using a custom developed coupled THMC solver.' Computers and Geotechnics, 161 (2023).

[2] Wani, Sahil, Ramesh Kannan Kandasami, and Wei Wu. 'Hypoplastic model for gas hydrate-bearing sediments considering pore morphology.' Computers and Geotechnics, 181 (2025).

[3] Rao, Mahima S., Sahil Wani, and Ramesh Kannan Kandasami. 'Effect of Hydrate Morphology on Geomechanical Behavior of Gas Hydrate Sediments.' In Geotechnical Frontiers (2025).

Acid-assisted subcritical crack propagation in carbonate rocks considering chemical ductillization

Xiaojie Tang[1, 2] and Manman Hu[2*]

[1.] College of Civil Aviation, Nanjing University of Aeronautics and Astronautics, China
E-mail: xjtang@connect.hku.hk
[2.] Department of Civil Engineering, The University of Hong Kong, Hong Kong
E-mail: mmhu@hku.hk

Keywords: Subcritical crack growth, Acidic environment, Chemo-mechanics, Micro-cracking, Chemical ductilization.

1. Introduction

For carbonate-rich reservoirs, acidizing treatment is often incorporated as it assists effectively in promoting the crack propagation in a subcritical regime[1]. How a crack propagates in a stressed geomaterial susceptible to mineral mass removal in an acidic environment remains an open question[2,3]. Meanwhile, the chemically induced "ductillization" by reactive environments and its interaction with rock inhomogeneities on crack propagation has rarely been explored. Here, we investigate using a reactive chemo-visco-plasticity model considering the effect of micro-fracturing enhanced chemical reaction and shrinkage. Numerical studies on a single blunt-tip crack propagating into a stressed medium with crack surface subject to fluid pressurization and a long-lasting acid exposure are presented.

2. Reactive chemo-visco-plasticity for carbonate rocks in a reactive environment

For the irreversible portion of the deformation, we follow the strategy proposed by Tang and Hu[4], where the magnitude of the plastic strain rate $\dot{\lambda}$ is expressed through deviatoric and volumetric components,

$$\dot{\lambda} = \sqrt{\dot{\varepsilon}_q^{pl\,2} + \dot{\varepsilon}_v^{pl\,2}} \tag{1}$$

where $\dot{\varepsilon}_q^{pl}$ and $\dot{\varepsilon}_v^{pl}$ represent the deviatoric and volumetric invariants of the plastic strain rate, respectively. Both components are assumed to follow Perzyna's overstress model of viscoplasticity:

$$\begin{cases} \dot{\varepsilon}_q^{pl} = \dot{\varepsilon}_{\mathrm{ref}} \langle \frac{q - y_q}{\sigma_{\mathrm{ref}}} \rangle^m \\ \dot{\varepsilon}_v^{pl} = \dot{\varepsilon}_{\mathrm{ref}} \langle \frac{p' - y_{p'}}{\sigma_{\mathrm{ref}}} \rangle^m \end{cases} \tag{2}$$

The effect of chemical mass removal on the irreversible component of the rock mechanical behaviour is expressed through a REV-averaged variable, ξ^{REV}, defined as

$$\xi^{REV} = \int_0^t (1 + \eta\hat{\varepsilon})\dot{\xi}^{loc} dt \tag{3}$$

The following expression is adopted for describing the effect of chemical degradation on the yield limits

$$y_{p',q} = Y_{p',q}(1 - \beta_{p',q}\, \xi^{REV}) \tag{4}$$

3. Subcritical growth of a single crack subject to chemically reactive environment

Numerical results based on the reactive chemo-visco-plasticity model on subcritical growth of a single fracture subject to fluid pressurization and a chemically reactive environment are illustrated in Fig. 1. The effect of material heterogeneity is considered by imposing a randomly distributed local mass removal, e.g. within the range of [0, 0.05] on the entire process zone as the initial conditions. Compared to the homogeneous case ($\xi_0^{loc} = 0$) where the initial mechanical properties are uniformly distributed within the process zone, the crack in rocks with initial defects propagate significantly faster under the same chemical environment. It is evident that a pronounced localization of deviatoric strain develops in proximity to the advancing crack tip, and that the nucleation of micro-bands from initial heterogeneities corresponds to where the crack propagation accelerates.

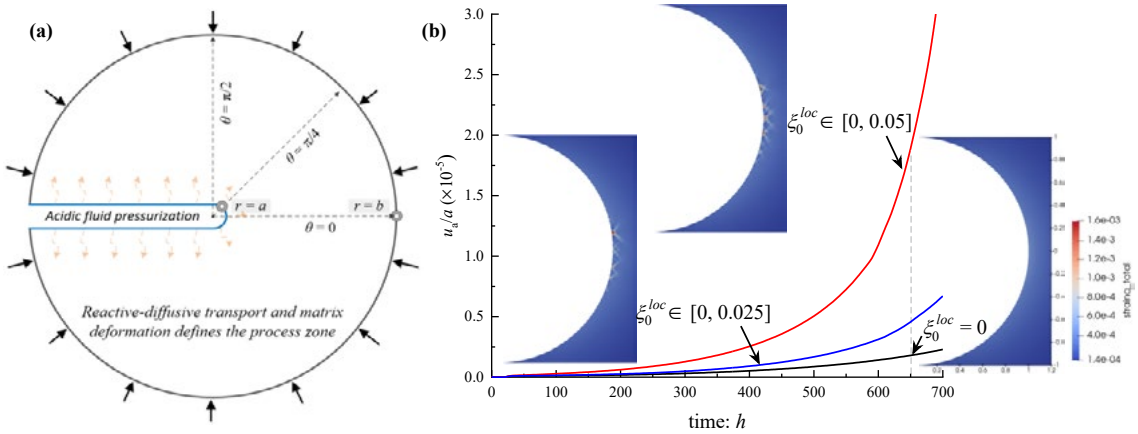

Fig. 1: ***(a)*** *Numerical setup of mode-I crack propagation in acidic environment.* ***(b)*** *Time evolution of the crack propagation for cases with various degrees of preset heterogeneity. Patterns of deviatoric strain (total strain) near the crack tip at a timestep of 650 hours' acid exposure are depicted.*

4. Conclusion

The current study presents a numerical investigation on the propagation of a single macroscopic crack in chemical environment, employing a reactive-visco-plasticity model. Our results show that the propagation of the macroscopic crack is significantly accelerated when an initial imperfection in the rock considered. Subcritical growth of the crack accelerates when a network of micro-bands self-organizes inside the chemically enabled plasticity zone in front of the macroscopic crack-tip.

5. References

[1] *Atkinson, B.K., 'Subcritical crack growth in geological materials', Journal of Geophysical Research: Solid Earth, 89(B6), 4077-4114 (1984).*
[2] *Hu, M.M., Hueckel, T., 'Modeling of subcritical cracking in acidized carbonate rocks via coupled chemo-elasticity', Geomechanics for Energy and the Environment, 19, 100114 (2019).*
[3] *Hu, M.M., Hueckel, T., 'Environmentally Enhanced Crack Propagation in a Chemically Degrading Isotropic Shale', Géotechnique, 63(4), 313-321 (2013).*
[4] *Tang, X.J., Hu, M.M., 'A Reactive-Chemo-Mechanical Model for Weak Acid-Assisted Cavity Expansion in Carbonate Rocks', Rock Mechanics and Rock Engineering, 56, 515-533 (2023).*

Fluid flow and hydraulic fracturing in soft sands

Charalampos Konstantinou[1,2], Panos Papanastasiou[1,2]

[1] Department of Civil and Environmental Engineering, University of Cyprus
[2] PHAETHON Centre of Excellence
E-mail: ckonst06@ucy.ac.cy, panospap@ucy.ac.cy
Keywords: artificial sandstones, MICP, infiltration, permeability, strength

1. Introduction

Fluid injection in reservoirs is crucial in geo-energy applications such as hydraulic fracturing—used to stimulate tight reservoirs and control sand production—and water flooding, where avoiding fracturing is key to ensuring a uniform reservoir sweep. In weakly cemented reservoirs, however, the shift between hydraulic fracturing and fluid infiltration is not well defined, as classical fracture mechanics do not fully apply; instead, fluid diffusion may dominate, influenced by in-situ stresses, rock strength, and injection parameters. In shallower ground, lower in-situ stresses allow for volume changes that lead to cavity formation rather than fractures, which is important for applications like managed aquifer recharge, hydraulic barriers, and groundwater decontamination. These principles also underpin emerging unconventional uses such as CO_2 and hydrogen storage. This study analyzes fluid flow experiments on weakly cemented sandstones to identify key parameters affecting the transition from infiltration to fracturing, with a particular focus on hydraulic fracturing behavior as indicated by pressure responses.

2. Methodology

Fluid injection and hydraulic fracturing tests were conducted on artificially created cemented weak rocks that simulated poorly consolidated sands. These experiments examined how applied stresses, rock strength, and pumping parameters influenced the outcomes. A custom-designed fracture capture apparatus was used specifically for conducting hydraulic fracturing in highly porous media. The artificially cemented sandstones are developed using microbially induced calcium carbonate precipitation (MICP), a bio-cementation method that introduces calcium carbonate within the porous network [1]. These specimens have various cementation levels which define the strength of the material and the hydraulic properties (hydraulic conductivity and porosity). The apparatus is designed for highly porous media where infiltration is the primary process. In this setup, a cylindrical specimen—150 mm in diameter and 40 mm thick—is subjected to three independent stresses [2]. A Perspex window at the base allows for real-time observation and recording of infiltration as well as fracture initiation and propagation.

3. Main Results

Figure 1 shows the fracture patterns observed during selected tests. With low cementation, the specimens exhibit widespread damage, featuring irregular fractures and grain-scale disaggregation that form a cavity near the injection point. In contrast, higher cementation leads to more localized damage with fractures oriented perpendicular to the minimum

horizontal stress, a behavior typical of brittle materials. Increasing the mean stress amplifies the damage: low cementation specimens collapse completely under high stress, while those with higher cementation, though still significantly damaged, fare better. The fracture modes shift from shear failure at low cementation to mixed shear-tensile failure at higher cementation. Additionally, pressure profiles reveal that generating fractures requires much higher pressures compared to tests with passive boundaries or those using strongly consolidated sandstones. The findings show that applied mean stress and flow rate are key in determining whether a specimen forms distinct, crack-like fractures (at higher cementation) or experiences cavity formation and disaggregation (at lower cementation). A Support Vector Machine regression model, which used variables like stress, flow rate, viscosity, permeability, and unconfined compressive strength, confirmed these results by accurately predicting peak pressure.

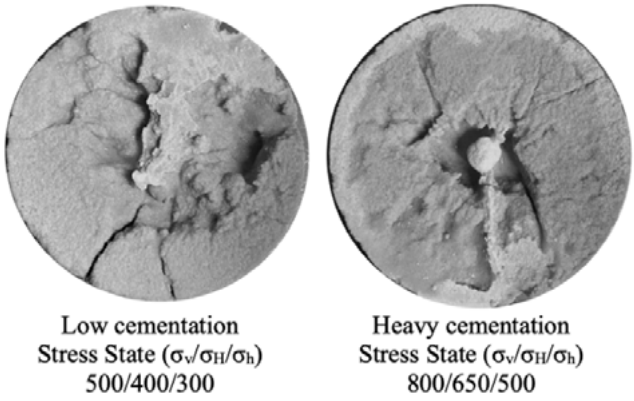

Fig. 1: Selected infiltration and fracturing patterns derived from the fluid flow experiments.

4. Conclusions

This study highlights the intricate relationship between mechanical and hydraulic properties in weakly cemented sandstones during fluid injection, offering valuable insights for optimizing geo-energy practices such as hydraulic fracturing, reservoir management, wellbore strengthening, and other subsurface hydrological applications

Acknowledgements

Funding from the European Regional Development Fund and the Republic of Cyprus through the Research Promotion Foundation (Cyprus RPF, RESTART 2016–2020 PROGRAMMES, Project H2StorEMed, BILATERAL/ISRAEL (MOST)/0224/0039.

5. References

[1] Konstantinou, C., Biscontin, G., Jiang, N. J., & Soga, K. (2021). Application of microbially induced carbonate precipitation to form bio-cemented artificial sandstone. Journal of Rock Mechanics and Geotechnical Engineering, 13(3), 579-592.

[2] Kandasami, R. K., Konstantinou, C., & Biscontin, G. (2023). Development of a fracture capture simulator to quantify the instability evolution in porous medium. arXiv preprint arXiv:2304.00207.

Numerical Investigation on the Influence of Acid-Insoluble Minerals in Acid Wormholing in Carbonates

Kenji Furui[1], Keita Yoshioka[2]

[1] *Department of Earth Sciences, Resources and Environmental Engineering, Waseda University, Tokyo, Japan*
E-mail: furui@waseda.jp
[2] *Department Geoenergy, Montanuniversität Leoben, Austria*
E-mail: keita.yoshioka@unileoben.ac.at

Keywords: phase-field approach, carbonate matrix acidizing, wormholing, reactive infiltration instability

1. Introduction

In matrix acidizing in carbonate reservoirs, high-permeability flow channels known as wormholes are formed. However, many aspects of the complex branching and extension behavior of wormholes remain unclear. In this study, we developed a hydro-chemical coupled numerical model that considers the mineral composition of rocks to evaluate the impact of acid-insoluble minerals on the wormhole geometry and efficiency.

2. Methodology

The numerical model in this study incorporates equations for phase-field evolution, acid advection-diffusion, and single-phase fluid flow in porous medium [1, 2]. Rock particles consist of dissolvable carbonate minerals and insoluble silica-based minerals, with dissolution represented by the phase-field variable. A linear relationship between porosity and phase-field variable is assumed, and permeability is computed using the Carman-Kozeny equation.

In the numerical experiment, a square domain of 0.5 m×0.5 m with a 1 m thick block is assumed. The acid (28 wt% HCl) is injected from the center hole at a constant rate of 2.4×10^{-2} m³/s creating radially extending wormholes. Case studies were performed for rocks with various carbonate contents and permeability fields to assess the effects of rock heterogeneity on well injectivities.

3. Main Results

For the homogeneous porosity and permeability rock that consists of pure calcite (100% carbonate mineral content), Initially, eight wormholes formed, but four dominant ones emerged, growing symmetrically (Fig. 1a). When carbonate mineral fractions were randomly distributed, increased branching reduced the lengths of dominant wormholes (Fig. 1b). For the rock with low-carbonate content, wormholes failed to form, and the borehole expanded as face dissolution (Fig. 1c). On the other hand, when the rock has high-carbonate content with some small variation, reduced leak-off resulted in smaller but longer wormholes (Fig. 1d).

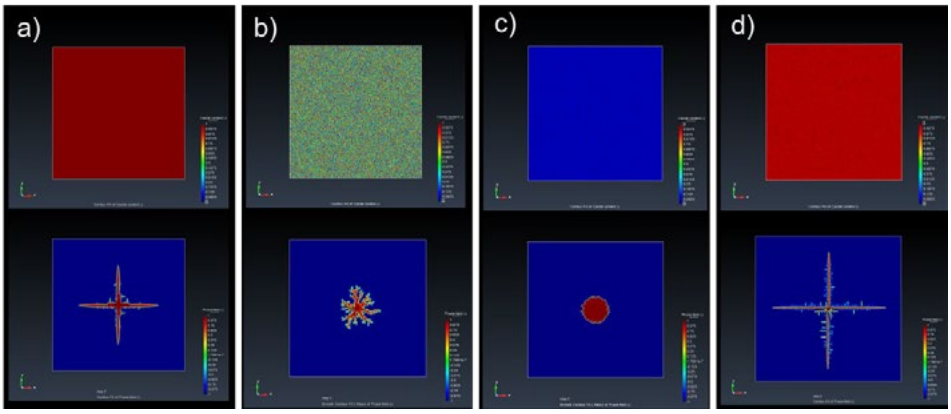

Fig. 1: Wormhole simulations in isotropic rocks with varying calcium carbonate content: (a) pure calcite (1.0), (b) random distribution (0.0-1.0), (c) low content (0.0-0.1), (d) high content (0.9 – 1.0). The top row shows calcium carbonate content while the bottom row shows phase-field values indicating liquid (-1) and solid (1) phases.

For heterogeneous permeability distribution, dominant wormholes developed but became asymmetric (Fig. 2a). Fewer dominant wormholes formed, but they grew longer. When carbonate content varied significantly, frequent branching hindered dominant wormhole formation (Fig. 2b).

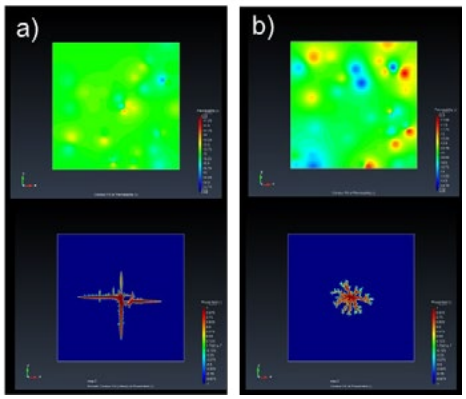

Fig. 2: Wormhole simulations in anisotropic rocks with varying calcium carbonate content: (a) pure calcite (1.0), (b) random distribution (0.0-1.0). The top row shows permeability values while the bottom row shows phase-field values.

4. Conclusion

A small presence of insoluble minerals may improve the wormhole efficiency. However, as the amount of insoluble minerals increases, it becomes an obstacle to wormhole growth, impairing stimulation results. Furthermore, permeability heterogeneity can either enhance or diminish wormhole efficiency, requiring careful consideration.

5. References

[1] Furui, K. and Yoshioka, K., 'A phase-field modeling study for reaction instability and localized fluid flow in carbonate rocks', Geoenergy Science and Engineering. Vol 245 (2025).
[2] Furui, K., Abe, T., Watanabe, T., Yoshioka, K., 'Phase-field modeling of wormhole formation and growth in carbonate matrix acidizing', Journal of Petroleum Science and Engineering, Vol 209 (2021).

Time-dependent thermo-viscoplastic deviatoric destressing of salt caprocks

Renato Poli[1], Maria-Aikaterini Nikolinakou[2], D. Nicolas Espinoza[1], Kamy Sepehrnoori[1]

[1] *Department of Petroleum and Geosystems Engineering, University of Texas at Austin, Austin, United States*
E-mail: rpoli@utexas.edu, espinoza@austin.utexas.edu, kamys@mail.utexas.edu
[2] *Bureau of Economic Geology, University of Texas at Austin, Austin, United States*
E-mail: mariakat@mail.utexas.edu

Keywords: THM, Viscoplasticity, Creep, Salt rock, Finite Element Method

This work investigates the behavior of salt as caprock of a reservoir under fluid injection for Enhanced Oil Recovery and fluid storage/disposal. Specifically, we model the time-dependent response of salt layers when exposed to an underlying reservoir with increased pressure and decreased temperature for an extended period. This investigation is relevant for fluid injection in deep reservoirs, for example, where salt is the sealing caprock, the temperature contrast between the injected fluid and the in-situ rock is high ($> 50°C$), and maximizing the injection rate is a practical objective.

We employ an in-house multi-physics finite element simulator, that uses iterative coupling to model the interaction between temperature, flow, and mechanics. The mathematical formulation of the simulator covers linear porothermoelasticity for the reservoir and thermoviscoplasticity for the salt layers. The simulator is validated to known analytical solutions in simple geometries.

We investigate the transient stress response of a salt layer under thermal stress, emulating the temperature around an injector well after a long-term cold-water injection (Figure 1). We observe an instantaneous (elastic) rotation in the direction of the principal stresses due to the arching effect caused by the thermal contraction of the reservoir. This effect is partially compensated by the reservoir dilation due to increased pore pressure. The arching effect protects the caprock from vertical fracture propagation within the cooled rock volume. We also observe significant transients in Von Mises stress around the cylindrical injection hole across a thick salt layer over short periods of time (Figure 2).

Finally, we present a parametric sensitivity investigation to estimate the characteristic time for the deviatoric destressing of the salt under uncertainties. Our results indicate that, unlike brittle rock, the transient-state response salt bodies act to significantly dissipate deviatoric transient states, so that, in steady-state, deviatoric stresses of the rock are small (<10MPa). The time constant of the system strongly depends on the model parameters and heterogeneities of the salt layers. Aside from extreme scenarios, our results show that significant deviatoric destressing is still expected inside the operational timeframe, lasting in the weeks-to-month range before approaching the steady-state asymptote.

These numerical estimates of the residual deviatoric stresses within the salt caprock suggest that EOR projects cannot rely on a steady isotropic state of stresses but can expect a residual constant in the short term. Although we build our parametric study on salt layers representing reservoir caprocks, we can extend our observation to broader cases, such as the deviatoric destressing of salt caverns subjected to seasonal loading and unloading. Our findings can also benefit well design through salt bodies and help mitigate risks associated with drilling in salt systems.

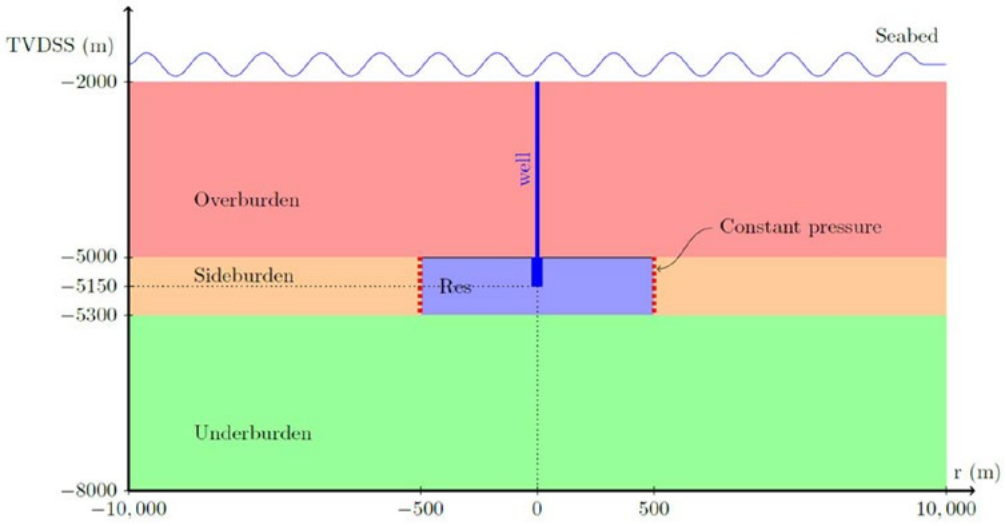

Figure 1 – The model used as a reference. The overburden caprock is a viscoplastic salt layer, and the reservoir is a brittle poroelastic carbonate.

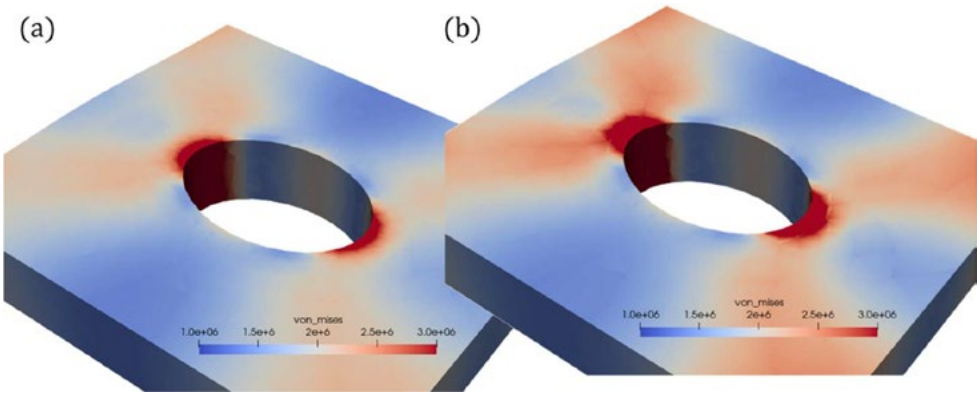

Figure 2 – Evolution of Von Mises stress around a cylindrical hole in a salt layer under asymmetric load. (a) Instantaneous elastic stress response; (b) Stress after 3 days. Comparison between the 2 illustrates the substantial Von Mises stress evolution despite that short time interval.

Impact of Boundary Conditions for Plants in Present and Future

M. S. Maddah Sadatieh[1,2], A. Tsoampousi[1], A. Paschalis[3,1]

[1] *Civil and Environmental Engineering, Imperial College London, London, UK*
E-mail: m.maddah-sadatieh22@imperial.ac.uk
[2] *Science and Solutions for a Changing Planet DTP, London, UK*
[3] *University of Cyprus, Civil and Environmental Engineering, Nicosia, Cyprus*

Keywords: Soil-plant-atmosphere interaction; Plants; Stability; Numerical analysis.

1. Introduction

Soil-plant-atmosphere interaction (SPAI) significantly affects slope's mechanical and hydraulic behavior. Therefore, rendering modelling this Boundary Condition (BC) important, for present and future years. Recently fully coupled hydro mechanical analysis have implemented SPAI as an infiltration BC [1]. However, this BC has generally been applied only at the soil surface. Whereas transpiration happens within the root zone.

In this paper, a typical cut slope in the UK has been chosen and assumed to be covered by trees. The analysis has been run with only surface BC and with surface and internal BCs. The Factors of Safety (FoS) for both analysis for the present and future are compared, to examine the effect of internal BCs.

2. Methodology

A cut slope, 8 m high and 28 m wide, is assumed to be covered by trees with a root depth of 2 m. The soil profile consists of 3 m of Weathered London Clay (WLC), 45 m of Intact London Clay (ILC) and 23 m of Lambeth Group Clay (LGC). SPAI is modelled using an ecohydrological model (T&C [2]) coupled with a geotechnical model (PLAXIS 2D [3]) using two approaches: A) only a surface BC, B) a surface BC for all hydraulic fluxes except transpiration and internal BCs for transpiration, positioned along the root zone.

A 2D plane-strain model, and all soil layers were modelled with Mohr-Coulomb failure criterion with isotropic small strain stiffness [4]. Permeability varied anisotropically with mean effective stress [5]. WLC was allowed to desaturate using a Van-Genuchten Soil Water Retention Curve [6], [7]. ILC and LGC were set to saturated. The analysis was run from 1997 to 2008 for initialization, and then from 2021 to 2040. For the future climate, data from UKCP18 for the worst-case scenario (RCP8.5) was used [8, 9].

3. Main Results

Fig. 1 (a) shows the FoS for both analysis from 1997 to 2008 and Fig. 1 (b) shows the FoS for the climate projection years, 2021 to 2040. As shown in Fig. 1 (a), FoS values are similar with instances with analysis B occasionally being slightly higher. The maximum difference is around 0.16 in Aug 2001. In future years, these differences are more visible, where the maximum difference in FoS is around 0.38 in November 2031.

4. Conclusion

Two modelling approaches were compared to investigate its effect on slope safety for present and future years: A) all hydraulic fluxes implemented at the soil surface and B) all hydraulic fluxes excluding transpiration applied at the surface and transpiration

applied at different depths of the root zone to mimic plant's behavior. During initial years, differences between approaches were minimal. As years passed, with the effect of climate change, these differences became more visible. However, they were not substantial enough to effect engineering decisions, meaning that for the considered cut slope, modeling SPAI at the soil surface appears to give adequate results.

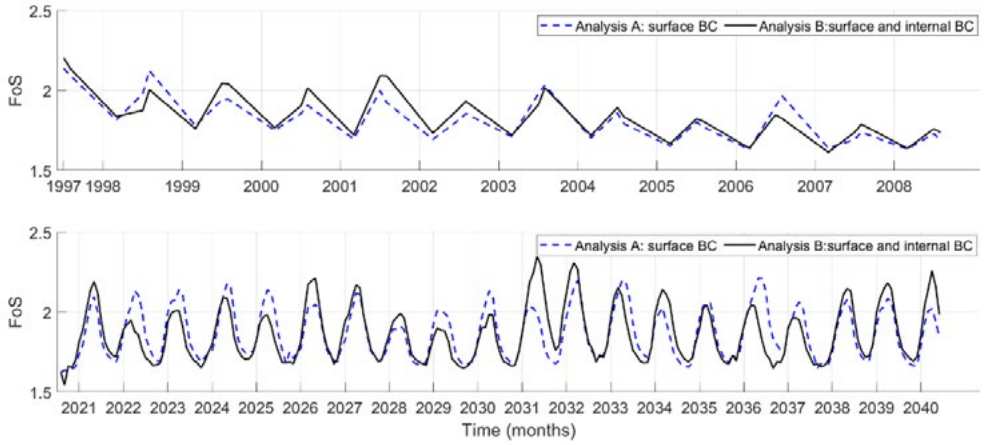

Fig. 1: FoS for the (a) initial years (1998 to 2008), and (b) Future years (2021 to 2040)

5. References

[1] A. Tsimapousi, D. M. Potts, e L. Zdravković, "Numerical study of the effect of soil–atmosphere interaction on the stability and serviceability of cut slopes in London clay", Canadian Geotechnical Journal, vol. 54, no 3, p. 405–418, mar. 2017, doi: 10.1139/cgj-2016-0319.

[2] S. Fatichi, "Tethys-Chloris (T&C) - Terrestrial Biosphere Model – Public release October 2021", 2021. Acessado: 15 de agosto de 2024. [Online]. Disponível em: https://codeocean.com/capsule/0294088/tree/v2

[3] Sequent, "PLAXIS 2D (2024.01)", 2024.

[4] D. M. G. Taborda, S. Kontoe, e A. Tsiampousi, "IC MAGE Model 01 - strain-hardening/softening Mohr-Coulomb failure criterion with isotropic small strain stiffness (Version 2.1)", Zenodo, 2023.

[5] D. M. G. Taborda, A. Tsiampousi, e S. Kontoe, "IC MAGE Flow Model 02 - Stress-dependent anisotropic permeability (1.0)", Zenodo, 2023.

[6] M. T. Van Genuchten, "A Closed-form Equation for Predicting the Hydraulic Conductivity of Unsaturated Soils 1", 1980.

[7] J. A. SMETHURST, D. CLARKE, e W. POWRIE, "Factors controlling the seasonal variation in soil water content and pore water pressures within a lightly vegetated clay slope", Géotechnique, vol. 62, no 5, p. 429–446, maio 2012, doi: 10.1680/geot.10.P.097.

[8] "UKCP18 Convection-Permitting Model Projections for the UK at 2.2km resolution", CEDA Archive, Acessado: 15 de agosto de 2024. [Online]. Disponível em: https://catalogue.ceda.ac.uk/uuid/ad2ac0ddd3f34210b0d6e19bfc335539/

[9] M. Meinshausen et al., "The RCP greenhouse gas concentrations and their extensions from 1765 to 2300", Clim Change, vol. 109, no 1, p. 213–241, nov. 2011, doi: 10.1007/s10584-011-0156-z.

A simple 1D model for simulating volume changes in clays caused by variations of the moisture content

Dimitrios Loukidis[1], Georgia Lazarou[1], Ploutarchos Tzampoglou[1], Thrasivoulos Stylianou[1]

[1] *Department of Civil & Environmental Engineering, University of Cyprus, Nicosia, Cyprus*
E-mail: loukidis@ucy.ac.cy

Keywords: clays, swelling/collapse, constitutive model, effective stress

1. Introduction

Soils and sedimentary rocks with significant clay content exhibit large tendency for development of volumetric strain due to changes in moisture content, often causing various degrees of damages to infrastructure that is in contact with them. More specifically, clays increase their volume upon wetting and shrink upon drying, This is because of changes in the effective stress and the hydration of the clay particles, with the latter being the main mechanism. As such, modeling these volume changes cannot be done by relying solely on a definition of effective stress for partially saturated soils. Moreover, under high vertical stresses, soil wetting may lead to a collapse of its matrix, i.e. development of contractive strains instead of swelling.

Herein, we present a simple effective stress model for the prediction of the clay heave and settlement due to changes in moisture content. To achieve this, the model combines an elastic effective stress law with a mechanism of development of additional inelastic strains. The model is calibrated for marls of various plasticity using swelling /collapse tests performed in the oedometer.

2. Effective stress model

The constitutive model uses the Bishop's effective stress definition [1]:

$$\dot{\sigma}'_{ij} = \dot{\sigma}_{ij} + (\chi s)\delta_{ij} \tag{1}$$

where σ'_{ij} and σ_{ij} are the effective and total stresses, s is the soil suction, and δ_{ij} is the Kronecker's delta. It is assumed that the variable χ is equal to the degree of saturation S_r. The elastic part of the model follows the Hooke's law:

$$\dot{\sigma}'_{ij} = D_{ijkl}\dot{\varepsilon}_{el,kl} = D_{ijkl}(\dot{\varepsilon}_{kl} - \dot{\varepsilon}_{pl,kl}) \tag{2}$$

where ε_{el} and ε_{pl} are the tensors of elastic and plastic strains, respectively, and D_{ijkl} is the isotropic elastic stiffness matrix defined in terms of Young's modulus E and Poisson's ratio v. The E is set to vary according to the following power law:

$$E = A\sigma'^{n}_{v} p_a^{1-n} \tag{3}$$

where σ'_v is the effective vertical stress, A and n are model parameters and p_a =100kPa. The plastic volumetric strain, which is assumed to be distributed evenly in the three normal strains, is computed through the following equation:

$$\dot{\varepsilon}_{\mathrm{vpl}} = -\left(\alpha \dot{s} \chi - (1-a)\langle -\dot{s}\rangle \chi\right) / D_{\mathrm{vpl}} \tag{4}$$

where α is a model parameter, <•> denote Macaulay brackets, and D_{vpl} is a plastic modulus, which is set to be a decreasing function of the total vertical stress:

$$D_{\mathrm{vpl}} = p_{\mathrm{a}} / 3 + \left[c_1 / \left(1 + c_3(\sigma_{\mathrm{v}} / p_{\mathrm{a}})\right) + c_2\right] \sigma_{\mathrm{v}}'^{m} p_{\mathrm{a}}^{1-m} \tag{5}$$

where c_1, c_2 and c_3 are model parameters.

3. Oedoemeter test simulations

Fig. 1 compares the experimental data from swelling/collapse tests performed in a classical oedometer [2] with the model's predictions for medium expansive Nicosia marl (plasticity index PI=23, clay content 20%) with an initial degree of saturation 52%. It can be seen in Fig. 1a that the constitutive model has the ability to predict soil collapse for vertical stress greater than the swelling pressure (90 kPa). If the mechanism that predicts inelastic volumetric strains (eq. 4) is ignored, the constitutive model predicts only swelling behavior which is practically independent of the applied vertical stress. The model predictions for very highly expansive marl (PI=43-50, clay content 43%-45%) with initial degree of saturation 85% are compared with experimental data in Fig. 1b. The model is able to predict the high free swelling strain of about 9%, which is twice as much what would be predicted in the absence of eq. (4).

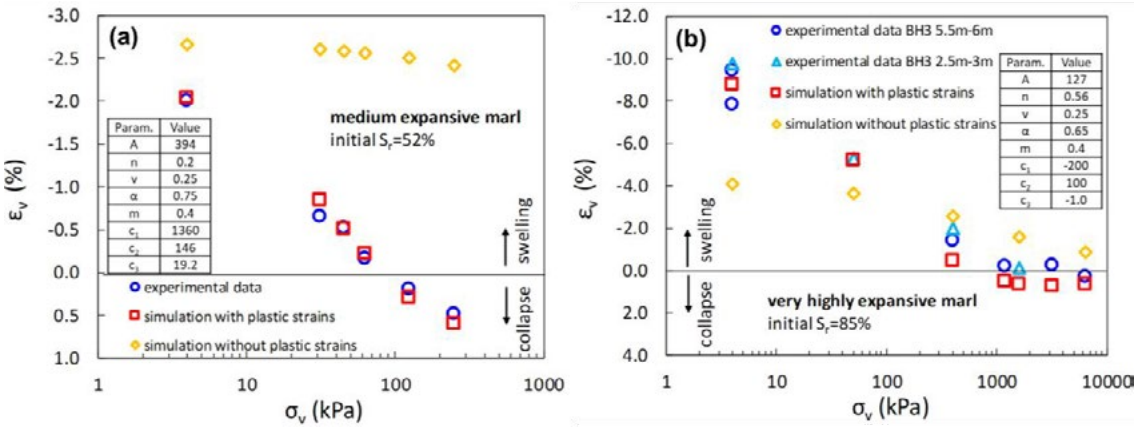

Fig. 1: Vertical strain upon inundation: a) medium expansive and b) very highly expansive marl

4. Conclusions

A simple one-dimensional constitutive model was presented for simulating the volumetric response of clays to moisture changes. Using a mechanism that predicts additional strains due to changes in suction, the model captures the experimentally observed behavior.

5. References

[1] Bishop, A.W. 'The principal of effective stress', Teknisk ukeblad, 39, pp. 859-863 (1959)

[2] ASTM (D4546 -14) Standard test methods for one-dimensional swell or collapse of soils. American Society for Testing of Materials, West Conshohocken

The future is green (hydrogen): THMC challenges for temporary subsurface hydrogen storage in depleted reservoirs and salt caverns

Suzanne Hangx[1]

[1] *High Pressure and Temperature Laboratory, Department of Earth Sciences, Faculty of Geosciences, Utrecht University, Utrecht, the Netherlands*
E-mail: s.j.t.hangx@uu.nl

Keywords: containment, microphysics, fluid-rock interactions,

1. Abstract

Renewable electricity generation, through solar and wind power, is increasing every year. However, the intermittent nature of renewable energy means that energy storage is becoming increasingly more important. Green hydrogen, generated using renewable energy, is considered to be an attractive low-carbon energy carrier, for the decarbonisation of the transport, power and heating sectors, as well as for fuel-energy intensive industries, such as the chemical and steel industries. While surface storage of hydrogen in tanks and pipelines offers limited storage and discharge capacity, subsurface storage in depleted oil/gas fields or salt caverns is able to cover GWh-energy supply.

Energy storage, in the form of natural gas, compressed air or oil, has already been proven successful. However, the small molecular size of hydrogen, its low viscosity and reactivity makes it a challenging fluid to contain. Though a handful of projects successfully storing hydrogen in salt caverns exist, the potential for reservoir storage is still largely unexplored. This form of energy storage will not only disturb the physical environment of the storage system, i.e. through changes in pore fluid pressure and effective stress, but also the chemical environment, by introducing a previously foreign fluid. In this keynote, I will outline the main thermal, hydrological, mechanical and chemical scientific challenges that exist when temporarily storing hydrogen fuel in depleted oil/gas fields and salt caverns.

Numerical modeling of hydrogen seep in Fairy Circles

Christine Detournay[1], Martin Schöpfer[2,3], Gabor Tari[4]

[1] *Itasca Consulting Group, Minneapolis, Minnesota, USA*
E-mail: christine@oneitasca.com
[2] *University of Vienna, Austria*
[3] *NiMBUC Geoscience, Vienna, Austria*
E-mail: martin.schoepfer@univie.ac.at
[4] OMV Exploration & Production, Vienna, Austria
E-mail: Gabor.Tari@omv.com

Keywords: fairy circle, natural hydrogen, two-phase flow, numerical modeling

1. Introduction

Fairy circles are natural circular surface depressions, devoid of vegetation, found in places such as Namibia, Brazil, Russia, Australia, and the U.S. [1]. They have been associated with hydrogen seeping to the surface, and recent prospections for green energy have revealed that they may be signs of renewable hydrogen reserves underground. Hydrogen is known to form underground when iron-rich rocks interact with water through a process called serpentinization [2]. It is envisioned that hydrogen seeps through fractures in the gas-generating basement and is released in localized sources at the contact with the overlying sedimentary layer [3]. Although little is known about the formation of the fairy circles, the speculation is that this natural gas reserve amounts to a considerable source of clean energy. This provides a strong incentive for further investigation on the topic.

2. Methodology

The paper explores the formation of fairy circles and their potential for hydrogen production using the fluid-mechanical commercial code FLAC [4]. The axi-symmetric model represents a 200 m thick layer of water-saturated sedimentary rock with a point source of gas at the base. Simultaneous flow of gas and water is simulated using Darcy's laws embedded in the two-phase flow logic. Buoyancy is accounted for via the density term in these laws. Capillary pressure and relative permeabilities are related to water saturation using Van Genuchten laws. Fluid-mechanical coupling is done in the extended framework of Biot poro-elasto-plastic theory. It relies on Bishop effective stress in which fluid pore pressure is taken as the average of water and gas pressures weighted by their respective saturation.

3. Main Results

The simulation results in Fig.1 show that the rock volume invaded by the gas is an inverted cone with circular footprint, a shape that is attributed to buoyancy. The simulations predict a larger gas flux near the centre of the fairy circle. The

measurements are in the range of published field data. The main parameters influencing the size of the fairy circle and the surface production are the source depth and intensity.

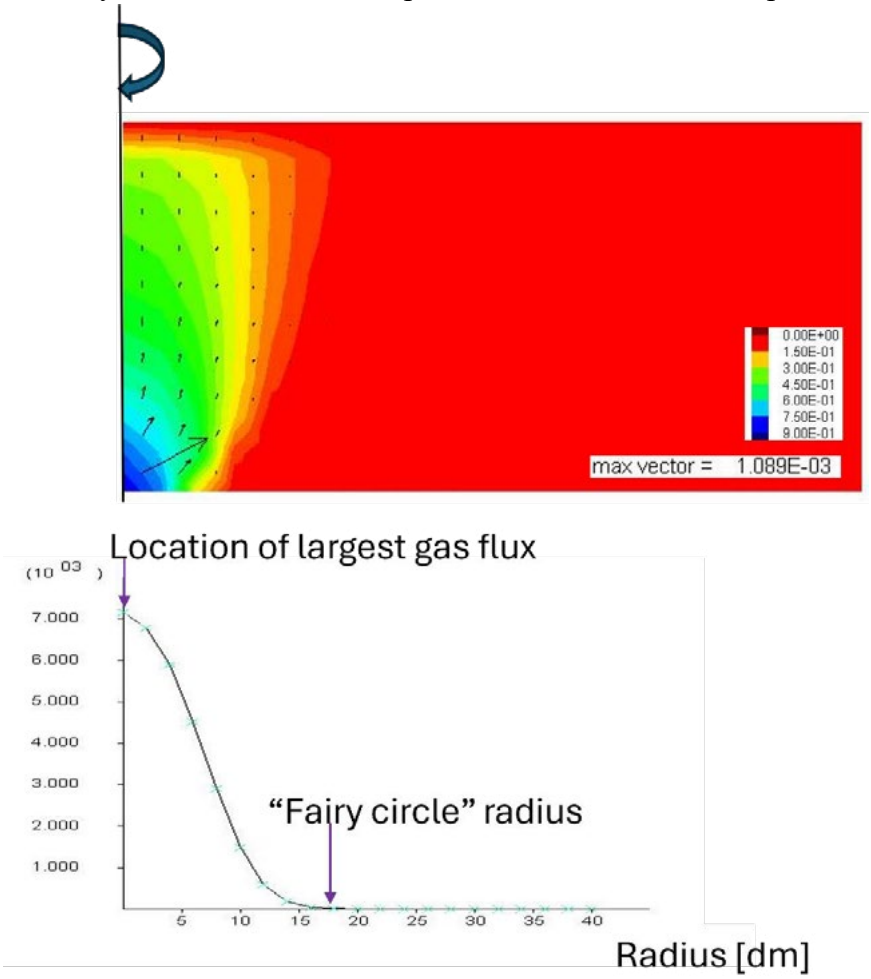

Fig.1: Gas saturation contours and flow vectors (top), gas production at the surface in m^3/m^2 over 3 years (bottom).

Numerical experiments are a valid tool to explore fairy circle formation. However, the findings must be sustained by field monitoring and laboratory experiments.

4. References

[1] Zaraska, M., "'Hydrogen fever' erupts after discoveries of large deposits of the clean gas", Scientific American. 8 May 2024.
[2] Zgonnik, V., 'The occurrence and geoscience of natural hydrogen: a comprehensive review', Earth-Science Reviews, 203, 103140. (2020).
[3] Tari, G., Natural Hydrogen Systems. De Gruyter Academic Publishing, Berlin, in press. (2025).[4] Itasca Consulting Group, Inc. FLAC — Fast Lagrangian Analysis of Continua, Ver. 8.1. Minneapolis: Itasca. (2019).
[4] Itasca Consulting Group, Inc. FLAC — Fast Lagrangian Analysis of Continua, Ver. 8.1. Minneapolis: Itasca. (2019).

Operational parameters assessment for a prospective pilot demonstration of underground hydrogen storage at Ketzin, Germany

Mrityunjay Singh[1*], Anna-Maria Eckel[2*], Cornelia Schmidt-Hattenberger[3*], Juliane Kummerow[4*], Lea Döpp[5*+], Maria Belen Febbo[6*], Marton Pal Farkas[7*], Peter Pilz[8*], Wisdom David[9*+], Ingo Sass[10*+]

[*]*Section 4.3 Geoenergy GFZ Helmholtz Center for Geosciences Department, Potsdam, Germany*
[+]*Institute of Applied Geosciences, Technical University Darmstadt, Darmstadt, Germany*
E-mail: [1]singh@gfz.de, [2]eckel@gfz.de, [3]conny@gfz.de, [4]jule@gfz.de, [5]doepp@gfz.de, [6]febbo@gfz.de, [7]farkas@gfz.de, [8]funghi@gfz.de, [9]wisdom@gfz.de, [10]sass@gfz.de

Keywords: Underground hydrogen storage, Operational parameters, THMCB processes

1. Introduction

The study aims to advance the technological readiness of green hydrogen storage in deep saline aquifers by comprehensively characterizing the thermo-hydro-mechanical-chemical-biological (THMCB) process controlling parameters. The Ketzin site, with its well-documented geological history and previous town gas and CO_2 storage operations at TRL levels 8 and 6, respectively, is an ideal prospective demonstration site for validating our integrated approach. By combining numerical simulations with targeted laboratory experiments, the study provides a scientific basis for operational decision-making, guiding the design of a prospective pilot demonstration at Ketzin. Figure 1 highlights 25 key operational parameters that govern hydrogen injection, storage, and recovery processes. Current work addresses both near-term operational challenges and long-term reservoir behavior, including the dynamic interactions among thermal gradients, two-phase fluid flow, rock deformation, geochemical reactions, and microbial hydrogen consumption, ensuring precise guidelines for injection protocols and overall reservoir management.

2. Methodology

We perform reservoir-scale multiphase flow simulations (COMSOL Multiphysics, and CMG GEM) and reactive transport modeling (PhreeqC, and Geochemist's Workbench) to capture THMCB interactions. The governing equations enforce mass and momentum balance [1], account for poroelastic stress-strain behavior, and incorporate kinetic rate laws for mineral dissolution - precipitation and microbial metabolism [2]. Laboratory experiments and data from literature supply growth rates and half-saturation constants for hydrogenotrophic microorganisms, and relative permeability-saturation relationships. Full coupling inside THM processes as well as in CB processes are adopted due to involved spatial and time scales.

3. Results

A comprehensive sensitivity analysis was conducted using numerical simulations and targeted laboratory experiments to assess the influence of key operational parameters on

reservoir performance. All 25 parameters were evaluated to determine their roles in driving pressure changes, plume migration, and fluid composition. Injection rate governs reservoir pressurization, while temperature variations affect fluid rheology and reaction kinetics. Permeability and porosity heterogeneities influence gas flow pathways, with wellbore design and completion procedures further shaping injection capacity. Chemical composition affects corrosion effects and mineral precipitation - dissolution, whereas microbial activity can consume hydrogen or generate secondary gases, altering local petrophysical conditions. Notably, our analysis reveals that small deviations in these parameters can initiate complex, non-linear feedback loops across thermal, hydraulic, mechanical, chemical, and biological domains, emphasizing the interdependent nature of these processes. Temperature fluctuations may accelerate or inhibit specific reactions, guiding injection strategies. Additional aspects, such as controlled overpressure limits, withdrawal protocols, and chemical additive injection, ensure storage integrity and longevity.

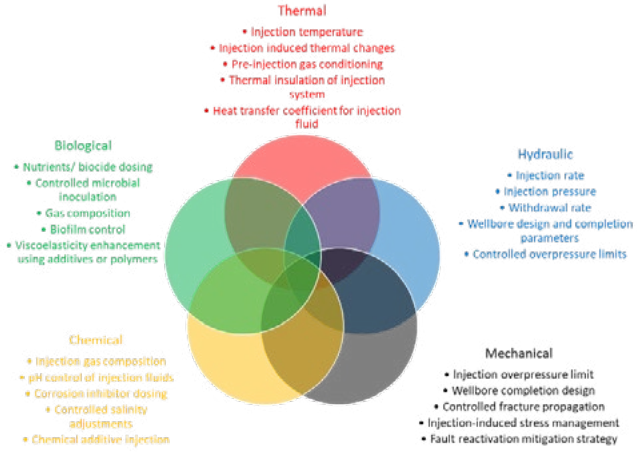

Figure 1: Operational or engineering parameters related to underground hydrogen storage in a deep saline aquifer.

4. Conclusions

Within GeoZeit/HyPrepare, this integrated framework systematically addresses the 25 important operational parameters that control hydrogen storage in deep saline aquifers for Ketzin site. Results emphasize the complex interaction of injection conditions, reservoir heterogeneity, geomechanical stability, chemical transformations, and biological processes. The coupled numerical modeling, and experimental data provide a scientific foundation for optimizing injection rates, temperature settings, well design, and injection fluid composition prior to a pilot demonstration at Ketzin.

5. References

[1] Ershadnia, Reza, Singh, M., et al. "Impact of geological and operational conditions on underground hydrogen storage." Int. J. of Hydrogen Energy 48, no. 4 (2023): 1450-1471.

[2] Würdemann, H., Möller, F., Kühn, M., et al. "CO_2SINK – From Site Characterisation and Risk Assessment to Monitoring and Verification: One Year of Operational Experience with the Field Laboratory for CO_2 Storage at Ketzin, Germany." Int. J. Greenhouse Gas Control, vol. 4, no. 6, (2010): 938–951.

A data-driven analysis for the changes in hydraulic properties of rocks under the presence of hydrogen

Eftychia Christodoulou[1], Charalampos Konstantinou[1,2], Panos Papanastasiou[1,2]

[1] *Department of Civil and Environmental Engineering, U of Cyprus, Nicosia, Cyprus*
[2] *PHAETHON Centre of Excellence*
E-mail: christodoulou.eftychia@ucy.ac.cy, konstantinou.charalampos@ucy.ac.cy, panospap@ucy.ac.cy

Keywords: hydrogen, porous media, porosity, permeability, Random Forests

1. Introduction

Green hydrogen is increasingly recognized as an effective energy storage medium, addressing intermittency challenges in renewable systems [1]. Large-scale hydrogen supply can only be achieved through underground storage. Currently, little is known about the changes in the hydraulic and mechanical properties of host rocks in the presence of hydrogen. This study assesses these changes in permeability and porosity using a data-driven approach on published experimental datasets. For example, an increase in porosity not only has important implications for hydrogen storage in depleted oil and gas reservoirs but also raises questions about the mechanical stability and integrity of the reservoir rocks [2]. These effects are analyzed in detail using machine learning (ML) algorithms.

2. Methodology

Data has been collected from the literature which relates to porosity and permeability changes of rock formations exposed to hydrogen. The input variables were the initial porosity and permeability, the different type of rocks (Sandstone/Siltstone, Carbonates/Limestone and Claystone/Mudstone), the temperature, pressure and the exposed time in hydrogen. The degree of saturation with brine along with hydrogen purity and the presence of natural gas or other gases (air, helium, or CO_2) were considered. A causality analysis was performed to identify the parameters with the most significant impact on fluid pressures. This analysis employed the random forest (RF) algorithm, an ensemble learning method that constructs multiple decision trees. In regression tasks, each decision tree generates a continuous prediction, and the final output is obtained by averaging the predictions from all trees. Beyond evaluating model accuracy, the importance of individual parameters was analyzed to determine their influence.

3. Results

For porosity changes, data have been collected from the literature, comprising 22 studies with a total of 194 data points. The output parameter for porosity changes is binary: 0 indicates no significant change in porosity (≤10%), while 1 represents a change in porosity (>10%). Random forests (RF) were used, with the model trained on 70% of the input data and tested on the remaining 30%. The RF model's accuracy is presented in the

form of a confusion matrix (Table 1). As shown, the model correctly predicts 47 out of 58 values, while classifying 5 values as significant porosity changes when, in reality, they were not. Additionally, it misclassifies 6 values as showing no change in porosity when they actually exhibited significant changes based on the collected data. The overall accuracy of the model is 0.8103, and the F1-score is 0.857.

Table 1. Confusion matrix

Prediction/Reference	**0**	**1**
0	33	6
1	5	14

Beyond evaluating model accuracy, the importance of individual parameters was analyzed to determine their influence on the outcome. As shown in Fig 1, the most important parameter for this classification task is the initial porosity, which is closely related to the type of rock (e.g., shales have very low porosity compared to sandstones). This is followed by environmental conditions—temperature, pressure, and experiment duration—which also play a significant role. The degree of specimen saturation has a lesser influence. Temperature and applied pressure are particularly important as they can induce changes in the porous medium's skeleton, facilitate chemical reactions, and affect hydrogen volume based on the pressure-temperature-volume relationship.

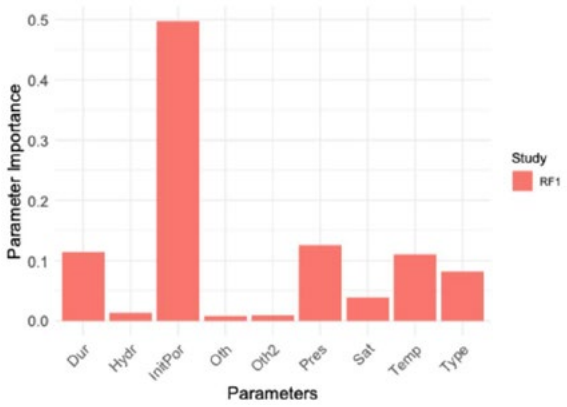

Fig. 1: The parameter importance of RF

Acknowledgements

This research is supported with funding from the European Regional Development Fund and the Republic of Cyprus through the Research Promotion Foundation (Cyprus RPF, RESTART 2016–2020 PROGRAMMES, Project H2StorEMed, BILATERAL/ISRAEL (MOST)/0224/0039.

4. References

[1] Ma et al., 'Large scale of green hydrogen storage: Opportunities and International Journal of Hydrogen Energy, pages 379-396 (2024).

[2] Aluah et al., 'An Experimental Study on the Caprock Integrity of Reservoirs to Assess the Repurposing Depleted Bakken Formation Oil and Gas Fields for Underground Hydrogen Storage', Society of Petroleum Engineers (2024).

Hydro-mechanical behaviour of carbonate reservoir rocks under cyclic hydrostatic loading for hydrogen storage application

Zhaochen XU[1], Philipp BRAUN[1], Jean SULEM[1]

[1] *Navier, Ecole Nationale des Ponts et Chaussées, Institut Polytechnique de Paris, Univ Gustave Eiffel, CNRS, Marne-la-Vallée, France*
E-mail: zhaochen.xu@enpc.fr, philipp.braun@enpc.fr, jean.sulem@enpc.fr

Keywords: geological hydrogen storage, hydrostatic cyclic loading, porous limestone, mechanical response, permeability evolution

1. Introduction

Underground hydrogen storage in porous formations (UHSP) provides a large-scale and long-term solution to balance the seasonal supply-demand mismatch of renewable energy [1]. UHSP involves repeated stress cycling from seasonal hydrogen injection and withdrawal, affecting the reservoir's porosity and permeability, which are key factors controlling its storage capacity and injectivity. Therefore, understanding their evolution under cyclic loading is essential to ensure the efficiency and safety of UHSP operations. Current studies on porous carbonate rocks under cyclic loading-unloading remain limited, often involving too few cycles to represent the lifespan of UHSP operations [2]. In this study, multi-cycle hydrostatic triaxial tests accompanied by permeability measurements were conducted to characterize the hydro-mechanical property evolution of the Saint-Maximin limestone (SML), a typical highly permeable reservoir rock with a highly heterogeneous microstructure [3], aiming at addressing this knowledge gap.

2. Methodology

Triaxial tests were performed at 25 °C on saturated SML samples under fully drained conditions. The hydrostatic load was applied by varying the confining pressure at a loading and unloading rate of 0.6 MPa/min. The change in pore volume was quantified by measuring the displacement of the pore fluid pressure generator with an angular encoder. In addition, permeability measurements along the axial direction of samples were performed using the steady-state technique. A pore pressure difference of 200 kPa was imposed between the top and bottom of the SML sample to continuously measure the permeability during selected loading-unloading cycles.

3. Main Results

Fig. 1 compares porosity and permeability changes over tens of cycles within the elastic stage and at the onset of inelastic stage. In the elastic stage, cyclic loading causes a noticeable ratcheting deformation, indicated by hysteresis loops shifting progressively with the accumulation of strain. After 1000 cycles, a reduction of 0.45% is observed for the porosity whereas the permeability decreases slightly from 4.1×10^{-14} to 3.5×10^{-14}

m². The limited damage accumulation may result from grain rearrangement or frictional sliding, though the precise mechanisms remain unclear. In contrast, once the plastic onset P^* is reached, significant irreversible porosity reduction occurs rapidly and accumulates with cycling, despite the maximum imposed confining pressure exceeding P^* by less than 1 MPa. Cyclic loading may lead to the development of interconnected microcrack networks, resulting in an increase of permeability (test IE30 in Fig.1(d)), or may induce the formation of localized compactive deformation bands, causing a monotonic decrease in permeability (IE300 in Fig.1(d)).

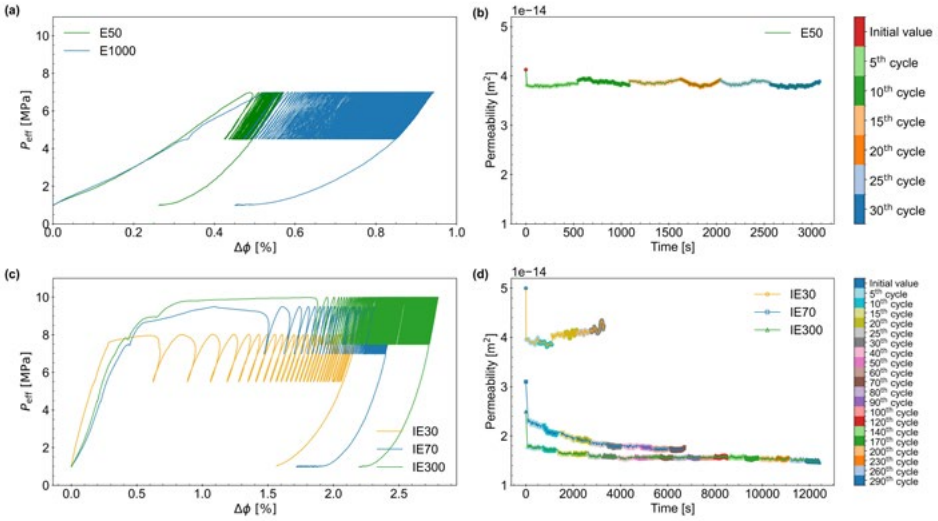

Fig. 1: Porosity and permeability evolution in the elastic stage (a &b, tests E50 and E1000 with 50 and 1000 cycles respectively below P) and inelastic stage (c &d, tests IE30, IE70 and IE300 with 30, 70 and 300 cycles respectively above P*)*

4. Conclusion

The experimental findings demonstrate that during cyclic loading, the maximum imposed stress dictates the activation of damage processes. The porosity heterogeneity of SML influences the evolution of permeability by affecting the propagation patterns of microcracks. Therefore, it is necessary to extend the permeability models that distinguish between pores and cracks to account for cyclic loading paths.

5. References

[1] Thiyagarajan, S. R., Emadi, H., Hussain, A., Patange, P., Watson, M., 'A comprehensive review of the mechanisms and efficiency of underground hydrogen storage', Journal of Energy Storage, 51, 104490 (2022).

[2] Zhou, J., Deng, G., Tian, S., Xian, X., Yang, K., Zhang, C., Dong, Z., 'Experimental study on the permeability variation of sandstone at cyclic stress: Implication for underground gas storage', Journal of Energy Storage, 60, 106677 (2023).

[3] Abdallah, Y., Sulem, J., Bornert, M., Ghabezloo, S., Stefanou, I., 'Compaction Banding in High-Porosity Carbonate Rocks: 1. Experimental Observations', Journal of Geophysical Research: Solid Earth, 126(1), e2020JB020538 (2020).

Stress-induced non-Fickian transport in 3D fractured rock

Chuanyin Jiang and Qinghua Lei

Department of Earth Sciences, Uppsala University, Uppsala, Sweden
E-mail: Chuanyin.jiang@geo.uu.se, Qinghua.lei@geo.uu.se

Keywords: 3D DFN; mesh quality; stress-flow-transport coupling; non-Fickian transport

1. Introduction

Non-Fickian transport is ubiquitous in fractured rock due to multi-scale heterogeneity – from single fracture-scale aperture variability to network-scale structural complexity. Characterized by early solute breakthrough and heavy tailing, it plays a key role in many geoengineering applications involving mass/heat transport.

Fractured rock is inevitably subjected to in-situ stress, leading to fracture closure and shear-induced dilation. 2D studies have observed stress-induced non-Fickian transport [1, 2], but due to simplified geomechanical boundary conditions and geometric topologies, 2D findings require further validation by 3D modeling. A few existing 3D insights relied on simplified assumptions, omitting fracture-fracture and fracture-matrix interactions as well as Coulomb's friction failure [3]. Thus, a high-fidelity understanding of non-Fickian transport in 3D fractured rock remains lacking.

This study introduces FracLab, a 3D discrete fracture network (DFN) generator that optimizes DFN geometry (Fig. 1a), enabling the computational efficiency of subsequent high-fidelity 3D coupled stress-flow-transport modeling. Using the FracLab-generated DFNs, we capture stress-induced non-Fickian transport phenomena in 3D fractured rock.

2. Methodology

We model a 10 m cubic domain with a DFN (~1600 fractures) generated by FracLab (Fig. 1b). Fracture radii follow a power-law distribution, while the orientations are purely random. FracLab's geometry control algorithm ensures high-quality meshing in both fracture and matrix domains (Fig. 1c). The coupled stress-flow-transport modeling is solved using the finite element method, incorporating nonlinear normal closure, shear slip, and dilatancy of fractures. We explored a differential stress condition (S_y = S_z = 1 MPa and S_x = 5 MPa) (Fig. 1d) with flow directed along the negative x-axis (Fig. 1f).

3. Main Results

Under the applied differential stresses, significant shear dilation emerges along the preferentially oriented long fractures (Fig. 1e), which simultaneously leads to pronounced shear deformation and stress concentration in the surrounding rock matrix (Fig. 1d). These highly dilated fractures form dominant flow pathways, channeling most of the fluid passing through the system. As a result, the breakthrough curve (BTC), represented by the probability density function (PDF) of average outlet concentration, exhibits strongly non-Fickian characteristics, i.e., a positively skewed, non-Gaussian-shaped BTC. In contrast, under the zero-stress condition with a uniform initial aperture, the BTC follows a Gaussian shape, indicating Fickian transport behavior.

4. Conclusion

We developed FracLab, a 3D DFN generator enabling coupled stress-flow-transport modeling in 3D fractured rock. We demonstrated that differential stress may greatly change transport dynamics, shifting Fickian transport under the unstressed condition to strongly non-Fickian behavior through shear-induced dilation and flow channeling.

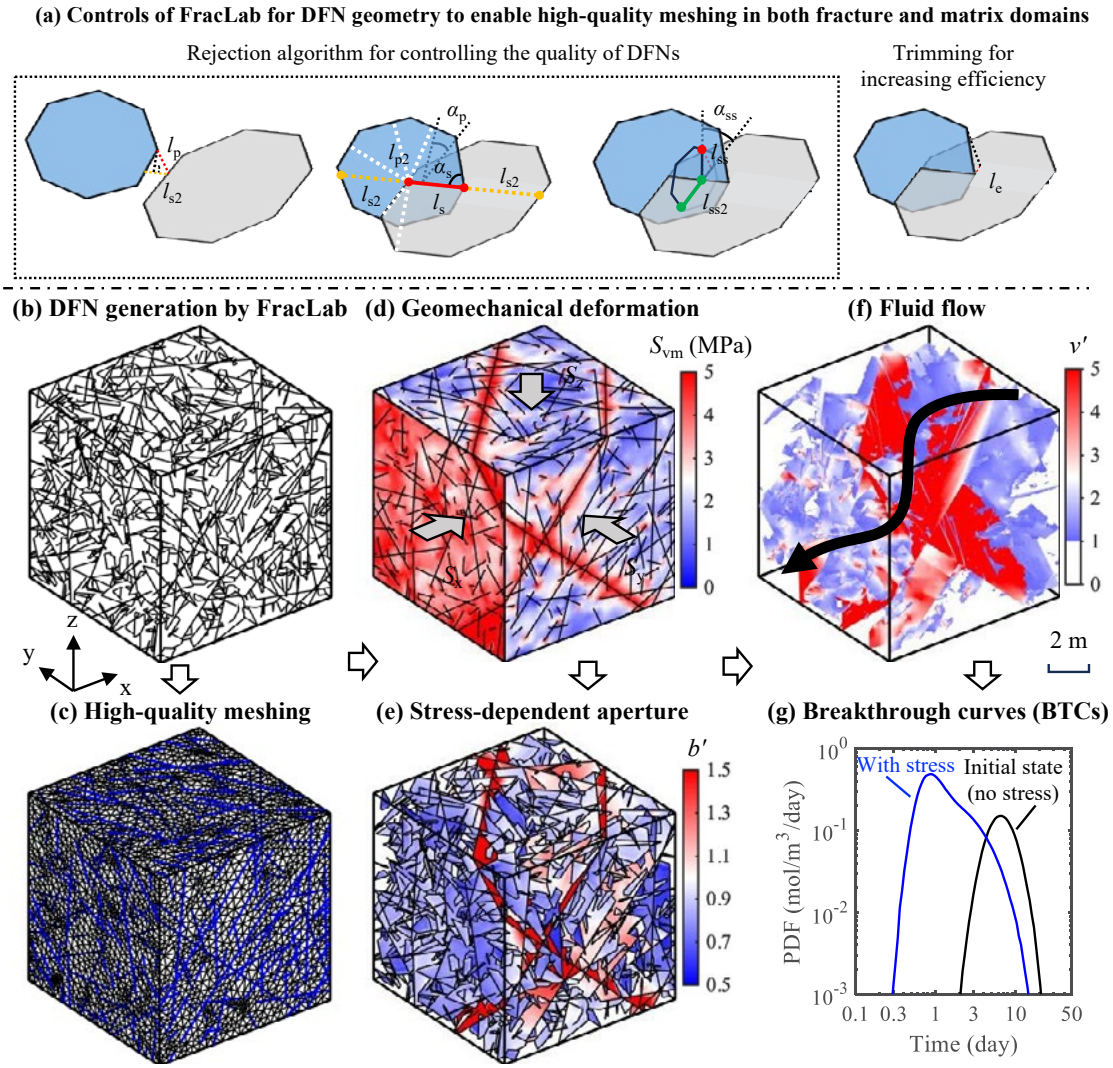

Fig. 1: Workflow for the stress-flow-transport modeling in 3D fractured rock

5. References

[1] Kang, P.K., Lei, Q., Dentz, M., Juanes, R. 'Stress-induced anomalous transport in natural fracture networks'. Water Resources Research, 55, 4163–4185 (2019).

[2] Wang, X., Jiang, C., Lei, Q., Liu, L., 'Impact of stress-driven crack growth on the emergence of anomalous transport in critically connected natural fracture networks', International Journal of Rock Mechanics and Mining Sciences, 170, 105532 (2023).

[3] Sweeney, M.R., Hyman, J., 'Stress effects on flow and transport in three-dimensional fracture networks', Journal of Geophysical Research: Solid Earth, 125, e2020JB019754 (2020).

Injection-induced deformation in porous media: the coupling between formation heterogeneity, flow, and strain types.

Yaniv Edery, Shaimaa Sulieman, Martin Stolar, Evgeny Shavelzon, and Arnold Bachrach

[1] *Technion - Israel Institute of Technology*
E-mail: yanivedery@technion.ac.il

Keywords: Porous media deformation, heterogeneity, transport and flow.

1. General instructions

The injection of pressurized fluids into the underground, commonly utilized in industrial processes such as carbon storage, geothermal energy production, and hydraulic fracturing, can induce seismic activity and deform the porous structure of the underground rocks. While pore pressure typically induces expansion, experimental studies suggest that under confined conditions—relevant to many injection operations into aquifers—fluid injection may lead to compaction of the porous medium. However, the coupling of flow and deformation exhibits a rich, dynamic range for the deformation type that has not been previously explored in porous structures, ranging from localized compaction to dilation and fracturing.

This study investigates injection-induced compaction localizations in a granular porous medium by tracking both the global and local deformation and monitoring the applied pressure and flux. For that, we developed a method to chemically sintered Poly(methyl methacrylate) (PMMA) grains so to simulate rock-like conditions. We employ refractive index-matching fluids to track the deformation by fluorescent imaging of fluorescently labeled beads that are embedded in the porous structure during the pressurized flow [1]. The results demonstrate continuous elasto-plastic compaction at the global scale, which follows the mean effective stress (Fig 1.). Surprisingly, this global compaction is punctuated by abrupt strain localizations that couple compaction and shear. These localizations are triggered by sudden pore collapses, followed by the shearing and rearrangement of adjacent regions, primarily upstream, due to stress gradients imposed by fluid flow (Fig 2.). This shear-induced rearrangement temporarily reduces stiffness, driving further compaction and stiffness recovery over time. Furthermore, while the flow condition should induce 1D compaction, we observe considerable dilation transverse to the flow (Fig 2.b.), which moderates the measured permeability reduction, producing a discrepancy between the stress-strain hysteresis and the stress-permeability hysteresis. We also show that under radial conditions, these compaction-dilation events may result in tensile fractures [2]. Our findings underscore the complexity and rich physical dynamics of injection-induced compaction localization, revealing the emergence of non-axial strains in what initially appears to be a one-dimensional problem.

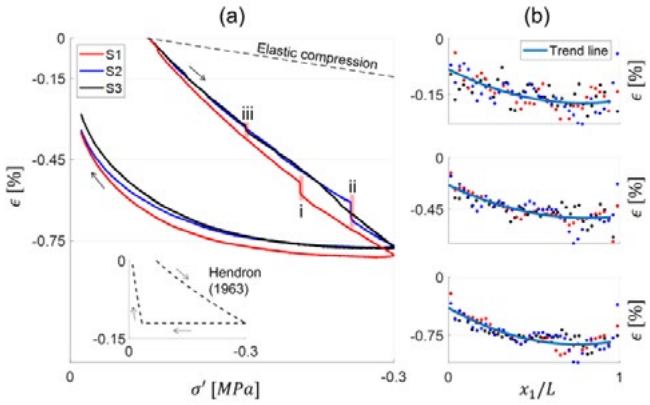

Fig. 1: a) Averaged strain-stress relation for three different samples: 'S1', 'S2' and 'S3'. The normal strain in the e1 direction (ϵ) is measured locally and averaged over both x1 and x2. The normal effective stress in the same direction (σ') is calculated through the concept effective stress using the measured injection pressure, and is averaged over x1. The elastic compression curve (marked by a dashed line) is calculated by assuming linear strain-stress relations and using the measured confined elastic modulus of the medium. The other dashed curve in the inset was calculated by using Hendron's mathematical model for confined compaction of a face-centered cubic array of equi-radi elastic spheres. (b) Internal distribution of ϵ, averaged over x2 only, plotted against the medium's normalized length (x1/L), for three different over-all averaged (over x1 and x2) strains (ϵ = −0.15, −0.45, −0.75%), for the loading path only. Note the increasing compaction along x1 which is in-line with the compression gradient, expected by the concept of effective stress.

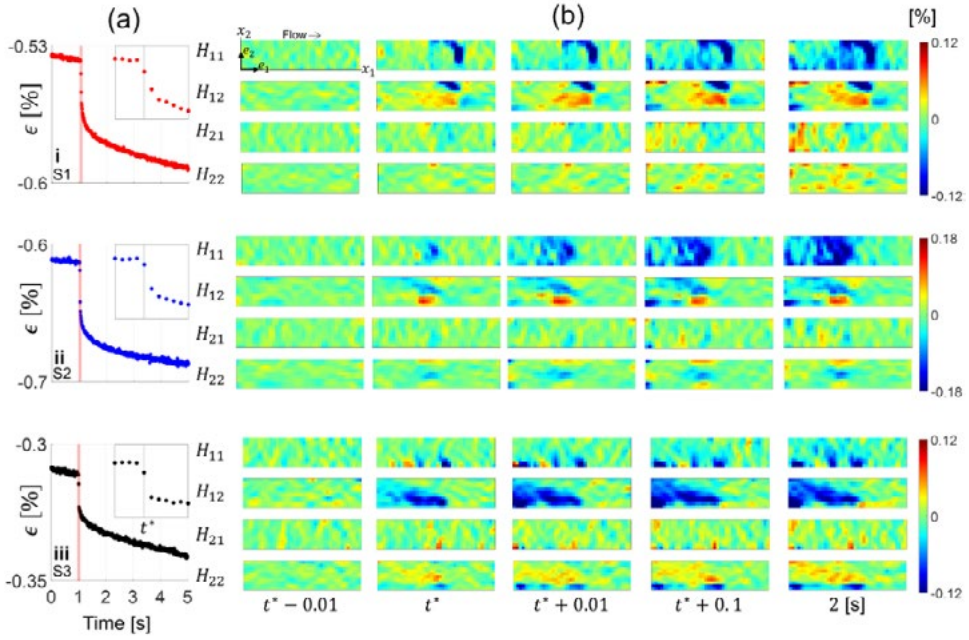

Fig. 2: a) A 5-second window around the average strain drops (i-iii). Under this time window, the

strain drops are not completely sharp but rather have some 'tail', most clearly seen between time=1 to time=2 seconds, with the strain rate gradually decreasing. The inset shows a finer strain analysis on an even smaller time window of 0.1 seconds (which can be traced to the red shaded patch) with 0.01 seconds interval between the measurements. (b) 2D displacement gradient maps, calculated relative to time=0, to isolate the localization signal from the continuous deformation prior to its initiation. Note the appearance of several components of Hij at t∗ and the continuous intensification of H11 at later times in 'i' and in 'ii'.

2. Acknowledgments

A.B. acknowledges The Nancy and Stephen Grand Technion Energy Program (GTEP) for supporting this research. YE and AB acknowledge the support of the MOST-RIF Cyprus-Israel Scientific Research Program (grant no. 0007592). YE and ES acknowledge the support of the Israel Science Foundation (grant no. 3774/24).

3. References

[1] Arnold Bachrach and Yaniv Edery. Technique for studying in high resolution poromechanical deformation of a rocklike medium. Phys. Rev. E, 108(2):L022901, August 2023.

[2] Shaimaa Sulieman, Martin Stolar, Ludmila Abezgauz, Shouceng Tian, and Yaniv Edery. Investigating the permeability evolution of artificial rock during ductile and brittle deformation under pressurized flow. arXiv preprint arXiv:2309.02231, 2023.

Applicability of equations of state across a range of pressure and temperature conditions for underground hydrogen storage

Konstantinos Charalampous[1,2], Charalampos Konstantinou[1,2], Panos Papanastasiou[1,2]

[1]*Department of Civil and Environmental Engineering, University of Cyprus, Cyprus*
[2]*PHAETHON Centre of Excellence for Intelligent, Efficient and Sustainable Energy Solutions*
E-mail: charalampous.konstantinos@ucy.ac.cy, konstantinou.charalampos@ucy.ac.cy, papanastasiou.panos@ucy.ac.cy

Keywords: hydrogen storage, equations of state, thermodynamic properties, gas deviation factor, renewable energy

1. Introduction

The transition to renewable energy highlights hydrogen as a sustainable energy carrier, but its storage requires understanding thermodynamic behavior under various conditions. This study evaluates eleven equations of state (EoS) for predicting the gas deviation factor (Z) of hydrogen across different storage applications, including salt caverns and depleted reservoirs. Using an extensive experimental dataset, the accuracy of these EoS was assessed with error metrics. The findings emphasize the suitability of EoS for specific storage applications, while regression models and contour plots provide insights for optimizing hydrogen storage systems, supporting its adoption in sustainable energy.

2. Methodology

Data from 16 studies (1973 data points with ranges of pressure and temperature 0.1MPa-2250MPa and 23K-873K, respectively.) have been analyzed to determine the accuracy of various equations of state (EoS) using error metrics such as the Root Mean Square Error and the Mean Absolute Errors. The study covers data acquisition, EoS analysis, and error metric evaluation. Experimental studies included hydrogen volume/mass measurements across varying temperatures and pressures. The dataset spans a wide range of conditions, providing valuable insights into hydrogen behavior. a collection of studies that have contributed significantly to the understanding of thermodynamic properties of hydrogen under various conditions. Various equations of state (EoS) are used to describe the thermodynamic properties of hydrogen based on the work by [1]. These models are essential for accurately predicting the behavior of hydrogen under various conditions, which is crucial for its applications across energy systems.

3. Main Results

A comparison of various EoS models highlights their modifications and impact on hydrogen thermodynamic predictions. The underground storage of hydrogen, similar to natural gas, is increasingly seen as a viable large-scale energy storage solutions [2]. Salt caverns and depleted reservoirs are common storage types, with operating pressures of 10 to 30 MPa and temperatures between 18 to 80°C for salt caverns, and 10 to 80 MPa with temperatures from 40 to 140°C for depleted reservoirs. The RKS equation of state (EoS) is found to be the most suitable for both storage types based on temperature and

pressure conditions, followed by NB for temperature and PTV for pressure. RKS is highlighted for its accuracy in predicting the gas deviation factor, with contour plots provided for estimation in Fig. 1. The gridfit function was used to create the contour plot for interpreting the data, with predictions trusted only where experimental data is available. This study evaluates the suitability of various EoS for predicting hydrogen's gas deviation factor under different storage conditions. For underground storage, RKS emerged as the most reliable for salt caverns and depleted reservoirs. Empirical equations and surface plots derived from this study offer practical solutions for hydrogen volume estimations, supporting the optimization of hydrogen storage systems in the transition to sustainable energy.

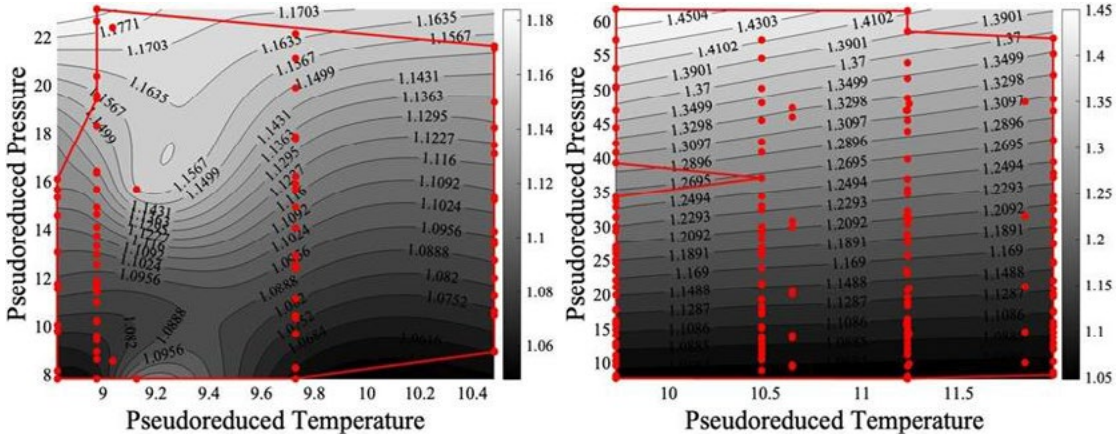

(a) (b)

Fig. 1 Contour plots for Z-factor against the pseudoreduced pressures and temperatures for salt caverns (a) storage and depleted reservoir storage (b)

4. Conclusions

This study evaluates the suitability of various equations of state (EoS) for predicting hydrogen's gas deviation factor under different storage conditions. For underground storage, RKS emerged as the most reliable for both salt caverns and depleted reservoirs. Empirical equations and surface plots derived in this study offer practical tools for estimating the gas deviation factor (Z) while balancing complexity and accuracy. The findings emphasize the importance of selecting tailored EoS based on storage conditions to optimize hydrogen storage design and support the transition to sustainable energy solutions.

5. References

[1] Nasrifar K. Comparative study of eleven equations of state in predicting the thermodynamic properties of hydrogen. Int J Hydrogen Energy 2010;35:3802–11. https://doi.org/10.1016/j.ijhydene.2010.01.032.

[2] Konstantinou C, Giakoumi M, Papanastasiou P, Olympios A V, Arsalis A, Georghiou GE. Green hydrogen storage capacity estimations in depleted gas reservoirs. 2024 3rd Int Conf Energy Transit Mediterr Area (SyNERGY MED) 2024:1–5. https://doi.org/10.1109/SyNERGYMED62435.2024.10799311.